JYU DISSERTATIONS 490

Kati Karvonen

Mechanisms and elimination of *Borrelia burgdorferi* persistence *in vitro*

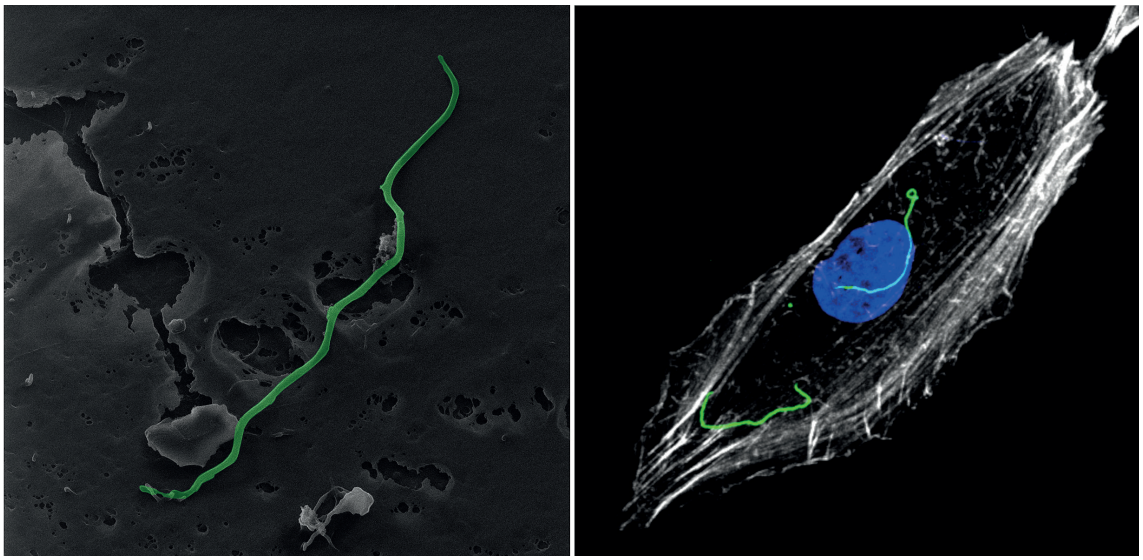

UNIVERSITY OF JYVÄSKYLÄ
FACULTY OF MATHEMATICS
AND SCIENCE

JYU DISSERTATIONS 490

Kati Karvonen

Mechanisms and elimination of *Borrelia burgdorferi* persistence *in vitro*

Esitetään Jyväskylän yliopiston matemaattis-luonnontieteellisen tiedekunnan suostumuksella
julkisesti tarkastettavaksi helmikuun 11. päivänä 2022 kello 10.

Academic dissertation to be publicly discussed, by permission of
the Faculty of Mathematics and Science of the University of Jyväskylä,
on February 11, 2022 at 10 a.m..

JYVÄSKYLÄN YLIOPISTO
UNIVERSITY OF JYVÄSKYLÄ

JYVÄSKYLÄ 2022

Editors
Varpu Marjomäki
Department of Department of Biological and Environmental Science, University of Jyväskylä
Timo Hautala
Open Science Centre, University of Jyväskylä

Permanent link to this publication: http://urn.fi/URN:ISBN:978-951-39-9007-7

ISBN 978-951-39-9007-7 (PDF)
URN:ISBN:978-951-39-9007-7
ISSN 2489-9003

ABSTRACT

Karvonen, Kati
Mechanisms and elimination of *Borrelia burgdorferi* persistence *in vitro*
Jyväskylä: University of Jyväskylä, 2022, 57 p.
(JYU Dissertations
ISSN 2489-9003; 490)
ISBN 978-951-39-9007-7
Yhteenveto: Persistentti *Borrelia burgdorferi* -infektio ja sen poistaminen *in vitro*
Diss.

Borrelia burgdorferi sensu lato complex are species of pleomorphic spirochete bacteria causing Lyme borreliosis (LB), the most common tick-borne disease in the Northern hemisphere. Although antibiotics usually kill the bacteria, some post-treatment patients suffer from long-term sequalae of LB, the development of which is currently unclear, although immune evasion and persistence of the bacteria are thought to play major roles. This study investigated the long-term infectivity and persistence of *B. burgdorferi* sensu stricto *(*henceforth referred to as *B. burgdorferi)* in human non-phagocytic cells *in vitro*, as well as, characterised borrelial outer membrane vesicles (BbOMVs), and assessed the cytotoxic effect of BbOMVs on these human cells. In addition, the bactericidal effects of two herbal compounds against *B. burgdorferi* pleomorphic forms were examined. The aim was to identify the mechanisms associated with *B. burgdorferi* persistence in human cells *in vitro*, and to provide future tools for eradicating such persistence. The results demonstrated that *B. burgdorferi* invaded and persisted in synovial and skin cells for nine days, without killing the host cells. Moreover, *B. burgdorferi* was observed in a variety of shapes, while simultaneously avoiding lysosomal colocalisation during the nine days of coculture. BbOMVs were on average 33 nm in diameter and contained antigenic proteins OspA, OspC, p39 and peptidoglycan, as well as double stranded DNA. However, the vesicles did not induce cell death after 72-h of coculture with the human cells. The analysis of two herbal compounds demonstrated effective eliminating of *B. burgdorferi* spirochetes, round bodies, and biofilm-like aggregates. In summary, this study demonstrated that *B. burgdorferi* can invade human cells with the possibility to evade host immune system, and with the help of different pleomorphic forms, persist inside a host. Furthermore, BbOMVs could be utilised as decoys and repositories for persisting antigens during a borrelial infection, and plant-based antimicrobials may offer a potential for therapeutics against long-term LB.

Keywords: Antimicrobial; *Borrelia burgdorferi*; Lyme disease; outer membrane vesicle; persistence.

Kati Karvonen, University of Jyväskylä, Department of Biological and Environmental Science, P.O. Box 35, FI-40014 University of Jyväskylä, Finland

TIIVISTELMÄ

Karvonen, Kati
Persistentti *Borrelia burgdorferi* -infektio ja sen poistaminen *in vitro*
Jyväskylä: Jyväskylän yliopisto, 2022, 57 s.
(JYU Dissertations
ISSN 2489-9003; 490)
ISBN 978-951-39-9007-7
Yhteenveto: Persistentti *Borrelia burgdorferi* -infektio ja sen poistaminen *in vitro*
Diss.

Borrelia burgdorferi sensu lato -ryhmän bakteerit ovat monimuotoisia spirokeettabakteereja, jotka aiheuttavat pohjoisen pallonpuoliskon yleisintä puutiaisten levittämää tautia, borrelioosia. Vaikka antibiootit yleensä tappavat bakteerin, osa potilaista kärsii hoidon jälkeisestä pitkäkestoisesta borrelioosista, jonka syntyyn johtavia tekijöitä ei vielä tiedetä, mutta immuunipuolustukselta piiloutumisen ja bakteerin pitkäaikaisen säilymisen eli persistenttiyden ajatellaan olevan avainrooleissa. Tässä tutkimuksessa tutkittiin solumaljalla *B. burgdorferi* sensu stricto -bakteerin (jatkossa *B. burgdorferi*) pitkäkestoista infektiota ja persistenttiyttä ihmissoluissa, jotka eivät ole syöjäsoluja. Tämän lisäksi bakteerin erittämiä ulommaisen solukalvon vesikkeleitä (USV) karakterisoitiin sekä arvioitiin vesikkelien sytotoksisuus soluille. Lopuksi kahden kasviperäisen yhdisteen antibakteerinen tehokkuus *B. burgdorferin* eri muotoja vastaan selviteltiin. Tutkimuksen tavoitteena oli tunnistaa *B. burgdorferin* persistenttiyteen ihmissoluissa liittyvät erilaiset mekanismit, sekä tarjota työkaluja tällaisen persistenttiyden poistamiseen. Tulokset osoittivat, että *B. burgdorferi* tunkeutui ja säilyi rusto- sekä ihosoluissa yhdeksän päivää tappamatta isäntäsolua. Lisäksi tänä aikana havaittiin bakteerin erilaisia muotoja, sekä bakteerin välttävän lysosomaalisen hajotuksen. USV:t olivat keskimäärin 33 nm halkaisijaltaan ja sisälsivät antigeenisiä proteiineja OspA, OspC, p39 ja peptidoglykaania, sekä kaksijuosteista DNA:ta. USV:t eivät kuitenkaan aiheuttaneet solukuolemaa 72 tunnin yhteiskasvatuksen jälkeen. Molemmat kasviperäiset yhdisteet tuhosivat tehokkaasti *B. burgdorferin* spirokeetta-, pallo- ja biofilmi muodot. Kaiken kaikkiaan tämä tutkimus osoitti, että *B. burgdorferi* pystyy tunkeutumaan ihmissoluihin ja näin mahdollisesti pakenemaan immuunivasteelta. Tämän lisäksi eri muotoja hyödyntäen bakteeri pystyy säilymään isännässä. Bakteeri saattaa käyttää USV:eita harhauttamaan immuunijärjestelmää, sekä persistenttien antigeenien säilytyspaikkana infektion aikana. Kasvipohjaiset antimikrobiset yhdisteet saattavat tulevaisuudessa tarjota hoitomuotoja pitkäkestoista borrelioosia vastaan.

Avainsanat: Antimikrobinen; *Borrelia burgdorferi*; Lymen tauti; persistenttiys; ulommaisen solukalvon vesikkeli.

Kati Karvonen, Jyväskylän yliopisto, Bio- ja ympäristötieteiden laitos PL 35, 40014 Jyväskylän yliopisto

Author

Kati Karvonen, MSc
Department of Biological and Environmental Science
P.O. Box 35
FI-40014 University of Jyväskylä
Finland
kati.s.karvonen@jyu.fi

Supervisors

Professor Varpu Marjomäki, PhD
Department of Biological and Environmental Science
P.O. Box 35
FI-40014 University of Jyväskylä
Finland

University teacher Jonna Nykky, PhD
Department of Biological and Environmental Science
P.O. Box 35
FI-40014 University of Jyväskylä
Finland

Reviewers

Senior Researcher MSc Natalie Rudenko, PhD
Institute of Parasitology Biology Centre
Biology Centre CAS
Branišovská 1160/31
370 05 Check Republic

Senior Scientist Anna-Liisa Välimaa, PhD
Natural Resources Institute Finland (Luke)
P.O. Box 413 (Paavo Havaksen tie 3)
FI-90014 University of Oulu
Finland

Opponent

Team leader, Sara Moutailler, PhD
Joint Research Unit for Molecular Biology and Parasitic Immunology
147 rue de l'université
75338 Cedex 07 France

CONTENTS

ABSTRACT
TIIVISTELMÄ
CONTENTS
LIST OF ORIGINAL PUBLICATIONS
RESPONSIBILITIES
ABBREVIATIONS

1 INTRODUCTION 11

2 Review of the literature 13
2.1 *Borrelia burgdorferi* 13
2.1.1 Pleomorphic forms 14
2.2 Lyme borreliosis 15
2.2.1 Prolonged disease manifestations 16
2.3 Borrelial persistence 17
2.3.1 Utilisation of tick proteins 18
2.3.2 Complement evasion 18
2.3.3 Antigenic variation via VlsE 19
2.3.4 Localisation into specific niches 20
2.3.5 Persister cells and persistent antigens 20
2.4 Bacterial outer membrane vesicles 21
2.4.1 *B. burgdorferi* OMVs 22
2.5 Plant-based antibacterials 23

3 AIMS OF THE STUDY 25

4 Overview of the methods 26

5 Results and discussion 27
5.1 Differences in *B. burgdorferi* infectivity between different host cells 27
5.1.1 Attachment to host cells 27
5.1.2 Long-term infectivity in host cells 28
5.2 Intracellular persistence 29
5.3 Persistence through pleomorphic forms 31
5.4 Characterisation of BbOMVs 33
5.4.1 Size analysis of BbOMVs 33
5.4.2 Protein characterisation of BbOMVs 34
5.4.3 BbOMVs did not induce death in human cells 36
5.5 Eradication of *B. burgdorferi* with novel herbal compounds 37

6 Conclusions 39

Acknowledgements 41

YHTEENVETO (RÉSUMÉ IN FINNISH) 43

REFERENCES 46
ORIGINAL PAPERS

LIST OF ORIGINAL PUBLICATIONS

The thesis is based on the following original articles, which will be referred to in the text by their Roman numerals I–III.

I Karvonen K., Nykky J., Marjomäki V., Gilbert L. 2021. Distinctive evasion mechanisms to allow persistence of *Borrelia burgdorferi* in different human cell lines. *Frontiers in Microbiology* 12: 711291.

II Karvonen K., Tammisto H., Nykky J., Gilbert L. 2022. *Borrelia burgdorferi* outer membrane vesicles contain antigenic proteins but do not induce cell death in human cells. *Microorganisms*. In press.

III Karvonen K., Gilbert L. 2018. Effective killing of *Borrelia burgdorferi in vitro* with novel herbal compounds. *General Medicine Open* 2 (6): 1-4.

RESPONSIBILITIES

Article I — The original idea to examine *Borrelia burgdorferi* infection in non-immune human cells came from Leona Gilbert. Leona Gilbert and I planned the helium ion microscopy, infectivity, cell death, and pleomorphic form analysis experiments. Varpu Marjomäki and I planned the electron microscopy, colocalization, GFP assessment, and the borrelial survival experiments. I performed the experiments. I analysed the data together with Leona Gilbert. Each author participated in reviewing and writing the article after I had written the first draft.

Article II — The original idea to study borrelial outer membrane vesicles was mine. Leona Gilbert and I planned and designed the experiments. Hanna Tammisto optimized the purification protocol, and we together performed the vesicle characterization experiments. I performed the cell cytotoxicity experiments. I analysed the data together with Leona Gilbert. Each author contributed to the writing of the article after I had written the first draft.

Article III — The original idea and the design of the experiments came from Leona Gilbert. I performed the experiments. I analysed the data and wrote the manuscript together with Leona Gilbert.

ABBREVIATIONS

BbOMV	*Borrelia burgdorferi* outer membrane vesicle
BFL	Biofilm-like aggregate
ECM	Extracellular matrix
EM	Erythema migrans
FH	Factor H
FHL-1	Factor H like-protein 1
GFP	Green fluorescent protein
LB	Lyme borreliosis
LSF	Biocidin LSF broad-spectrum liposomal formula
MBD	Minimum bacterial death
MIC	Minimum inhibitory concentration
Osp	Outer surface protein
RB	Round body
vls	Variable major protein-like sequence
VlsE	Variable major protein-like sequence expressed

1 INTRODUCTION

Lyme borreliosis (LB) is a multifaceted disease caused by bacteria belonging to the *Borrelia burgdorferi* sensu lato complex (Burgdorfer *et al.* 1982). The bacterium is transmitted via hard-bodied *Ixodes* ticks, and currently, there are three main species whose infection results in LB in humans: *B. burgdorferi sensu stricto*, *B. afzelii*, and *B. garinii* (Trevisan *et al.* 2021). LB can manifest in a multitude of signs and symptoms, ranging from mild flu-like symptoms with or without a red rash called erythema migrans (EM), to more severe manifestations involving the skin, joints, the nervous system, or even the heart (Cardenas-de la Garza *et al.* 2019). Antibiotic therapy is effective against the bacteria, especially if treatment is started promptly after initiation of infection. However, an important subset of patients continues to exhibit prolonged signs and symptoms months to years after initial diagnosis and the receival of treatment (Kullberg *et al.* 2020).

Presently, the scientific community is divided over whether long-term sequalae of LB is a true consequence of *B. burgdorferi* sensu lato infection or not. Because the infective agent has not been able to be reproducibly cultured from patient samples, the presence of persistent infection, and thus, the cause for the enduring distress in patients, has not been satisfactorily confirmed (Cardenas-de la Garza *et al.* 2019, Shor *et al.* 2019, Schoen 2020, Lantos *et al.* 2021). However, non-cultivable spirochetes, as well as persisting antigens such as borrelial DNA fragments and certain borrelial proteins have been located from patient tissue samples after treatment with antibiotics (Nanagara *et al.* 1996, Hulïnská *et al.* 1999, Pícha *et al.* 2014, Jutras *et al.* 2019). Therefore, signs of borrelial infection in patients treated with antibiotics can still be detected, but the lack of evidence for viable, dividing bacteria prevents doctors from identifying the cause as a persistent ongoing infection. Consequently, the enduring long-term sequalae of LB in some patients have left the research community puzzling over the question why some patients continue to suffer when others recover rapidly? Furthermore, how exactly is *B. burgdorferi* sensu lato bacteria involved in the progression of continued manifestations of a variety of signs and symptoms in LB

patients? The answers to these questions would help develop better treatment options for patients suffering from long-term LB signs and symptoms.

In this study, the aim was to investigate long-term *B. burgdorferi* sensu stricto infection in human cells *in vitro,* in order to examine mechanisms of persistence in host cells, as well as to identify options to eliminate such persistence. The results illustrated that *B. burgdorferi* sensu stricto was able to invade and remain inside human cells without killing the cells. A variety of different forms of the bacterium was observed, which could assist in its persistence. Borrelial outer membrane vesicles were examined to contain certain antigenic molecules and could therefore be utilised by the bacteria as decoy targets for host immune response, or as convenient agents for persistent antigens. In addition, two herbal compounds efficiently eradicated the pleomorphic forms of the bacteria, thus offering possibilities as future treatment options.

2 REVIEW OF THE LITERATURE

2.1 *Borrelia burgdorferi*

Borrelia burgdorferi sensu lato complex is part of the phylum Spirochaetes to which also belongs such pathogenic bacteria as *Treponema pallidum* (syphilis), *Leptospira interrogans* (leptospirosis), and *Borrelia recurrentis* (relapsing fever) (LPSN 2021, Trevisan *et al.* 2021). Three respective groups of bacteria belong to the genus *Borrelia*, two of which cause diseases in humans (Lyme group and Relapsing fever group), and Echidna-Reptile group, whose pathogens only infect reptiles (LPSN 2021, Trevisan *et al.* 2021). The Lyme group of bacteria or *B. burgdorferi* sensu lato complex currently consist of 20 accepted and three proposed different species of *Borrelia*, out of which eight have been found pathogenic in humans (Wolcott *et al.* 2021). However, the three main species currently involved in human pathogenesis are *B. burgdorferi* sensu stricto (henceforth referred as *B. burgdorferi*), *B. garinii* and *B. afzelii* (Borchers *et al.* 2015). The Lyme group bacteria are spirochetes or spiral / coiled in shape, reaching 10 – 30 μm in length and approximately 0.2 – 0.5 μm in width (Burgdorfer *et al.* 1982, Trevisan *et al.* 2021), and cause Lyme borreliosis (LB), a multisystemic disease in humans (reviewed in Section 2.2). For clarity, from hereafter *Borrelia* is used as an umbrella term for LB pathogenic bacteria.

Borrelia is transmitted via *Ixodes* ticks throughout the Northern hemisphere, and while all three abovementioned genospecies have been detected in patients in Europe, in the USA mostly *B. burgdorferi* is the causative agent of LB (Cardenas-de la Garza *et al.* 2019, Trevisan *et al.* 2021). *Borrelia* has a parasitic life cycle, shifting between the tick vector and its vertebrate host. A tick goes through four transformations during its lifetime, from eggs to larvae, to nymph, and ultimately into adult. The different stages span over approximately two years, during which ticks feed off of a variety of reservoir hosts of *Borrelia* such as small rodents, hedgehogs and birds, as well as other mammals and lizards, before molting into each next stage (Mead 2015, Wolcott *et al.* 2021, Trevisan *et al.* 2021). Unlike the reservoir hosts, in which *Borrelia* can persist without caus-

ing disease and be transmitted into a feeding tick, humans are a dead-end host for *Borrelia*. The nymphal stage is the most dangerous for human transmission, because the ticks are small and hard to detect, and in fact most human infections occur in late spring and summer during the nymphal phase (Mead 2015).

The variation of different hosts and the parasitic lifestyle of *Borrelia*, can be seen in its fairly small genome (Tilly *et al.* 2008). *B. burgdorferi* has a linear chromosome of about 900-kbp and several plasmids (9 linear and 12 circular) (Fraser *et al.* 1997, Casjens *et al.* 2000). The linear chromosome encodes genes that are common in other bacteria, while the rapidly evolving plasmids are more unique to the *Borrelia* genus (Fraser *et al.* 1997, Casjens *et al.* 2000, Tilly *et al.* 2008). No apparent virulence factors, such as genes for the production of toxins, have been located from *B. burgdorferi* chromosome (Fraser *et al.* 1997). However, several plasmid-encoded genes, required for mammalian infection, have been identified (Tilly *et al.* 2008). For instance, certain lipoproteins are known to induce an immune response in mammals, and specifically outer surface protein C (OspC) was demonstrated to be necessary in successful infection in mice (Grimm *et al.* 2004, Tilly *et al.* 2008). As the small genome lacks several genes for synthesizing nucleotides, amino acids, fatty acids and enzyme cofactors (Fraser *et al.* 1997, Tilly *et al.* 2008), the bacterium requires these nutrients from its host or from the complex *in vitro* culture media.

2.1.1 Pleomorphic forms

In normal culture conditions, *Borrelia* is mostly found as a spirochete. However, being a pleomorphic bacterium, *Borrelia* can alter its form into metabolically inactive round body form (RB), into biofilm-like aggregates (BFLs), and it can be seen producing outer membrane vesicles (OMVs; also called blebs) (Meriläinen *et al.* 2015, Rudenko *et al.* 2019). Figure 1 below illustrates borrelial pleomorphic forms with *B. burgdorferi* strain GCB726 which has been genetically modified in its flagella with green fluorescent protein (GFP) (Moriarty *et al.* 2008). The corkscrew shape of spirochetes is evident in 1A, while in 1B a blebbed bacterium can be located. The rounding up of RBs is depicted in 1C, and a cluster of bacterial cells as a BFL can be observed in 1D. While each of these pleomorphic forms can be detected from normal growth cultures, they can also be deliberately induced. Specifically, RBs have been demonstrated to form by osmotic pressure, changes in pH, serum starvation and in increased temperatures, but also with antibiotics (Kersten *et al.* 1995, Brorson and Brorson 1998, Alban *et al.* 2000, Murgia and Cinco 2004, Meriläinen *et al.* 2015). Blebbing has been illustrated to increase in amount by treatment with antibiotics, human sera, and certain mammalian cell culture media (Barbour *et al.* 1982, Kersten *et al.* 1995, Meriläinen *et al.* 2015). BFLs were noticed to be pH, temperature and growth phase -dependent (Srivastava and De Silva 2009). However, reversion from the pleomorphic form back to its parental spirochetal form can occur, once the culture conditions become favourable again (Brorson and Brorson 1998, Alban *et al.* 2000, Murgia and Cinco 2004, Meriläinen *et al.* 2015).

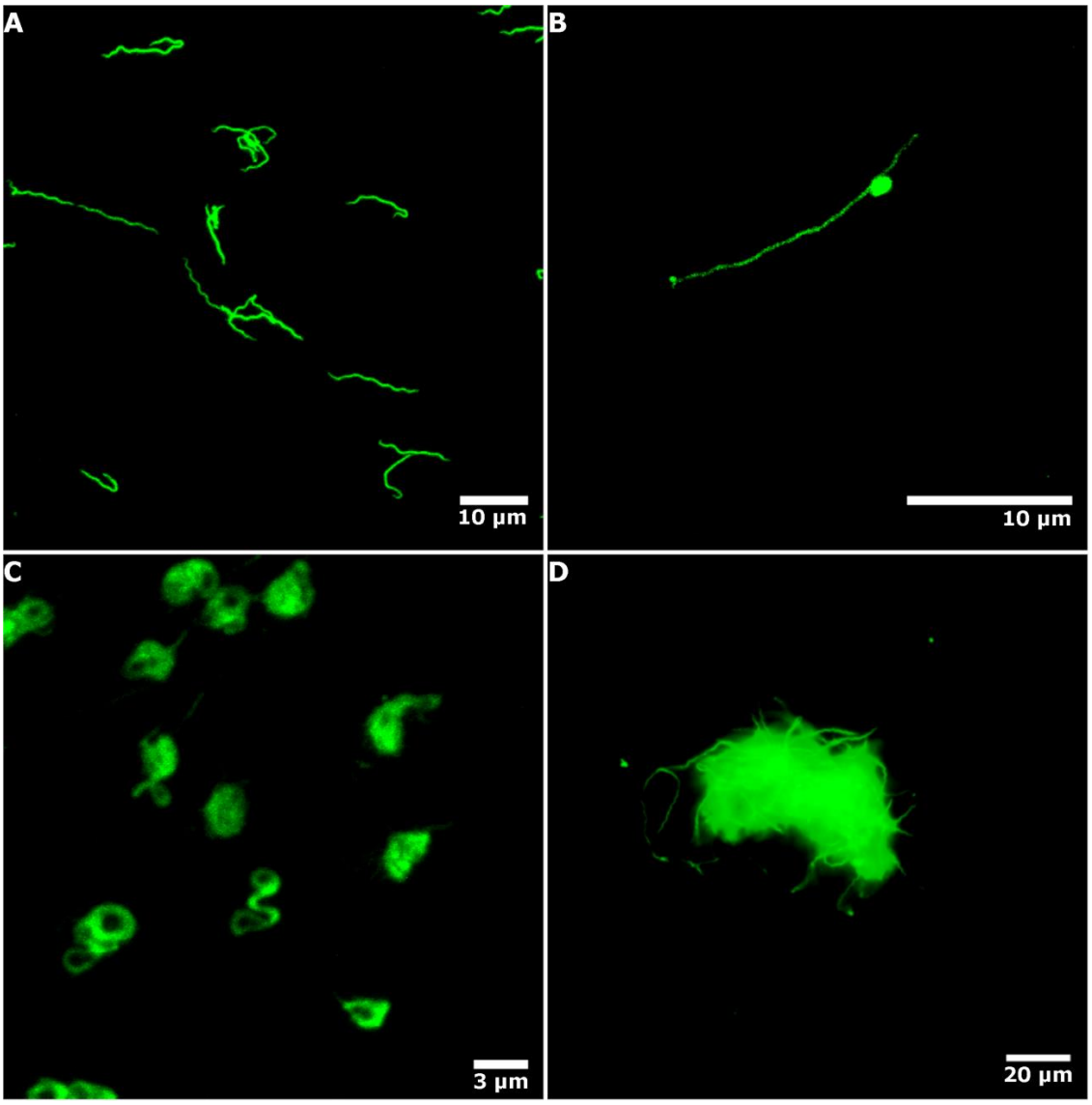

FIGURE 1 Different pleomorphic forms of *B. burgdorferi*. Genetically modified *B. burgdorferi* strain GCB726 fluorescing in green due to green fluorescent protein located in the flagella, indicting the parental corkscrew shaped spirochete (A), bleb (B), round body (RB; C), and biofilm-like aggregate (BFL; D) forms. Scale bars: A & B: 10 µm, C: 3 µm, D: 20 µm.

2.2 Lyme borreliosis

Presently, the most common vector-borne disease in North America and Europe is LB (Mead 2015). It is estimated that approximately 476 000 clinically diagnosed LB cases occur yearly in the USA (Kugeler *et al.* 2021), while the European Parliament in a resolution on Lyme disease (Borreliosis) (2018/2774 (RSP)) estimated the case number in Europe to be as high as 850 000 (Anon 2018). *Borrelia* infection can lead to multisystemic manifestations and can be divided into three stages: early localised, early disseminated and late stages (Cardenas-de la

Garza *et al.* 2019). Signs and symptoms in the early localised stage usually include a red-bluish EM rash, which appears within the first week of the infection, and may accompany fever and other flu-like symptoms (Cardenas-de la Garza *et al.* 2019, Schoen 2020). *Borrelia* can disseminate from the initial tick bite site to other locations in the body including the skin, joints, the nervous system, and rarely the heart. Thus, the symptoms in the disseminated stage, occurring weeks to months after the initiation of infection, can comprise of secondary EM lesions in the skin, Lyme neuroborreliosis (presenting for example as meningitis, painful radiculoneuritis or facial palsy), Lyme arthritis and Lyme carditis (Cardenas-de la Garza *et al.* 2019, Schoen 2020). The late stage develops when *Borrelia* infection has been left untreated during the initial stages, resulting in disease manifestations including acrodermatitis chronica atrophicans, Lyme arthritis, and Lyme neuroborreliosis (Cardenas-de la Garza *et al.* 2019, Schoen 2020). Since *Borrelia* lacks genes for producing toxins, the resulting tissue damage in patients is considered to be the outcome of inflammatory reactions by the host immune response (Fraser *et al.* 1997, Borchers *et al.* 2015).

The three main pathogenic *Borrelia* species have been demonstrated to present slightly differently in patients. For instance, it has been noted that *B. burgdorferi* infection mostly results in arthritic symptoms, while *B. garinii* induces neurological disorders, and *B. afzelii* affects the skin (Baranton *et al.* 1992, Canica *et al.* 1993, Van Dam *et al.* 1993, Jungnick *et al.* 2015, Trevisan *et al.* 2021). Furthermore, these three pathogens have been identified in varying degrees in different continents with mostly only *B. burgdorferi* infecting humans in the USA, while all three species have been detected from patients in Europe (Baranton *et al.* 1992, Trevisan *et al.* 2021). Thus, patients in different parts of the world can manifest *Borrelia* infections in diverse manners, which can hinder accurate diagnosis especially if there is no recognition of a tick bite.

2.2.1 Prolonged disease manifestations

LB is treated with antibiotics, which in most cases efficiently eliminate *Borrelia*, especially when treatment was started early on in the infection. Oral doxycycline is recommended for 10 days, while 14-day course is suggested for amoxicillin and cefuroxime axetil (Lantos *et al.* 2021). Although most LB patients recover after receiving a course of antibiotics, approximately 5 – 20 % remain, who suffer from lingering signs and symptoms (Kullberg *et al.* 2020, Bobe *et al.* 2021), and have been defined as post-treatment Lyme disease syndrome (PTLDS) or chronic Lyme patients (Shor *et al.* 2019, Lantos *et al.* 2021, Bobe *et al.* 2021). These symptoms vary from fatigue, unexplainable pain and cognitive difficulties, among others (Kullberg *et al.* 2020). Presently, LB research lacks sufficient data to explicitly and unequivocally diagnose patients with PTLDS or chronic Lyme, which has prompted an ongoing debate whether or not either disease actually even exists or at least is due to an ongoing *Borrelia* infection (Cardenas-de la Garza *et al.* 2019, Shor *et al.* 2019, Schoen 2020, Lantos *et al.* 2021). However, as patients with long-term sequalae do exist, the exact mechanisms of how such distresses develop, are continuously being investigated.

2.3 Borrelial persistence

In order for *Borrelia* to be able to establish an infection and persist inside a mammalian host, the bacteria must escape the host's immune responses. *Borrelia* has developed several ingenious mechanisms, such as, utilisation of tick proteins, complement evasion, antigenic variation, localisation into specific niches, and deployment of persister cells, in order to circumvent the mammalian immune system, subsequently, being able to survive and persist (Berndtson 2013, Bockenstedt *et al.* 2020). Figure 2 below depicts these mechanisms, which are further discussed in the following subsections.

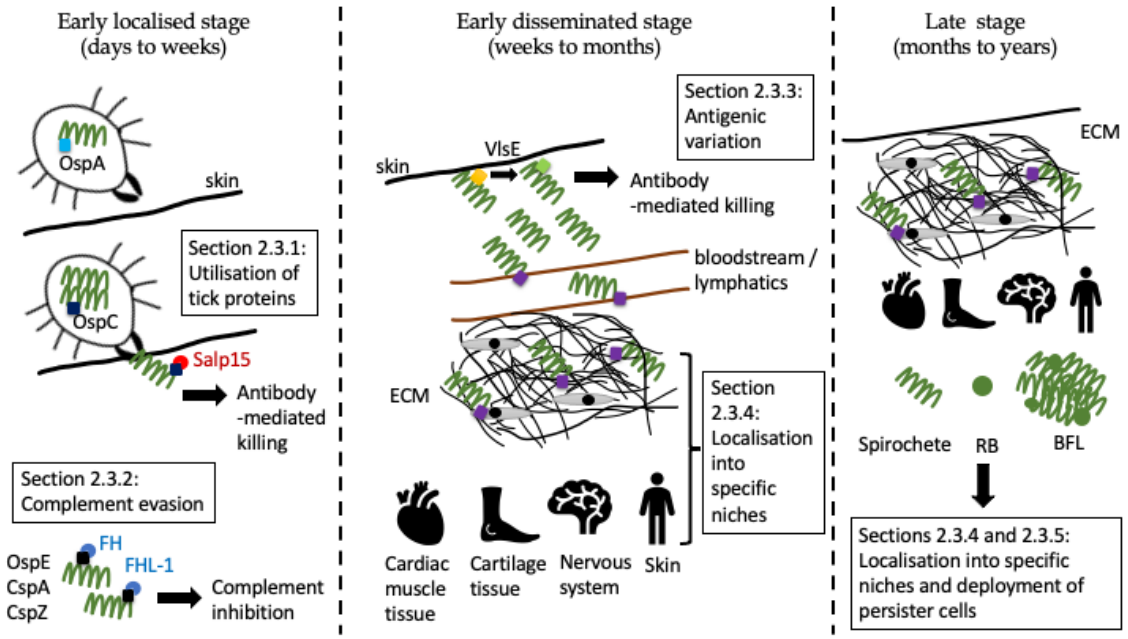

FIGURE 2 Illustration of different mechanisms for immune evasion utilized by *Borrelia*. *B. burgdorferi* is transmitted via *Ixodes* ticks. The blood meal changes *B. burgdorferi* protein expression. Especially the expression of OspA shifts to OspC, which signals the bacteria to migrate from the gut of the tick towards the tick salivary glands, and from thereon spread into the host. During the early localized stage of Lyme borreliosis (LB), *B. burgdorferi* can be found replicating in the immediate proximity of the tick bite site. With the help of tick proteins, such as, Salp15 binding to OspC, *B. burgdorferi* can avoid antibody-mediated killing. Furthermore, in order to avoid the host complement system, several *B. burgdorferi* surface proteins bind host complement inhibiting molecules, such as factor H and factor H like-protein 1 (FH/FHL-1), thus impeding complement activation. After weeks to months from the initial bite and *B. burgdorferi* transmission, bacteria can be found disseminating via the blood and lymphatics to distal parts of the body into several different tissues. Through antigenic variation of the VlsE surface protein, *B. burgdorferi* can deceive the adaptive immune response, especially the humoral antibody response. Moreover, by locating away from the bloodstream and into the extracellular matrix (ECM) and a variety of tissues, *B. burgdorferi* manages to avoid different immune cells, thus, avoiding detection. In the late stage of LB, *B. burgdorferi* is rarely observed from the blood, rather it can be found in the ECM and different tissues. Furthermore, different pleomorphic forms such as round body forms (RB) and biofilm-like aggregates (BFLs) can be visualized from tissue samples. (Based on Berndtson 2013; Bockenstedt *et al.* 2020.)

2.3.1 Utilisation of tick proteins

Borrelia infection begins with a tick bite to a vertebrate host. The spirochete resides in the tick gut where the incoming blood meal changes the environment, resulting in alterations in gene expression and consequently, in the protein expression of the bacterial outer membrane (Bockenstedt *et al.* 2020). Specifically, the expression of outer surface protein A (OspA) switches to OspC due to the increase in temperature and decrease in pH brought on by the blood flow (Schwan *et al.* 1995). Tick feeding is also a signal for replication, after which *Borrelia* begins to travel towards the tick salivary glands and into the host (Bockenstedt *et al.* 2020). The *Ixodes* tick saliva contains several anti-haemostatic, anti-inflammatory, vasodilatory and immunosuppressive properties, which facilitate tick feeding for extended periods of time without alerting the host immune system of the intruder (de Silva *et al.* 2009). Hence, it is no surprise that pathogens transmitted by the ticks have evolved to utilise some of these molecules to support the infection of a new host.

The most examined tick salivary protein is Salp15, which was first identified in 2005 to bind with OspC, consequently protecting *B. burgdorferi* from antibody-mediated elimination (Ramamoorthi *et al.* 2005, Schuijt *et al.* 2008, Wen *et al.* 2020). Moreover, *B. burgdorferi* infection was observed to increase Salp15 expression in ticks thus facilitating the infection (Ramamoorthi *et al.* 2005). In addition, a recent analysis indicated that *Borrelia* infection altered the expression of numerous tick salivary proteins to enhance borrelial transmission and survival at the bite site (Kim *et al.* 2021). Additionally, several studies have demonstrated enhanced infectivity of *Borrelia* in mice co-inoculated with tick salivary gland extract (Bockenstedt *et al.* 2020) further exhibiting the utilisation of tick proteins in infection by these bacteria.

Several tick proteins have been detected to inhibit host complement pathways. For instance, tick salivary lectin pathway inhibitor protein (TSLPI) bind lectin pathway pattern recognition molecules, hence, inhibiting the activation of the lectin pathway and protecting *Borrelia* from lysis, while Ixodes scapularis anti-complement (Isac) family of proteins block the alternative complement pathway (de Silva *et al.* 2009, Nuttall 2019). Furthermore, sialostatin L2, a cysteine protease, inhibited chemokine production and toll-like receptor signalling in infected murine dendritic cells (Nuttall 2019). Hence, *Borrelia* has developed several mechanisms for utilising the molecules secreted in the saliva of the tick vector to aid in borrelial infectivity and survival inside a host (see Fig. 2).

2.3.2 Complement evasion

Complement is a major part of the innate immune system, and it serves as a link between the innate and adaptive immunities. The complement system consists of over 30 proteins in the plasma and on cell surfaces, and it is divided into three pathways: classical, lectin and alternative (Walport 2001). The classical pathway is activated through antibody-antigen interaction, the lectin by the binding of mannan binding lectin, and the alternative is constantly activated by

spontaneous activation of complement component 3 (C3) (Zipfel and Skerka 2009). Each pathway ultimately converts C3 into C3a and C3b, which results in either opsonisation of the microbe by multiple C3b molecules ensuing in phagocytosis, or the generation of C5 convertase by C3a, which can lead to inflammatory reaction via C5a, and the formation of a membrane attack complex through the combination of C5b and several other complement components (C6-C9) (Walport 2001, Zipfel and Skerka 2009).

As was mentioned above in Section 2.3.1, some of the tick proteins aid *Borrelia* in evading host complement (Salp15, TSLPI, Isac) (Ramamoorthi *et al.* 2005, de Silva *et al.* 2009, Nuttall 2019). However, there are several borrelial proteins that alone can also induce survival from each complement pathway (Bockenstedt *et al.* 2020, Dulipati *et al.* 2020). Complement factor H (FH) and factor H-like protein-1 (FHL-1) are some of the proteins that *Borrelia* utilise in evading the complement system (Dulipati *et al.* 2020). FH and FHL-1 control C3b formation, and by binding these factors, *Borrelia* can effectively stop the complement activation cascade. For example, the OspE family of proteins (ErpA, ErpP, ErpC, p21), CspA and CspZ bind FH and FHL-1 inhibiting the alternative complement pathway (Dulipati *et al.* 2020; Lin *et al.* 2020a). Additionally, a 43-kDa protein, p43, as well as, OspC both inhibit classical and lectin pathways by binding C4b-binding protein (C4bp), while the outer surface protein BBK32 blocks the activation of C1 complex, thus inactivating the classical pathway (Caine *et al.* 2017; Dulipati *et al.* 2020; Lin *et al.* 2020a). In summary, a multitude of borrelial surface proteins acting in cohort facilitate the survival of *Borrelia* from complement, and therefore, assist in persistence (see Fig. 2).

2.3.3 Antigenic variation via VlsE

Upon encountering a foreign antigen, a B cell matures into a plasma cell, which starts to produce antibodies specific to that antigen. Hence, during infection, a pathogen is constantly in a race with the immune system, where the pathogen attempts to escape eradication while the immune system tries to capture and eliminate the escapee. Antigenic variation, or the process whereby microbes alter their surface antigens in order to avoid detection from host adaptive immune response, is one of the most common and effective attribute of immune evasion by a variety of human pathogens, such as *T. pallidum*, *Mycoplasma* species, *Neisseria* species, and *Borrelia*, among others (Vink *et al.* 2012, Bockenstedt *et al.* 2020, Chaconas *et al.* 2020). *Borrelia* expresses a variable major protein-like sequence (*vls*) gene locus, which contains the *vlsE* gene that encodes the 35-kDa surface exposed lipoprotein VlsE (Zhang *et al.* 1997, Vink *et al.* 2012). The *vls* system contains the *vlsE* expression site and 15 silent cassettes providing a multitude of possible recombination events for producing a variety of VlsE epitopes (Zhang *et al.* 1997, Norris 2014, Chaconas *et al.* 2020). Furthermore, the recombination changes seem to occur only during *in vivo Borrelia* infections, with *VlsE* sequence changes noticed as early as four days post-infection, while the complete loss of the "parental" sequence occurs by day 28 (Norris 2014). Hence, the rapid and constant change of surface antigens provides *Borrelia* with an effec-

tive mechanism for deceiving the humoral immune response, thus abetting in borrelial persistence in the host (see Fig. 2).

2.3.4 Localisation into specific niches

Borrelia is known to disseminate from the site of the tick bite to a variety of locations in the human body via the bloodstream and the lymphatics (Bobe *et al.* 2021). However, the bacteria does not stay in blood, but rather utilises it as a means to colonise other tissues, as can be deduced from the fact that detection of spirochetemia or borrelial DNA with PCR analysis from blood samples is almost always impossible (Kullberg *et al.* 2020, Bobe *et al.* 2021). The host extracellular matrix (ECM) is a dynamic network of macromolecules affecting cellular proliferation, adhesion, migration, polarity, differentiation, and apoptosis (Yue 2014). *Borrelia* has several membrane proteins that have been demonstrated to interact with the ECM, thus evoking a hypothesis for ECM functioning as a protective niche for *Borrelia* infection and persistence (Berndtson 2013). Specifically, borrelial proteins BBK32, RevA / RevB and BB0347 have been exhibited to bind fibronectin, while decorin binding proteins A and B bind decorin, BBA33 and CRASP-1 interact with collagen, and ErpX and BmpA with laminin (Bernard *et al.* 2019). In addition, several *Borrelia* proteins that bind host plasmin (enolase, OspA, OspC, Erp proteins, BBA70), aggrecan (BbHtrA) and integrins (P66, BB07, BB0172) have been identified (Bernard *et al.* 2019). Furthermore, OspC was recently observed to bind fibronectin and / or dermatan sulphate in a specific OspC variant -dependent manner, thus suggesting an additional role for OspC as a possible instigator for the *Borrelia* strain specific LB manifestations (Lin *et al.* 2020b). Nevertheless, the multitude of different protein interactions between *Borrelia* and the host ECM suggest a favouritism towards this milieu. Moreover, the ECM provides a convenient microhabitat for *Borrelia* to evade host immune system and persist (Berndtson 2013) (see Fig. 2).

In addition to locating into the ECM of a host, *Borrelia* was illustrated to invade such human non-phagocytic cells as endothelial cells (Comstock and Thomas 1991, Ma *et al.* 1991), dermal fibroblasts (Klempner *et al.* 1993, Rozwadowska *et al.* 2017), synovial cells (Girschick *et al.* 1996), and neural cells (Livengood and Gilmore 2006, Miklossy *et al.* 2008), among others. Moreover, elongated spirochetes have been detected in phagocytic macrophages (Naj and Linder 2015) and dendritic cells (Filgueira *et al.* 1996, Suhonen *et al.* 2003), suggesting that *Borrelia* can even escape being degraded by a professional phagocyte. Subsequently, invasion of human cells without killing the host cells has been suggested as one mechanism for immune evasion for *Borrelia* (Ma *et al.* 1991, Girschick *et al.* 1996, Livengood and Gilmore 2006).

2.3.5 Persister cells and persistent antigens

Among a bacterial cell population a persister can arise, for instance, due to antibiotics (Bigger 1944). A persister is a bacterial cell which is insensitive to the action of an antibiotic most likely because the bacterium is in a dormant, non-

dividing phase, and if placed into a suitable environment, would start diving again (Bigger 1944). It is believed that in a bacterial cell culture there is a small but not constant population of persisters that will individually be unaffected by antibiotics, but this ability is not passed on to offspring, much like resistance genes would be (Bigger 1944). Additionally, persister cells are not antibiotic resistant, rather they can be considered as dormant "sleeper" cells that tolerate the effects of antibiotics (Lewis 2010, Rudenko *et al.* 2019). Antibiotic tolerance can be understood as a passive function, in which dormant cells survive antibiotic induced killing without any specific drug resistance mechanism (Lewis 2010). Meanwhile, antibiotic resistant cells actively prevent antibiotics from working because of a specific resistance mechanism, such as the activity of β-lactamases that destroy penicillin (Lewis 2010). Therefore, persisters should ultimately be able to be killed with antibiotics provided that their dormancy is first overcome (Lewis 2010, Sharma *et al.* 2015, Rudenko *et al.* 2019).

Antibiotics are the main treatment against *B. burgdorferi* infection, and in most cases, efficiently eradicate the bacterium. However, studies have illustrated the inefficiency of antibiotics against *B. burgdorferi* pleomorphic forms *in vitro*, specifically RBs and BFLs, thus labelling these forms as persisters (Sapi *et al.* 2011, Sharma *et al.* 2015, Feng *et al.* 2016, Rudenko *et al.* 2019). Furthermore, *Borrelia* or borrelial antigens have been detected from mice (Bockenstedt *et al.* 2012, Hodzic *et al.* 2014) and primates (Embers *et al.* 2012), as well as from human patient samples several months after receiving antibiotics (Nanagara *et al.* 1996, Hulïnská *et al.* 1999, Pícha *et al.* 2014, Sapi *et al.* 2016, 2019, Jutras *et al.* 2019). Although *Borrelia* could be visualized from infected tissue samples after antibiotic treatment, recultivation was not successful, raising the question whether or not the bacterium was still viable (Hulïnská *et al.* 1999, Bockenstedt *et al.* 2012, Hodzic *et al.* 2014). However, the detection of *Borrelia* and borrelial antigens months after antibiotic treatment, does indicate that the bacterium can persist in an infected host (see Fig. 2).

2.4 Bacterial outer membrane vesicles

Gram-negative bacteria generate vesicles from their outer membrane (McBroom and Kuehn 2005). Gram-positive bacteria can also produce vesicles, but since these bacteria only have a single membrane bilayer, their vesicles are called cytoplasmic membrane vesicles (Toyofuku *et al.* 2019). However, due to the Gram-negative -like nature of *Borrelia*, this section will focus solely on outer membrane vesicles (OMVs). Bacteria produce outer membrane vesicles in normal growth cultures, but stressors such as temperature, oxidative stress and detergents, among others, can be used to induce the formation of OMVs (Qing *et al.* 2019). OMVs are considered to be formed by two distinct manners: by membrane blebbing or explosive cell lysis (Toyofuku *et al.* 2019). Sized approximately between 10 – 300 nm, OMVs are spherical nanostructures with a single membrane bilayer, which consist of almost the same outer membrane proteins, poly-

saccharides and lipids as the membranes of the bacteria that the OMVs originated from (McBroom and Kuehn 2005, Orench-Rivera and Kuehn 2016, Qing *et al.* 2019). OMVs can function as signal delivery vehicles by carrying specific cargoes such as periplasmic proteins, toxins and other virulence factors, as well as genetic material (McBroom and Kuehn 2005, Unal *et al.* 2011). Furthermore, studies have identified bacterial OMVs from both *in vitro* cocultures with mammalian cells and bacteria, as well as, from *in vivo* animal and human fluid and tissue samples (Forsberg *et al.* 1981, Dorward *et al.* 1991, Brandtzaeg *et al.* 1992, Hellman *et al.* 2000, Hynes *et al.* 2005, Perez Vidakovics *et al.* 2010). Therefore, OMVs have been suggested to function, for example, as a means for bacterial inter- and intracellular communication, reaction to the surrounding environment, transport mechanism for signals even to remote locations, expulsion mechanism of potentially harmful factors from the surface of the bacterial outer membrane, and transforming agents (McBroom and Kuehn 2005, Ellis and Kuehn 2010, Unal *et al.* 2011, Kaparakis-Liaskos and Ferrero 2015, Toyofuku *et al.* 2019). In addition, OMVs have been exhibited to aid in bacterial survival by affecting host immune responses via modulating pro- and anti-inflammatory signalling and by acting as decoy molecules for the immune system (Unal *et al.* 2011, Kaparakis-Liaskos and Ferrero 2015). For instance, *Helicobacter pylori* OMVs have been demonstrated to independently activate growth arrest and interleukin 8 (IL-8) production in gastric epithelial cells (Ismail *et al.* 2003). Meanwhile, OMVs from *Neisseria meningitidis* were observed to induce both proinflammatory cytokines TNF-α, IL-1, IL-6 and IL-8, as well as, anti-inflammatory cytokine IL-10 in human whole blood, suggesting a delicate balance between OMV induced inflammation and immunosuppression (Mirlashari *et al.* 2001). Additionally, *Moraxella catarrhalis* produces OMVs that function as decoy targets for the immune cells by directly interacting with B cells, thus leaving the bacteria to escape detection (Perez Vidakovics *et al.* 2010). Likewise, OMVs from serum-resistant strains of *Neisseria gonorrhoeae* significantly reduced serum killing of whole bacteria (Pettit and Judd 1992). In summary, bacterial OMVs contain various properties that confer beneficial functions for the bacterium to not only initiate infection but also to survive once inside a host.

2.4.1 *B. burgdorferi* OMVs

Borrelia produces outer membrane vesicles, or blebs, like many other bacteria. Previously, both naturally occurring and chemically induced *B. burgdorferi* OMVs (BbOMVs) have been described *in vitro* (Dorward *et al.* 1989, Shoberg and Thomas 1993, Skare *et al.* 1995). Moreover, Dorward and colleagues (1991) demonstrated BbOMVs *in vivo* from infected mice, dogs, humans and ticks (Dorward *et al.* 1991). A variety of proteins have been located from BbOMVs, specifically, OspA, OspB, OspC and OspD, as well as various unspecified proteins sized between 14 – 110 kDa (Dorward *et al.* 1991, Shoberg and Thomas 1993, 1995, Whitmire and Garon 1993, Yang *et al.* 2011). In addition to proteins, genomic material in the form of linear and circular DNA originating mostly from plasmids, but also from the chromosome, have been reported (Dorward *et*

al. 1989, Dorward and Garon 1990). Similarly, plasmid encoded RNA transcripts have been illustrated to be contained in BbOMVs (Malge *et al.* 2018). BbOMVs have been confirmed to interact with host cells by attaching to human umbilical vein endothelial (HUVE) cells (Shoberg and Thomas 1993), and by binding and entering human fibroblast and dendritic cells, as well as, T and B lymphocytes (Beermann *et al.* 2000). Figure 3 below exemplifies BbOMVs (arrow) originating from the outer membrane of *B. burgdorferi* spirochete in a transmission electron micrograph with flagella (F) separately indicated to avoid confusion.

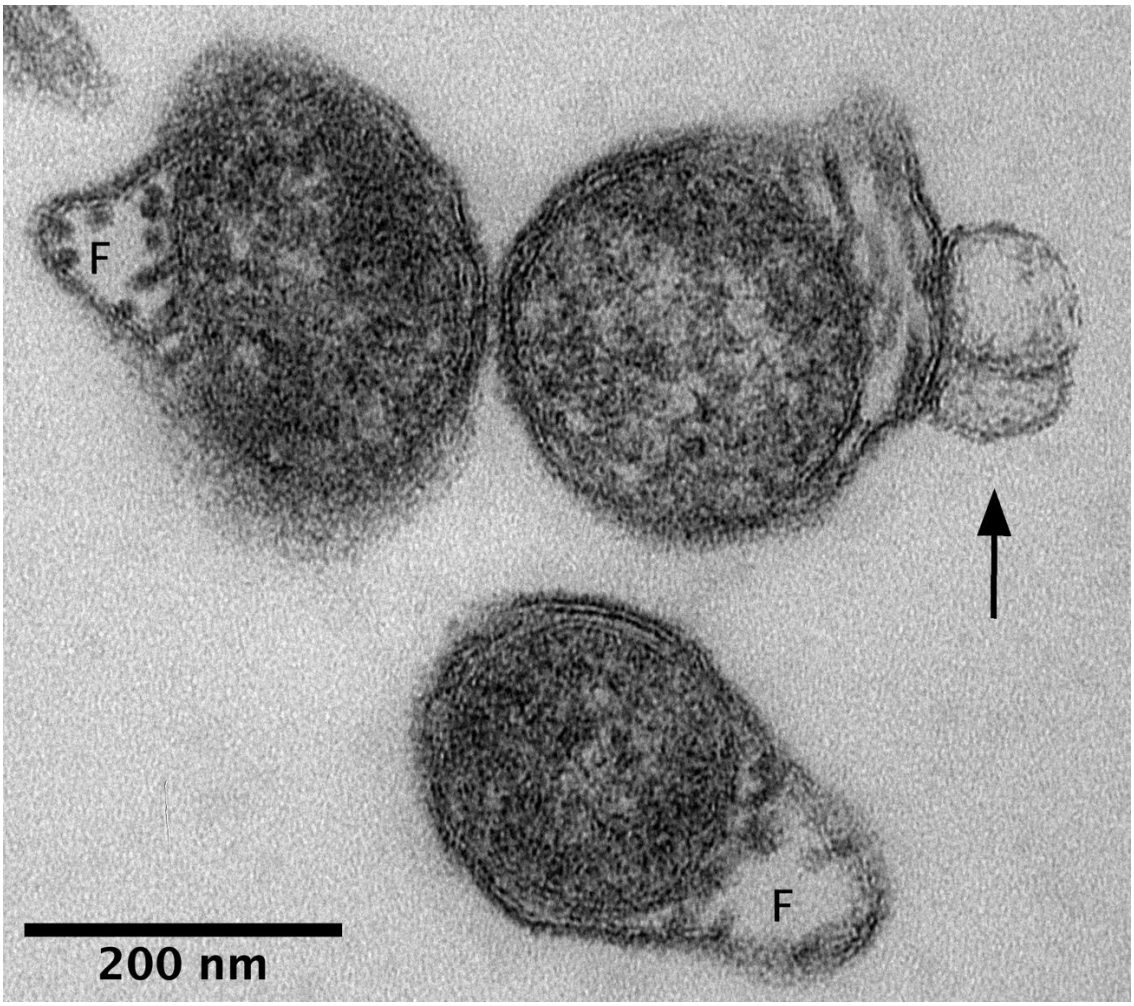

FIGURE 3 Transmission electron micrograph of epon embedded *B. burgdorferi* spirochetes exhibiting the formation of outer membrane vesicles as indicated by the arrow. Flagella (F) are indicated. Scale bar 200 nm.

2.5 Plant-based antibacterials

Multidrug resistant bacteria have become a major problem for the 21st century medical care (Uddin *et al.* 2021). Currently, there are already several antibiotic

resistant bacterial species including *Escherichia coli*, *Staphylococcus aureus*, *Streptococcus pneumoniae*, *Klebsiella pneumoniae*, *Salmonella* and *Shigella* species (Dhama *et al.* 2014, Uddin *et al.* 2021). Hence, scientific exploration for alternative antimicrobials has begun, especially from herbal and spice compounds (Tajkarimi *et al.* 2010, Dhama *et al.* 2014). The antibacterial activity of a specific plant compound depends on the phytochemicals, such as flavonoids, steroids, β-carotene, alkaloids, tannins, for example, as well as the concentration of the phytochemical, and bioactive principals (plant secondary metabolites, which are responsible for the therapeutic properties of a medicinal plant) of the herbal compound (Dhama *et al.* 2014, Chikezie *et al.* 2015). However, herbal compounds have been demonstrated to possess immunomodulatory benefits by enhancing humoral and cell mediated immunity, ameliorating stress and immunosuppression, regulating cytokines, inhibiting pathogens, and having anti-inflammatory, as well as antioxidative properties (Dhama *et al.* 2014). The effectiveness of multiple plant / spice extracts, phytochemicals, and oils against a variety of microbes have been scientifically examined (Nascimento *et al.* 2000, Khan *et al.* 2009, Tajkarimi *et al.* 2010, Dhama *et al.* 2014, Chikezie *et al.* 2015). Furthermore, certain plant extracts / phytochemicals together with antibiotics were observed to be synergistically bactericidal against antibiotic resistant bacteria such as *Pseudomonas aeruginosa, K. pneumoniae*, *Proteus* spp. and *Enterobacter aerogenes* (Nascimento *et al.* 2000).

Due to the ability to sometimes survive and persist through antibiotic treatment, research interest in antibacterial herbal compounds and phytochemicals against *Borrelia in vitro* has increased in the 21st century. Feng and colleagues, for example, have investigated the eradicative capabilities of several essential oils on the persister forms (BFLs and stationary phase cultures) of *B. burgdorferi* (Feng *et al.* 2017, 2018). Meanwhile, research by Goc and colleagues demonstrated phytochemicals, specifically, cis-2-decenoic acid, baicalein, monolaurin, and kelp to function against *B. burgdorferi* and *B. garinii* spirochetes and RBs, while only baicalein and monolaurin were effective against BFLs (Goc *et al.* 2015). Furthermore, a synergistic bactericidal effect against all pleomorphic forms of *B. burgdorferi* and *B. garinii* was observed with doxycycline and baicalein and luteolin (Goc *et al.* 2016), as well as, with only phytochemicals and micronutrients combined without the addition of antibiotics (Goc *et al.* 2017). Others have identified grape fruit seed extract to be effective against both *B. afzelii* spirochetes and RBs (Brorson and Brorson 2007), while Stevia whole leaf extract was observed to be more effective against *B. burgdorferi* persisters (RBs and BFLs) than antibiotics (Theophilus *et al.* 2015). Although currently examined only *in vitro*, these and other studies reveal the increasing trend in scientific interest in discovering alternative treatment options for LB patients, and the possibility for utilising herbal compounds alone or synergistically with antibiotics to treat antibiotic resistant or otherwise persistent infections.

3 AIMS OF THE STUDY

I To investigate *B. burgdorferi* infectivity and the factors that lead to long-term persistence in two human non-phagocytic cell lines.

II To characterise *B. burgdorferi* outer membrane vesicles (BbOMVs) with respect to size, as well as by specific protein markers, and to investigate the cytotoxic effect of BbOMVs on human cells.

III To examine the bactericidal effect of two novel herbal compounds against *B. burgdorferi* pleomorphic forms.

4 OVERVIEW OF THE METHODS

The materials and methods used in this study are listed in Table 1 below. Detailed descriptions of each method can be found in the original publications indicated by Roman numerals.

TABLE 1 Summary of the methods used in the original publications included in the thesis.

Methods	Publication
B. burgdorferi cultures	I, II, III
Human cell cultures	I, II
Infection of human cells	I, II
Helium ion microscopy	I
Transmission electron microscopy	I, II
Confocal microscopy	I, II,
Fluorescence microscopy	I, II, III
Human cell viability assays	I, II
Immunolabeling	I
Colocalization analysis	I
Vesicle purification	II
Qubit fluorometer assay	II
SDS-PAGE and Western blot	II
Flow cytometry analysis	I, II
Minimum inhibitory concentration analysis	III
Minimum bacterial death analysis	III
Time-kill analysis	III
Image analysis	I, II, III
Statistical analysis	I, II, III

5 RESULTS AND DISCUSSION

5.1 Differences in *B. burgdorferi* infectivity between different host cells

B. burgdorferi is able to infect such non-immune human cells as neuroblastoma (Thomas *et al.* 1994, Strnad *et al.* 2015), neuroglial (Rittig *et al.* 1992, Livengood and Gilmore 2006, Williams *et al.* 2018), neural cells (Strnad *et al.* 2015), as well as, primary synovial cells (Girschick *et al.* 1996), umbilical vein endothelial cells (Comstock and Thomas 1989, 1991, Szczepanski *et al.* 1990, Ma *et al.* 1991, Livengood and Gilmore 2006), and foreskin fibroblasts (Georgilis *et al.* 1992, Klempner *et al.* 1993). Due to the multisystemic nature of LB, we utilized two non-phagocytic and non-immune human cell lines, chondrosarcoma (SW1353) and dermal fibroblast (BJ), to model specific disease manifestations, arthritis and skin disorders, respectively (Georgilis *et al.* 1992, Liu *et al.* 2017, Chen *et al.* 2017). We investigated borrelial infectivity from early attachment (at 30-min post-infection) to internalization during a nine-day time period. The results indicated differences in borrelial infectivity between these two human cell lines.

5.1.1 Attachment to host cells

Firstly, *B. burgdorferi* attachment onto chondrosarcoma and dermal fibroblast cells was investigated with helium ion microscopy at 30-min post-infection. *B. burgdorferi* was observed as spirochetes on top of the SW1353 cells, whereas both coiled forms and spirochetes were located with the infected BJ cells (I, Figs. 1E, F, G). Previous research on *B. burgdorferi* infected murine fibroblasts has suggested "cyst-like" (probably RB) forms located inside these cells to possibly aid in host immune evasion by harbouring the bacterium in an inactive state, and after relocation into nutritionally replete environment, it could revert back to an active spirochetal form (Wu *et al.* 2011). In addition, coiling phagocytosis has been demonstrated to occur less with RBs than spirochetes (Meriläinen *et al.* 2016), suggesting that different receptors in the bacterial membrane have an ef-

fect on borrelial invasiveness. Moreover, the coiled borrelial forms located on the infected BJ cells (I, Fig. 1F), indicated that *B. burgdorferi* utilized different bacterial membrane interactions when invading BJ cells than during SW1353 cell invasion.

Secondly, *B. burgdorferi* was detected to interact with SW1353 cells, as indicated by the cell surface micro-protrusion visualized in the samples (I, Fig. 1E, black arrow). However, as has been demonstrated previously (Klempner *et al.* 1993, Rittig *et al.* 1996), interaction between BJ cells and *B. burgdorferi* was observed less often (I, Fig. 1F), suggesting variances in host cell adhesion by *Borrelia* possibly due to different receptors on the human cells, as well as on the bacterial membrane between the different forms.

Additionally, as the SW1353 cells were observed interacting with *Borrelia* (I, Fig. 1E), it was considered that some form of actin filament involvement was required for borrelial entry into these cells. However, even though coiled phagocytosis of *Borrelia* has been demonstrated to occur in macrophages (Rittig *et al.* 1998, Hoffmann *et al.* 2014, Naj and Linder 2015, Meriläinen *et al.* 2016), human dendritic cells (Filgueira *et al.* 1996, Rittig *et al.* 1996, Suhonen *et al.* 2003), and neuroglial cells (Livengood and Gilmore 2006, Williams *et al.* 2018), we did not observe coiling phagocytosis in either infected SW1353 or BJ cells (I, Fig. 1). This could be because of the early time point used (30-min), or because of a different invasion mechanism utilized by the bacteria. All in all, these results suggested distinctive host cell entry mechanisms for *B. burgdorferi* based on the host cell type. Hence, *B. burgdorferi* might utilise invasion of different cell types as protective niches to evade the host immune system.

5.1.2 Long-term infectivity in host cells

Infected SW1353 and BJ cells with GFP-mutated strain of *B. burgdorferi* (GCB726) were screened for nine days in order to examine the long-term infectivity of the bacterium. The cells exhibited a distinctive variation of infectivity by 48-h when, in the SW1353 cells, a peak in the percentage of infected cells was reached and after which a steady decline was observed (I, Fig. 2A). Even though infectivity increased in a dose-dependent manner in the infected SW1353 cells, the increase was not significant ($p \leq 0.05$). On the contrary, in the BJ cells, borrelial infectivity increased throughout the nine days (I, Fig. 2C). A significant dose-dependent increase in infectivity in BJ cells was observed at 48-h between MOIs 10 and 40 ($p \leq 0.05$). Likewise, there was a significant increase of infectivity ($p \leq 0.05$) in both MOIs 20 and 40 at day nine when compared to 24-h (I, Fig. 2C). In an experiment where GFP signal intensities from infected SW1353 and BJ cells at 24-h and nine days post-infection were compared, a significant decrease ($p \leq 0.005$) in the SW1353 samples at day nine was observed (I, Fig. S1). Meanwhile, GFP signal intensities did not vary in the infected BJ cells between the two time points (I, Fig. S1). Thus, the infectivity of BJ cells was both time- and dose-dependent as has been observed previously in HUVE and endothelial cells (Thomas and Comstock 1989, Szczepanski *et al.* 1990, Klempner *et al.* 1993, Isaacs 1994). Interestingly, in normal HUVE cells a similar peak in infec-

tivity at 48-h, as illustrated here with SW1353 cells, has been previously demonstrated (Ma *et al.* 1991). However, borrelial infectivity in either cell line, SW1353 or BJ, did not decrease completely throughout the nine-day time period (I, Fig. 2). Hence, *B. burgdorferi* infection persisted in both SW1353 and BJ cells at least for nine days.

5.2 Intracellular persistence

Previous findings in monocytes (Cruz *et al.* 2008), peripheral T lymphocytes (Petricarari *et al.* 2003), neural cells (Myers *et al.* 2009, Ramesh *et al.* 2013), and dermal fibroblasts (Rozwadowska *et al.* 2017), have demonstrated cell death of these cells after a *Borrelia* infection. Contrary to previous findings, SW1353 and BJ cells infected with *B. burgdorferi* for 96-h continued to grow similarly to the non-infected control cells even at a high MOI (200) (I, Fig. 3). Two respective viability assays were performed for infected SW1353 and BJ cells. Initially, live cells were counted at each time point (24, 48, 72, 96-h, seven and nine days) using Trypan Blue exclusion method, where living cells exclude the stain. This analysis illustrated significant growth ($*p \leq 0.05$; $**p \leq 0.005$) in each time point in both cell lines when compared to the staurosporine treated controls (I, Figs. 3A, B). Additionally, viability was assessed using a stain for mitochondrial membrane potential and flow cytometric analysis. Again, both cell lines illustrated viability since both had significantly ($*p \leq 0.05$; $**p \leq 0.005$) more fluorescence signal in each time point than the staurosporine induced apoptotic cell control (I, Figs. 3C, D). In Supplementary Figure 2, representative flow cytometry dot plots, as well as confocal images of the 96-h samples can be located. In the dot plots, unstained controls were used to adjust the signals, and the viable cell populations are denotated with red circles while *B. burgdorferi* controls are in red squares (I, Fig. S2). Corroborating conclusions to the viability of infected cells have been validated in human primary synovial cells (Girschick *et al.* 1996), HUVE and neuroglia cells (Livengood and Gilmore 2006), as well as in murine fibroblasts (Wu *et al.* 2011).

Since *B. burgdorferi* infection did not kill the human cells, it was important to examine whether the bacterium remained viable once internalized. Consequently, the two cell lines were infected with *B. burgdorferi* for 24 and 72-h, after which the cells were thoroughly washed and placed into BSK II media for a total of six weeks. The cultures were analysed with a fluorescence microscope, and growth was considered in cultures containing numerous motile *B. burgdorferi* spirochetes. *B. burgdorferi* grew in only one out of nine samples (from triplicate experiments) in both time points from the SW1353 cells (I, Fig. 4). Similarly, the samples from BJ cells exhibited growth in only one culture from the 24-h infected samples, whilst a total of six out of nine cultures from the 72-h time point had several motile spirochetes after six weeks of incubation (I, Fig. 4). Hence, similarly to previous studies (Georgilis *et al.* 1992, Thomas *et al.* 1994, Livengood and Gilmore 2006, Wu *et al.* 2011), we confirmed the viability of *B.*

burgdorferi after internalization into mammalian cells. Therefore, it is possible that *Borrelia* evade the host immune responses by hiding in these non-phagocytic mammalian cells, and simultaneously induce a sustained infection in the host (Ma *et al.* 1991, Klempner *et al.* 1993, Girschick *et al.* 1996, Embers *et al.* 2004, Livengood and Gilmore 2006, Wu *et al.* 2011, Naj and Linder 2015).

The intracellularity of *B. burgdorferi* even after nine days post-infection, was confirmed using anti-GFP and Protein A-gold immunolabelling with cryo-electron microscopy. From the transmission electron micrographs, immuno-labeled *B. burgdorferi* was located near the nucleus, freely in the cytosol, attached to plasma membranes, and inside vesicles (I, Figs. 5B – E). Similarly, previous studies have described *Borrelia* freely in the cytosol of human primary dendritic and synovial cells (Filgueira *et al.* 1996, Girschick *et al.* 1996), as well as in the cytoplasm of primate epithelial cells (Hechemy *et al.* 1992), and mouse primary macrophages (Rittig *et al.* 1996). Furthermore, *B. burgdorferi* has been detected to move through HUVE cell monolayer (Szczepanski *et al.* 1990, Comstock and Thomas 1991). In addition, a host membrane has been observed to surround intracellular *B. burgdorferi* in infected HUVE cells (Comstock and Thomas 1989). Hence, because the human cells survived, even flourished, during long-term infection (nine days) with *B. burgdorferi* (I, Fig. 3), it was speculated that *Borrelia* might exploit these different locations inside mammalian cells for initially evading the hostile external environment, and later to escape the intracellular endosomal processing pathways.

Borrelia is phagocytosed and degraded in lysosomes of macrophages (Rittig *et al.* 1994, Montgomery and Malawista 1996, Naj and Linder 2015, Meriläinen *et al.* 2016), and in phagolysosomes of dendritic cells (Suhonen *et al.* 2003). To establish a possible endosomal processing pathway, we investigated whether *B. burgdorferi* colocalized with Lamp2, a lysosomal marker, in SW1353 and BJ cells. Contrary to the findings in phagocytic immune cells mentioned above, *B. burgdorferi* colocalized with lysosomes only negligibly (I, Fig. 6, and Table 2). However, it was noticed that in the SW1353 samples at nine-day time point, *B. burgdorferi* did colocalize with Lamp2 more than in the BJ cells (I, Table 2). Moreover, *B. burgdorferi* was observed in coiled, rounded, and at times damaged -looking forms in the SW1353 cell samples (I, Figs. 6A, B), as has been previously exhibited in macrophages (Klose *et al.* 2019). These results indicated that *B. burgdorferi* was processed more in the chondrosarcoma cells than in the fibroblasts, demonstrating yet again differences of *B. burgdorferi* infection in these human cells. Interestingly, the processing of *B. burgdorferi* in SW1353 cells did not result in the full eradication of the bacteria from these cells as was previously observed (I, Figs. 2, 5).

However, others have demonstrated borrelial degradation without lysosomal participation in both macrophages and dendritic cells (Rittig *et al.* 1996). Furthermore, several studies have visualized elongated spirochetes in the cytoplasm of synovial cells (Girschick *et al.* 1996), HUVECs (Thomas and Comstock 1989, Szczepanski *et al.* 1990), fibroblasts (Klempner *et al.* 1993), dendritic cells (Filgueira *et al.* 1996, Suhonen *et al.* 2003), and macrophages (Naj and Linder 2015). Correspondingly, we detected *B. burgdorferi* as elongated, not damaged-

looking spirochete, seemingly free in the cytoplasm of especially BJ cells in multiple experiments (I, Figs. 2D, 6C, 6D). On the other hand, *B. burgdorferi* RBs have been demonstrated to colocalize less with lysosomes than spirochetes in macrophages, suggesting different processing pathway for RBs (Meriläinen *et al.* 2016). Since we observed *B. burgdorferi* in other forms than spirochetes in the SW1353 cells (I, Figs. 6A, B), this indicates of an alternative processing to lysosomal degradation in these cells. This further illustrated the different handling of *B. burgdorferi* between the two human cell lines, and yet another possible mechanism for borrelial survival through avoidance of lysosomal processing pathway. Therefore, it can be concluded that *B. burgdorferi* did not induce cell death in SW1353 and BJ cell lines. As the bacterium itself remained viable after internalization into these cells by avoiding lysosomal degradation, the invasion of human cells without harming them and avoidance of lysosomes would provide a possible mechanism of survival and persistence in human host cells for *Borrelia*.

5.3 Persistence through pleomorphic forms

Borrelia must escape the host immune response to be able to persist inside the host. The persistent forms of *Borrelia* (RBs and BFLs) are thought to be a possible mechanism for the bacterium to evade the host immune system (Rudenko *et al.* 2019). These persistent forms can be induced especially in unfavourable culture conditions. For instance, RBs have been established to form at high temperatures (≥ 40 °C), by changes in pH, with serum starvation, and by osmotic pressure (Alban *et al.* 2000, Murgia and Cinco 2004, Meriläinen *et al.* 2015, Sharma *et al.* 2015). Meanwhile, temperature, pH, and growth phase were observed to stimulate BFL formation (Srivastava and De Silva 2009). Penicillin have been shown to induce blebbing in *Borrelia* (Barbour *et al.* 1982). As pleomorphic forms were observed in the infected samples, an analysis of these forms was performed. From confocal images of infected SW1353 and BJ cells, 300 GFP-fluorescent attached or internalized *B. burgdorferi* from each cell line were examined, and the detected forms were divided into five categories: spirochetes, blebs, RBs, aggregates (or BFLs), and damaged (Meriläinen *et al.* 2015) (I, Table 1). The analysis of pleomorphic forms revealed distinctions in *B. burgdorferi* infections between the chondrosarcoma (SW1353) and fibroblast (BJ) cells during the nine-day time period. Specifically, while in both cell lines the number of pleomorphic forms increased the longer the experiment lasted (max nine days), the SW1353 samples demonstrated markedly more blebs and RBs the first 96-h with an increase of damaged forms in the last two time points, seven and nine days post-infection (I, Fig. 7A). Initially in the infected SW1353 cells blebs decreased while the number of RBs increased until the 96-h time point, after which blebs started to increase again and the total number of RBs was less than 10 % at days seven and nine. During the last two time points, the number of damaged forms in the SW1353 cells increased to over 55 % (I, Fig. 7A). More-

over, in the SW1353 cell samples, the shift from the parental spirochetal form occurred early on in the infection with less than 40 % of the population being spirochetes at 24-h (I, Fig. 7A).

Contrarily to the SW1353 cells, in the BJ samples spirochetes remained the main form throughout the nine days with over 65 % still in the parental corkscrew shape at the end of the examined time period (I, Fig. 7B). Inversely to the SW1353 cells, in the infected BJ cells blebbed forms increased until the 96-h time point, though with less than 30 % of the whole population being blebs at that time, after which the number of blebs decreased to 10 % at day nine (I, Fig. 7B). The number of both RBs and damaged forms in the BJ samples increased towards the last two time points but with less than 20 % each being in their respective forms (I, Fig. 7B). Interestingly, the number of aggregates (BFLs) in the infected SW1353 samples remained the same (1.67 %) between the 72-h and nine-day time points, while in the infected BJ cells their numbers steadily increased up to 5.33 % by day nine (I, Figs. 7A, B). Hence, borrelial infectivity in these two human cell lines induced the formation of *B. burgdorferi* pleomorphic forms in varying degrees. Therefore, the manifestation of pleomorphic forms in borrelial infection of different human cell lines was considered to be a mechanism utilized by the bacterium to aid in its survival and/or persistence.

Studies have visualised globular "cyst-like" forms of *B. burgdorferi* from macrophages (Naj and Linder 2015), HUVE and neuroglial cells (Livengood and Gilmore 2006), as well as from murine fibroblasts (Wu *et al.* 2011). The globular forms of *Borrelia* have been suggested to be formed in a response to the elongated spirochetal shape by the host cell as the bacterium is taken up inside a phagosome (Naj and Linder 2015). As the two cell lines used here were non-phagocytic, and no coiling phagocytosis was observed in this study (I, Fig. 1), the pleomorphic forms detected here were considered to arise due to the bacterium's response to its environment rather than the host cell's response to the bacterium.

Previous research on the reversion of long-term H_2O induced RBs have documented that reversal into spirochetes took at least three months (Brorson and Brorson 1998, Gruntar *et al.* 2001, Murgia and Cinco 2004). Consequently, cultivation attempts of *Borrelia* from patient samples should take this time point into consideration, and an analysis for the pleomorphic forms should be performed, as well. As illustrated in Fig. 7A in article I, a plethora of pleomorphic forms might be hiding in the synovial tissue samples of LB patients. Moreover, since the infected SW1353 cells demonstrated an abundance of damaged forms (I, Fig. 7A), a prolonged immune response by the infected hosts could result in chronic inflammation of the joints without the presence of live *Borrelia* (Carlson *et al.* 1999).

5.4 Characterisation of BbOMVs

B. burgdorferi has been observed to produce outer membrane vesicles that carry molecules with capabilities for affecting host-pathogen interaction (Dorward *et al.* 1989, Shoberg and Thomas 1993, Skare *et al.* 1995, Beermann *et al.* 2000, Yang *et al.* 2011, Crowley *et al.* 2013, Malge *et al.* 2018, Wawrzeniak *et al.* 2020). Therefore, we purified BbOMVs from log phased (four days) cultures by ultracentrifugation with filtering followed by concentration steps, and subjected these vesicles to a variety of staining and immunolabelling examinations in order to characterise them.

5.4.1 Size analysis of BbOMVs

The mean diameter of BbOMVs (n = 600) was calculated from electron micrographs of negatively stained BbOMVs, and based on the sizes, the vesicles were divided into four categories: 0 – 20 nm, 20.1 – 60 nm, 60.1 – 100 nm and 100.1 – 140 nm. To our knowledge, this was the first time the diameter of naturally occurring BbOMVs was measured. On average, BbOMVs were small, only 33 nm in diameter (II, Fig. 1). The smallest diameter was 11.41 nm and the largest 107.70 nm. Most of the BbOMVs were between 20.1 – 60 nm with over 400 vesicles in that category (II, Fig. 1). Only three analysed BbOMVs were over 100 nm in diameter. These findings contradict previous results where chemically induced borrelial membrane blebs were measured to be 300 – 1000 nm in diameter (Skare *et al.* 1995), indicating that there is a noticeable difference in the size of naturally occurring and chemically induced membrane vesicles. The vast size difference between chemically induced and naturally occurring vesicles was considered to be the result of the unnatural means that the vesicles are "forced" to form when chemically produced.

From negatively stained epon embedded BbOMV micrographs, heterogenic but mostly rounded BbOMVs with single membrane bilayer were observed (II, Fig. 2A). Furthermore, the vesicles were both light and dense upon visualisation, although some of the denser BbOMVs were undoubtedly due to ruptured membranes and the consequent leakage of stain inside the vesicle (II, Fig. 2A). Interestingly, previous examination of *P. aeruginosa* OMVs has indicated the uptake of extracellular DNA into empty membrane vesicles (Renelli *et al.* 2004), thus validating the role for extracellular vesicles as a means for communication. Therefore, the possibility for some of the lighter BbOMVs observed here to be empty and be utilized in a similar manner to *P. aeruginosa* was considered. Consequently, *Borrelia* might employ BbOMVs in the induction of LB - related autoimmune-like conditions (such as Lyme arthritis) via the uptake of host extracellular DNA, and wrongly initiating host immune system to attack itself by deeming the signal as foreign. However, this hypothesis requires further validation.

The analysis of 30 epon embedded BbOMV micrographs revealed residual *B. burgdorferi* spirochetes in the purified vesicle samples (II, Fig. S1). Thus, eval-

uation of the ratio between such spirochetes and close to 3000 (n = 2889) BbOMVs was performed. Since only 1.8 % of residual spirochetes were calculated from the purified BbOMV samples, the purification protocol and further characterisation analyses were considered valid.

5.4.2 Protein characterisation of BbOMVs

Different types of cargo have been identified from bacterial membrane vesicles (McBroom and Kuehn 2005, Kaparakis-Liaskos and Ferrero 2015, Toyofuku *et al.* 2019). Here purified BbOMVs were examined for the presence of several protein and glycoprotein markers, as well as double stranded DNA (dsDNA). Firstly, by using a fluorometer and Qubit fluorophore assay kit, dsDNA could be easily detected from the samples (II, Fig. 3A), thus confirming previous results of DNA localized inside borrelial membrane vesicles (Garon *et al.* 1989, Dorward and Garon 1990). Moreover, plasmid-encoded RNA transcripts have been found enriched in BbOMVs (Malge *et al.* 2018). Hence, *Borrelia* appears to employ its membrane vesicles in the transfer of information between bacterial cells if not with the host, as well.

Secondly, BbOMVs were stained with Coomassie Blue and a commercial glycoprotein staining kit for proteins and glycoproteins, respectively (II, Figs. 3B, C). Both stains indicated the presence of proteins and glycoproteins in BbOMVs. Although, especially in the Coomassie Blue stain, the BbOMV lanes closely followed the positive control for the stain, albumin (II, Fig. 3B), suggesting that there were traces of media in the purified samples. The presence of glycoproteins in BbOMVs was evident from the signal intensity analysis, since the *B. burgdorferi* lysate controls and BbOMVs had similar values (II, Fig. 3C).

Lastly, detection of known antigenic proteins OspA, OspC, peptidoglycan and p39 was performed by western blotting from BbOMV samples (II, Figs. 3D-G). Similarly to previous studies (Dorward *et al.* 1991, Shoberg and Thomas 1993, Whitmire and Garon 1993, Yang *et al.* 2011), we also identified OspA and OspC from BbOMVs with bands sized 28 and 20.7 kDa (II, Figs. 3D, E). The spirochete expresses OspA in the tick gut, but both the change in temperature and influx of blood during tick feeding alters the protein expression to favour OspC instead (Schwan *et al.* 1995). OspC is utilized during the transmission from the arthropod vector into a mammalian host. Studies have identified OspC as a requirement for successful establishment of *B. burgdorferi* infection (Grimm *et al.* 2004). Recently OspC was identified as an antiphagocytic mechanism utilized by *Borrelia*, consequently enhancing bacterial survival and immune evasion during early dissemination into the host (Carrasco *et al.* 2015). Additionally, as both OspA and OspC have been recognised to be immunogenic in arthritic patients, especially with increased IgG response to OspA during the late stages (months to years) of Lyme arthritis (Akin *et al.* 1999), it would reason to conclude that the presence of these immunogenic lipoproteins in BbOMVs could result in an inflammatory response, thus contributing to the pathology of LB.

Interestingly, the bands for OspC were scarcely visible in the *B. burgdorferi* lysate control lanes (II, Fig. 3C, lanes 1, 6). Studies have indicated that certain

proteins can be enriched in bacterial vesicles. For example, enterotoxigenic *E. coli* and *P. aeruginosa* release OMVs enriched with enterotoxin and aminopeptidase, respectively, which increased the association of the vesicle with the host endothelial cells (Kesty *et al.* 2004, Bauman and Kuehn 2009). The OspC results examined here suggested a similar instance for *B. burgdorferi*. Furthermore, since OspC has antiphagocytic properties (Carrasco *et al.* 2015), *Borrelia* might deploy BbOMVs enriched with OspC in order to establish a suitable environment for infection, thus avoiding phagocytosis by the host immune cells.

In addition, our analysis identified immunogenic proteins peptidoglycan and p39 (basic membrane protein A) in BbOMVs (II, Figs. 3F, G). Peptidoglycan labelling detected a 37 kDa protein in each BbOMV lane and two smaller bands (~25 – 26 kDa) in one of the samples (lane 4), while p39 was visualised in the expected 39 kDa size (II, Figs. 3F, G). As Lyme arthritis is a late manifestation of *Borrelia* infection (Cardenas-de la Garza *et al.* 2019), and both peptidoglycan and p39 are markers for Lyme arthritis (Pal *et al.* 2008, Jutras *et al.* 2019), it would suggest a pathogenic role for these two proteins in LB. As late markers for Lyme arthritis, the two proteins would require remaining in the host long-term. Thus, BbOMVs might provide a convenient mechanism for these immunogenic proteins to persist in the host during progression of LB.

Lastly, as a control for the western blots, we immunolabeled BbOMVs with anti-*B. burgdorferi* antibody, which has been raised against whole bacterial cell lysate, thus labelling unspecified *B. burgdorferi* proteins. Indeed, the lanes for *B. burgdorferi* lysates illustrated strong signals throughout the lanes (II, Fig. 3H, lanes 1, 6). BbOMV lanes exemplified smaller proteins approximately the same sizes as the abovementioned proteins OspA, OspC, and p39, further validating these labels (II, Fig. 3H, lanes 3-5). Moreover, two further bands were located in the BbOMV lanes suggesting the presence of additional unspecified proteins in the membrane vesicles (II, Fig. 3H).

Presently, additional validation for borrelial persistence in LB patients is required. Furthermore, the role for BbOMVs in the disease pathology should be extensively investigated. Especially because of the confirmation of known immunogenic antigens OspA, OspC, and p39, and the detection of peptidoglycan in BbOMVs, the potential for borrelial outer membrane vesicles to induce an array of effects in the human host is evident. One study has suggested that membrane lipid exchange between BbOMVs and host cells might participate in the induction of autoimmune-related consequences in patients (Crowley *et al.* 2013). In addition, since previous work has demonstrated bacterial OMVs to be able to take up extracellular DNA (Renelli *et al.* 2004), BbOMVs might function in a similar manner. Hence, *Borrelia* might utilize BbOMVs in varying tactics to aid the bacterium to initiate infection, as well as to sustain a prolonged immune response at a remote location from the initial tick bite site, and possibly even to participate in autoimmune-like consequences through the utilisation of self-antigens in the form of host lipids and / or host DNA. Therefore, BbOMVs should be further examined in other cell lines, as well as, in animal models, and from patient tissue samples to validate their role in borrelial persistence in LB disease manifestations.

5.4.3 BbOMVs did not induce death in human cells

Bacterial membrane vesicles can affect the host in various respects. For instance, *H. pylori* OMVs were observed to induce growth arrest, IL-8 production, and cytotoxicity in gastric epithelial cells (Ismail *et al.* 2003). Furthermore, *E. coli* was demonstrated to secrete Shiga toxins in its OMVs (Yokoyama *et al.* 2006). BbOMVs have been identified to contain known immunogens, and to be able to adhere to endothelial cells without causing cell death (Shoberg and Thomas 1993). Hence, we investigated the possible cytotoxic effect of BbOMVs in chondrosarcoma (SW1353) and dermal fibroblast (BJ) cells. The human cells were cocultured with *B. burgdorferi* spirochetes and RBs, used as controls for cellular reaction to the bacterium, as well as BbOMVs for 72-h, and double stained with a pan-caspase inhibitor peptide, which was conjugated to a fluorochrome and a ketone group (FAM-VAD-FMK) and a DNA stain (7-AAD). Untreated and 1 μM staurosporine treated cells functioned as controls for viability and death, respectively. The samples were analysed using a flow cytometer, with the double staining generating quadrant sections in a dot plot from which viable, early apoptotic, late apoptotic / necrotic, and dead cell populations could be identified.

As was already established in the first study (I, Fig. 3), *B. burgdorferi* did not induce cell death in SW1353 or BJ cells (Karvonen *et al.* 2021). Similarly, the results here exhibited 80 % viability in both SW1353 and BJ cells after 72-h of coculture with *B. burgdorferi* spirochetes, RBs, and BbOMVs, respectively (II, Fig. 4). Particularly in the viable SW1353 cells, a significant difference ($p \leq 0.05$) was observed between the staurosporine treated and the untreated cells, as well as the BbOMV cocultured sample (II, Fig. 4A). Even higher significant difference ($p \leq 0.01$) was detected between the staurosporine treated sample and *B. burgdorferi spirochetes* and RBs (II, Fig. 4A). Furthermore, both the untreated and *B. burgdorferi* cocultured samples exhibited less than 10 % of early apoptotic or late apoptotic / necrotic cells after the 72-h time point (II, Fig. 4A). Additionally, very few dead cells were located from each sample of the SW1353 cell experiment, thus further displaying the lack of cytotoxic effect of *B. burgdorferi* on these cells (II, Fig. 4A).

Correspondingly, less than 2 % and 1 % of the BJ cell samples were early apoptotic or dead, respectively, after coculture with *B. burgdorferi* spirochetes, RBs, or BbOMVs (II, Fig. 4B). Significantly more ($p \leq 0.01$) *B. burgdorferi* fed cells remained viable when compared to the staurosporine treated cells (II, Fig. 4B). Similarly, significant differences were also observed in the late apoptotic / necrotic BJ cell populations between the staurosporine treated and the untreaded and BbOMV cocultured samples ($p \leq 0.01$), as well as in the staurosporine sample and *B. burgdorferi* spirochetes and RBs ($p \leq 0.001$) (II, Fig. 4B). As the *B. burgdorferi* fed cells exhibited less than 15 % of late apoptosis / necrosis each, and the untreated cells close to 18 % (17.6 %), the non-lethal effect of *B. burgdorferi* on BJ cells was evident (II, Fig. 4B). As neither of the *B. burgdorferi* forms, spirochetes or RBs, nor BbOMVs induced cell death in either human cell line, it was concluded that *B. burgdorferi* was not cytotoxic to chondrosarcoma or der-

mal fibroblast cells *in vitro*. Consequently, as already mentioned in Section 5.4.2, BbOMVs should be further examined for their role in the pathogenesis of LB as possible antigen repositories, as well as tools for deceiving host immune system, since these vesicles contain immunogenic molecules but lack cytopathic effects on the host cell.

5.5 Eradication of *B. burgdorferi* with novel herbal compounds

Although in most cases antibiotics effectively kill *Borrelia*, especially if treatment is started early on in the infection, the lingering long-term sequelae in some patients (Stanek *et al.* 2012, Shor *et al.* 2019) urges researchers for the discovery of novel treatment possibilities. Here we investigated the eliminating potentials of *B. burgdorferi* persistent forms *in vitro* by two dietary supplements: Biocidin Liquid formula and Biocidin LSF Broad-Spectrum Liposomal formula (LSF) (Bio-Botanical Research Inc.). Both of the compounds consist of several different plant extracts and essential oils and are marketed as having a variety of health benefits ranging from supporting gut health to immunomodulation and detoxification. Minimum inhibitory concentration (MIC) or the lowest concentration of an antibacterial required to inhibit microbial growth, and minimum bacterial death (MBD) or the lowest concentration of an antibacterial that kills a microbe, were determined for both herbal compounds on *B. burgdorferi* spirochetes, RBs and BFLs as previously described (Dever *et al.* 1992) (III, Methods). Because the compounds were liquids, dilutions instead of concentrations were utilised.

The MICs for both Liquid and LSF formulas with *B. burgdorferi* spirochetes, RBs and BFLs during a 96-h time period indicated that the herbal compounds effectively inhibited the growth of each borrelial pleomorphic form. Specifically, the MIC for *B. burgdorferi* spirochetes was 1:10 and 1:25 dilutions of Liquid formula and LSF, respectively (III, Figs. 1A, B). For RBs both formulas inhibited growth at 1:50 dilution (III, Figs. 1C, D), whilst for BFLs the MICs for both compounds were determined to be 1:10 dilution (III, Fig. 1E).

The MBDs for both formulas were deduced from the 72-h MIC samples by placing the bacterial cells into fresh media for three weeks and analysing borrelial growth during the first and last weeks. The results for both herbal compounds illustrated that 1:5 dilution resulted in lack of growth for each pleomorphic form even after three weeks of culture (III, Table 1), demonstrating effectiveness against the persistent forms of *B. burgdorferi*. The observed MBD dilutions for Liquid formula at week one corroborated the MIC results for each *B. burgdorferi* form (III, Figs. 1A, C, E, Table 1). Similarly, the LSF formula followed the MIC results for RBs and BFLs at the first week time point (III, Figs. 1D, E, Table 1). However, the 1:25 dilution for spirochetes acquired during the MIC experiment, yielded growth in the MBD analysis at week one (III, Table 1), thus somewhat contradicting the MIC for the compound. However, as the last MIC time point was 96-h and the MBD analysis was performed after seven days of culture, the slight inconsistency might be due to the lengthier time point in the

MBD experiment. Nonetheless, as only the 1:5 dilution was effective at killing each *B. burgdorferi* form after three weeks, this dilution should be used in future examinations of these compounds.

Lastly, the rate of bacterial death was examined to assess the antimicrobial effectiveness of the herbal compounds against *B. burgdorferi*. By treating the MICs of Liquid formula and LSF compounds, respectively, to *B. burgdorferi* spirochetes for 10, 20, 30, 60, and 120-min and counting the bacteria post-treatment, the rate of cell death was acquired. Both herbal compounds effectively reduced the number of viable bacteria in each culture with Liquid formula being marginally more effective than LSF (III, Fig. 2).

Combined, these results indicated that both tested compounds were effective at eliminating each *B. burgdorferi* form: spirochetes, RBs, and BFLs. Subsequently, these dietary supplements might offer an additional treatment option for patients suffering from LB, since both were effective against the persistent forms of *B. burgdorferi*. Naturally, as these experiments were performed *in vitro*, the compounds should be further examined *in vivo*. However, these results offer a promising foundation for such endeavours.

6 CONCLUSIONS

The main conclusions of this thesis are:

I *B. burgdorferi* invaded two non-phagocytic human cell lines without affecting the cells' viability even after nine days, thus providing a possibility for borrelial persistence inside these cells. Furthermore, the bacterium remained viable after 72-h of coculture with human cells. Internalised *B. burgdorferi* lacked lysosomal colocalisation with the human cells and survived in multiple pleomorphic forms. These abilities could contribute to different strategies for *Borrelia* to evade host immune system and persist long-term (see Fig. 4 below).

II *B. burgdorferi* OMVs were characterised with respect to their size and four different antigenic proteins: OspA, OspC, p39 and peptidoglycan. In addition, BbOMVs were not cytotoxic to human chondrosarcoma or dermal fibroblast cells. Consequently, BbOMVs could be a beneficial method for *Borrelia* to avoid the host immune system by acting as decoy targets, as well as providing a repository for persisting antigens detected in some symptomatic post-treatment patients (see Fig. 4 below).

III Two novel herbal compounds proved successful in eliminating *B. burgdorferi* spirochetes, round bodies, and biofilm-like aggregates. Hence, plant-based antimicrobials could provide an alternative treatment option for persistent *Borrelia* infections.

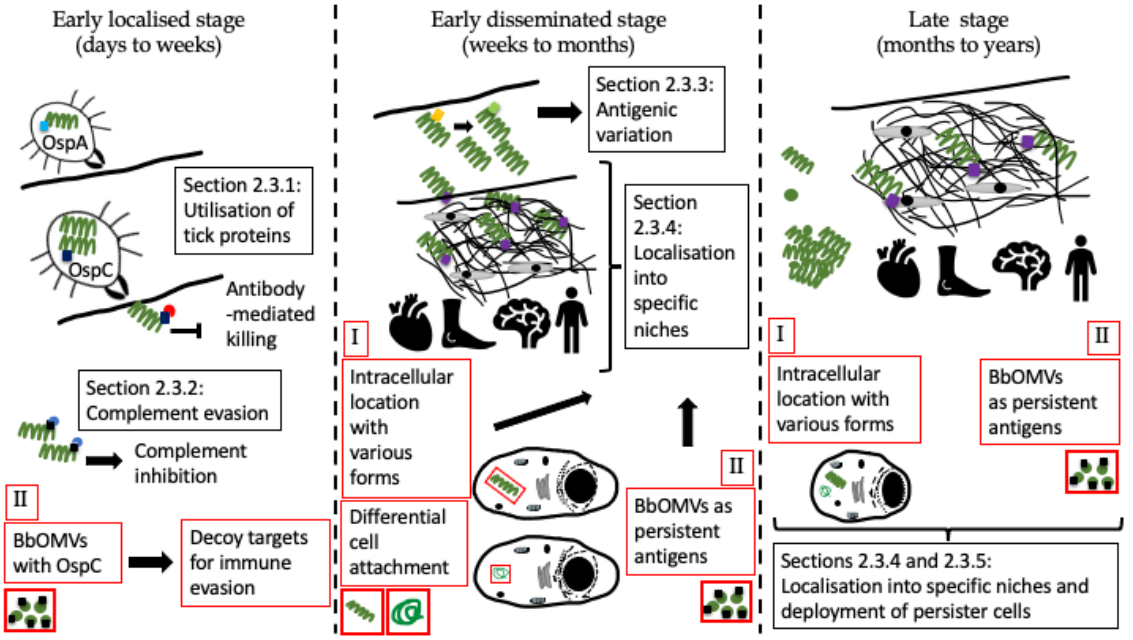

FIGURE 4 Graphical illustration of the mechanisms for immune evasion by *Borrelia* with findings made in this thesis (continuation from Figure 2). During the transmission of *B. burgdorferi* from the tick vector, borrelial outer membrane vesicles (BbOMVs) containing OspC surface protein might be deployed as decoy targets for immune cells, thus protecting the bacterium from elimination and providing time for replication and dissemination (Article II). Furthermore, BbOMVs would present as optimal repositories for persisting antigens during the progression of the infection, since several antigenic proteins (OspA, OspC, p39, peptidoglycan) and double stranded DNA were located in BbOMVs (Article II). While examining *B. burgdorferi* infection in chondrosarcoma and dermal fibroblast cells, *B. burgdorferi* was attached to the cells in different shapes depending on the cell type (Article I). Hence, the utilisation of varying shapes could provide a means for invading different cell types in differing means and sheltering surface antigens away from detection. Moreover, *B. burgdorferi* was localised inside the two human cell lines for nine days without affecting the viability of these cells (Article I). Different pleomorphic forms were observed, again in differing degrees, varying between the human cell lines (Article I). Consequently, *B. burgdorferi* might utilise the intracellular location and different pleomorphic forms to evade the immune system and persist in the host.

Acknowledgements

This work was carried out at the University of Jyväskylä, at the Department of Biological and Environmental Science and Nanoscience Center, Division of Biosciences, Section Cell and Molecular Biology during 2018 – 2022. This project was funded by the Department of Biological and Environmental Science and the Schwartz foundation.

I would like to express my gratitude towards the people who have participated in my PhD journey in any fashion, big or small. Firstly, thank you Adjunct Professor Leona Gilbert, my first kickass supervisor (and ass kicker). You first took me under your wing as an intern in 2014 and from then on have guided me and encouraged me to become an independent and resourceful researcher (and hopefully a future ass kicker). There were some rough seas at times, but your confidence in me and my abilities never wavered, for which I am very grateful.

Thank you to Professor Varpu Marjomäki, you are always so joyful, helpful, and welcoming. You graciously took me under your wing when I needed it the most and steered me through the finish line on time. I cannot thank you enough for that. I cannot wait for the new challenges and opportunities that now await me as part of your team!

I would also like to offer my sincere gratitude to Dr. Jonna Nykky, my second supervisor. You have offered me a helping hand in the lab, as well as, provided much needed science and non-science -related discussions about anything and everything throughout these years. I don't think I would have managed without you, so thank you for everything.

Next, I want to thank my thesis reviewers, Dr. Natasha Rudenko and Dr. Anna-Liisa Välimaa for their thorough and helpful feedback. Thank you to Dr. Sara Moutailler for generously agreeing to act as my opponent. In addition, I'd like to thank my follow-up group members Professor Vett Lloyd and CTN Robert Miller. Your supportive and helpful comments and questions kept me pushing forwards and helped me find new solutions to problems.

Thank you to Hanna and Jasmin, my awesome kickass MSc students. You both worked extremely hard and competently in the lab and made my life easier by requiring minimal supervision. I am so glad you two chose my projects to work in. Thank you both! I would also like to thank all the past members of Lee's team who made the team what it was: a fun, awesome and a supportive place to grow as a scientist, as well as, a person, thanks and CUBYE!

I am also very grateful for all my colleagues in and outside Jyväskylä. Lina, my Puscia! Thank you for the amount of love and support you have provided me with during this process, it is unaccountable, especially with my maths skills! Mira, you made this process look so easy, how did you do that? Thank you for all the discussions, advice, and encouragement you've given me through the years. Visa, thank you for all the times you helped me with the confocal microscopes or with ImageJ, and thanks for all the helpful tips in writing the thesis. Thanks to ("our") Heini, Heidi, Anni, Annu, Heini & Tommi, Sailee,

Dhanik, Chandan, Salla and all the countless others with whom I've shared interesting and insightful discussions about science, the hardships of a PhD student, and anything and everything under the sun throughout these years.

A special thank you to our lab technicians. Laura, you have helped me both in and outside the lab, and offered continuous support, as well as puppy therapy whenever needed! Thank you! Alli, you are always so friendly and eager to help. I don't know how you do it with that busy schedule of yours, but I am deeply grateful. Petri, thank you for your guidance (and patience) in teaching me to how to use both TEM and HIM.

The process of doing a PhD can be very tiring without the necessary support system. Thankfully, I have had the best friends and family just for that! I want to thank Tuikku for always being such a strong support pillar for me starting from 2005, when dancing on tables was still an acceptable thing for us to do! We've had countless, but much needed, game & sparkling nights with and without Mario, and hopefully we'll continue with this joyous tradition for the foreseeable future! I'm so happy that you are my friend! Thank you! Anna and Eevis, you both have respectively inspired me with your positive and optimistic views on life. Our discussions are always a delight, and I'm hoping we'll continue to have more wonderful exchanges and adventures in the future. Thank you both for being the awesome people that you are!

To all my friends near and far, thank you to each and every one for being awesome, supportive, fun, and enough distracting to keep me sane. I am so lucky to know and be able to call you all my friends!

Last, but definitely not least, thank you to my super awesome and supportive family! My superwoman of a sister, you listen to my constant jibberjabber even when you don't understand most of it, you give advice, help around, kick my ass when I need it, offer a drink when I need it and make me laugh and ease my stress, all the while having your own busy life. Thank you, for being a steady rock to rely on during hardships, and a warm soft blanket to wrap around when needed. Thank you to my extended family, Ville, Juuso, Leevi, Alisa and Lotta, for always welcoming me into your home and loving arms. Alisalle ja Lotalle, kiitos kaikista lämpimistä haleista ja märistä pusuista!

Thank you, my kickass little brother, whose endless sense of humour offers such a relief in the dark (and not so dark) days! Your tech support has been, and will continue to be, a valuable asset. Continue to be your awesome self! Oh, and thanks to you both, Kurpitsa & Iipeli, for the times I could crash on your couches while travelling! I know I should have stayed a bit longer at times and not just use you as a hotel… Kiitos ja anteeksi!

Lastly, Dad, thank you for always providing a safe and encouraging environment at home, together with mom. Both of you always quizzed me before exams and pushed and encouraged me to reach for my goals and aim higher. I would not have made it very far without your love and support. Thank you! I think one reason I've come this far is because you always told me to "stay in school", hence, I decided to go all the way!

YHTEENVETO (RÉSUMÉ IN FINNISH)

Persistentti *Borrelia burgdorferi* -infektio ja sen poistaminen *in vitro*

Borrelioosi (Lymen tauti) on mustajalkaisten *Ixodes* -lajiin kuuluvien puutiaisten välittämä infektiotauti, jota ihmisissä aiheuttavat *Borrelia burgdorferi* sensu lato -ryhmään kuuluvat spirokeettabakteerit. Tällä hetkellä borrelioosia aiheuttavat erityisesti kolme eri *Borrelia* -lajia: *B. burgdorferi* sensu stricto (jatkossa *B. burgdorferi*), *B. garinii* ja *B. afzelii*. Borrelioosi on pohjoisen pallonpuoliskon yleisin puutiaisvälitteinen tauti, ja sitä esiintyykin erityisesti Pohjois-Amerikassa sekä Euroopassa, mutta myös muualla maapalloa. Tyypillisimpinä borrelioosin alkuvaiheen oireina ovat puutiaisen puremakohdassa tai sen välittömässä läheisyydessä esiintyvä vaeltava punertava ihottuma (erythema migrans) sekä väsymys, päänsärky, kuume ja muut flunssan kaltaiset oireet. Jos *B. burgdorferi* -infektio pääsee leviämään, niin sanotun leviämisvaiheen oireina voivat muun muassa olla muualla vartalossa esiintyvä ihottuma, nivelkipu, hermostolliset oireet (neuroborrelioosi) sekä harvoin sydämen oireilu esimerkiksi sydänlihastulehduksena. Infektion myöhäisessä vaiheessa edellä mainitut oireet muuttuvat pysyvämmiksi ja infektiota voi olla hankala hoitaa, sillä *B. burgdorferi* on päässyt leviämään eri kudoksiin, joissa se voi piiloutua immuunijärjestelmältä sekä antibioottien vaikutukselta. Aikainen borrelioosin diagnosointi onkin tärkeää taudin hoidossa, sillä antibiootit useimmiten tappavat bakteerin tehokkaasti. Kuitenkin toisinaan hoito voi epäonnistua tai se on aloitettu liian myöhään, ja potilas voi oireilla vielä vuosikausia diagnoosin ja hoidon jälkeen. Tämän niin sanotun pitkäkestoisen borrelioosin (*engl. chronic Lyme*) synnyn syitä ei vielä kunnolla tiedetä, mutta bakteerin jäänteitä on havaittu potilaiden kudosnäytteistä. Elävää bakteeria ei ole kuitenkaan pystytty todistettavasti löytämään potilasnäytteistä, minkä vuoksi tieteellisessä yhteisössä onkin käynnissä kiista siitä, onko taudin pitkäkestoisuuden syynä *B. burgdorferi* -bakteerin aiheuttama infektio vai jokin muu tekijä.

Tutkimukset ovat osoittaneet, että *B. burgdorferi* sensu lato -ryhmän bakteerit ovat pleomorfisia eli ne pystyvät muuttamaan muotoaan epäsuotuisissa ympäristöolosuhteissa alkuperäisestä spirokeetta- eli korkkiruuvimuodosta esimerkiksi pyöreiksi pallomaisiksi muodoiksi (*engl. round body form*) tai yhdistyä useasta erillisestä bakteerista koostuvaksi rykelmäksi, jossa on myös solunulkoista materiaalia, eli biofilmiksi (*engl. biofilm*). Lisäksi bakteerit kykenevät lähettämään ympäristöönsä solunulkoisia vesikkeleitä laajentamalla ulommaista solukalvoaan. Nämä erilaiset muodot ja ulommaisen solukalvon vesikkelit todennäköisesti edesauttavat bakteeria sekä selviytymään erilaisissa ympäristöissä että mahdollisesti parantavat bakteerin infektiokykyä. Pallomaisten muotojen sekä biofilmien tiedetään nimittäin kestävän antibioottien aiheuttamaa solukuolemaa paremmin kuin spirokeettien. Tämän lisäksi joidenkin antibioottien tiedetään jopa aiheuttavan näitä muotoja. Tästä syystä näitä kahta *B. burgdorferi* -bakteerin muotoa, pallomuotoa ja biofilmiä, kutsutaan toisinaan persistenteiksi (*engl. persistent*) eli sinnikkäiksi muodoiksi, ja ne saattavatkin olla osasyyllisiä

pitkäkestoisen borrelioosin syntyyn. *B. burgdorferi* -bakteerin ulommaisen solukalvon vesikkelien roolia bakteerin patogeenisyydessä ei vielä tunneta. Kuitenkin niiden tiedetään sisältävän esimerkiksi DNA:ta sekä antigeenisiä proteiineja eli molekyylejä, jotka voivat aiheuttaa immuunireaktion isännässä.

Tässä tutkimuksessa tarkasteltiin pitkäkestoista ja persistenttiä *B. burgdorferi* -infektiota kahdessa eri ihmissolulinjassa solumaljalla sekä luonnehdittiin *B. burgdorferi* -bakteerin erittämiä ulommaisen solukalvon vesikkeleitä niiden koon ja sisältämien molekyylien osalta. Tämän lisäksi tutkimuksessa analysoitiin kahden kasviperäisen yhdisteen kykyä hävittää *B. burgdorferi* ja sen eri muodot. Tutkimustyön tavoitteena oli tunnistaa tapahtumasarjat, jotka voivat johtaa *B. burgdorferi* -bakteerin aiheuttamaan pitkäkestoiseen ja persistenttiin infektioon ihmissoluissa, sekä löytää uusia keinoja tämänkaltaisen infektion poistamiseen. Tutkimus koostuu kolmesta osatyöstä, jotka on eritelty seuraavaksi.

Ensimmäisessä osatyössä *B. burgdorferi* -bakteerin aiheuttamaa infektiota analysoitiin solun pintaan tarttumisesta aina solun sisään tunkeutumiseen ja sisällä säilymiseen. Yhteensä tarkasteltavia eri aikapisteitä oli seitsemän ja ne vaihtelivat 30 minuutista yhdeksään päivään asti. Kahta eri ihmissolulinjaa käyttämällä huomattiin eroja *B. burgdorferi* -infektioissa solulinjojen välillä. Ihosoluihin tarttunut *B. burgdorferi* oli useimmiten kippuralla, kun taas rustosolujen pinnalla bakteeri nähtiin pelkästään spirokeettana. *B. burgdorferi* havaittiin soluihin tunkeutuneena kaikkina tarkasteltuina ajankohtina kuitenkaan vahingoittamatta isäntäsolua. Solumaljoilta myös huomattiin, että ihmissolut eivät kokonaan poistaneet bakteeri-infektiota, vaikka rustosoluissa *B. burgdorferi* -bakteeria havaittiin vähemmän kahden päivän jälkeen ja näissä soluissa oli myös hieman enemmän lysosomaalista bakteerin hävittämistä. Tämän lisäksi *B. burgdorferi* -bakteerin eri muotoja löydettiin ihmissolujen sisältä vaihtelevasti niin, että ihosoluissa enemmistö oli spirokeettoja koko yhdeksän päivän ajan, kun taas rustosoluissa valtaosa oli pallomaisina neljänteen päivään saakka, ja tästä eteenpäin pääosa bakteereista oli vahingoittuneita. Näin ollen voitiin siis todeta, että *B. burgdorferi* infektoi eri ihmissoluja eri tavoin, mikä mahdollisesti edesauttaa bakteeria sopeutumaan erilaisiin ympäristöihin ja selviytymään isäntäsolussa pitkäkestoisesti. Bakteerin kyky tunkeutua soluihin vahingoittamatta niitä voi myös olla yksi keino piiloutua immuunijärjestelmältä.

Toisessa osatyössä *B. burgdorferi* -bakteerin luontaisesti tuottamien ulommaisen solukalvon vesikkelien halkaisija analysoitiin ensimmäistä kertaa. Vesikkelit olivat kohtalaisen pieniä noin 11 – 108 nm halkaisijaltaan. Tämän lisäksi erilaisia värjäysmenetelmiä käyttäen pystyttiin vesikkeleistä tunnistamaan kaksijuosteista DNA:ta sekä neljää erilaista antigeenistä proteiinia. Kun vesikkeleitä syötettiin iho- ja rustosoluille, huomattiin solujen säilyvän hengissä. Niinpä *B. burgdorferi* -bakteerin ulommaisen solukalvon vesikkelien arvellaan avustavan bakteeria infektion aloittamisessa immuunivastetta harhauttamalla, jolloin itse bakteeri säilyy vahingoittumattomana. Vesikkelit voivat myös toimia pitkäkestoisina antigeenien varastoina infektoidussa isännässä, leviten verenkierron mukana kauas alkuperäisestä bakteerista.

Kolmannessa osatyössä kahden kasviperäisen yhdisteen antimikrobista tehokkuutta eli niiden kykyä tuhota *B. burgdorferi* testattiin. Tutkimuksessa oltiin erityisen kiinnostuneita yhdisteiden kyvystä eliminoida *B. burgdorferi* -bakteerin persistentit muodot. Sekä spirokeetta-, pallo- ja biofilmi muotoja altistettiin yhdisteiden eri laimennoksille neljän päivän ajan. Tulokset osoittivat, että bakteerin eri muotojen tuhoamiseen vaadittiin erilaiset pitoisuudet, mutta molemmat yhdisteet kuitenkin tehokkaasti hävittivät kaikki kolme *B. burgdorferi* -bakteerin muotoa koeputkessa. Erilaisista kasviperäisistä yhdisteistä voikin jatkossa löytyä apukeino pitkäkestoisen borrelioosin hoitoon.

Tämä tutkimustyö osoitti, että *B. burgdorferi* kykenee tunkeutumaan erilaisten ihmissolujen sisään ja säilymään niissä ainakin yhdeksän päivää. Soluun tunkeutuminen voi olla yksi keino paeta immuunivastetta ja eri muotoja hyväksikäyttäen bakteeri pystyy selviytymään ja aiheuttamaan pitkäkestoisen infektion isännässä. Bakteerin erittämät ulommaisen solukalvon vesikkelit saattavat toimia eräänlaisina houkuttimina immuunivasteelle, jolloin itse bakteeri jää huomioimatta ja pystyy näin ollen pakenemaan immuunijärjestelmältä. Tämän lisäksi *B. burgdorferi* -bakteerin ulommaisen solukalvon vesikkelien sisältämät antigeeniset molekyylit saattavat edesauttaa pitkäkestoisen borrelioosin syntyä toimien tulehdustilan aiheuttajina eri puolilla vartaloa ilman bakteerin läsnäoloa. Kasviperäisistä yhdisteistä saattaa tulevaisuudessa olla apua pitkäkestoisesta borrelioosista kärsiville potilaille, varsinkin jos niillä pystytään tuhoamaan *B. burgdorferi* -bakteerin persistentit muodot.

REFERENCES

Akin E., McHugh G.L., Flavell R.A., Fikrig E. & Steere A.C. 1999. The immunoglobulin (IgG) antibody response to OspA and OspB correlates with severe and prolonged Lyme arthritis and the IgG response to P35 correlates with mild and brief arthritis. *Infect. Immun.* 67: 173–181.

Alban P.S., Johnson P.W. & Nelson D.R. 2000. Serum-starvation-induced changes in protein synthesis and morphology of Borrelia burgdorferi. *Microbiology* 146: 119–127.

Anon. 2018. *European parliament resolution on Lyme disease (borreliosis) 2018/2774 (RSP) -web page.* https://www.europarl.europa.eu/doceo/document/B-8-2018-0514_EN.html (Last visited 6/1/2022).

Avila-Calderón E.D., Araiza-Villanueva M.G., Cancino-Diaz J.C., López-Villegas E.O., Sriranganathan N., Boyle S.M. & Contreras-Rodríguez A. 2015. Roles of bacterial membrane vesicles. *Arch. Microbiol.* 197: 1–10.

Baranton G., Postic D., Girons I. Saint, Boerlin P., Piffaretti J.C., Assous M. & Grimont P.A.D. 1992. Delineation of Borrelia burgdorferi sensu stricto, Borrelia garinii sp. nov., and group VS461 associated with Lyme borreliosis. *Int. J. Syst. Bacteriol.* 42: 378–383.

Barbour A.G. 1984. Isolation and cultivation of Lyme disease spirochetes. *Yale J. Biol. Med.* 57: 521–525.

Barbour A.G., Todd W.J. & Stoenner H.G. 1982. Action of penicillin on Borrelia hermsii. *Antimicrob. Agents Chemother.* 21: 823–829.

Bauman S.J. & Kuehn M.J. 2009. Pseudomonas aeruginosa vesicles associate with and are internalized by human lung epithelial cells. *BMC Microbiol.* 9.

Beermann C., Groscurth P., Filgueira L. & Wunderli-Allenspach H. 2000. Lipoproteins from Borrelia burgdorferi applied in liposomes and presented by dendritic cells induce CD8+ T-lymphocytes in vitro. *Cell. Immunol.* 201: 124–131.

Bernard Q., Thakur M., Smith A.A., Kitsou C., Yang X. & Pal U. 2019. Borrelia burgdorferi protein interactions critical for microbial persistence in mammals. *Cell. Microbiol.* 21: e12885.

Berndtson K. 2013. Review of evidence for immune evasion and persistent infection in Lyme disease. *Int. J. Gen. Med.* 6: 291–306.

Bigger J.W. 1944. Treatment of Staphylococcal infections with penicillin by intermittent sterilisation. *Lancet* 244: 497–500.

Bobe J.R., Jutras B.L., Horn E.J., Embers M.E., Bailey A., Moritz R.L., Zhang Y., Soloski M.J., Ostfeld R.S., Marconi R.T., Aucott J., Ma'ayan A., Keesing F., Lewis K., Mamoun C. Ben, Rebman A.W., McClune M.E., Breitschwerdt E.B., Reddy P.J., Maggi R., Yang F., Nemser B., Ozcan A., Garner O., Carlo D. Di, Ballard Z., Joung H.-A., Garcia-Romeu A., Griffiths R.R., Baumgarth N. & Fallon B.A. 2021. Recent progress in Lyme disease and remaining challenges. *Front. Med.* 8: 666554.

Bockenstedt L.K., Gonzalez D.G., Haberman A.M. & Belperron A.A. 2012. Spirochete antigens persist near cartilage after murine Lyme borreliosis therapy. *J. Clin. Invest.* 122: 2652–2660.

Bockenstedt L.K., Wooten R.M. & Baumgarth N. 2020. Immune response to Borrelia: Lessons from Lyme disease spirochetes. *Curr. Issues Mol. Biol.* 42: 145–190.

Borchers A.T., Keen C.L., Huntley A.C. & Gershwin M.E. 2015. Lyme disease: A rigorous review of diagnostic criteria and treatment. *J. Autoimmun.* 57: 82–115.

Brandtzaeg P., Bryn K., Kierulf P., Øvstebø R., Namork E., Aase B. & Jantzen E. 1992. Meningococcal endotoxin in lethal septic shock plasma studied by gas chromatography, mass-spectrometry, ultracentrifugation, and electron microscopy. *J. Clin. Invest.* 89: 816–823.

Brorson Ø. & Brorson S.H. 1998. A rapid method for generating cystic forms of Borrelia burgdorferi, and their reversal to mobile spirochetes. *APMIS* 106: 1131–1141.

Brorson & Brorson S.H. 2007. Grapefruit seed extract is a powerful in vitro agent against motile and cystic forms of Borrelia burgdorferi sensu lato. *Infection* 35: 206–208.

Burgdorfer W., Barbour A.G., Hayes S.F., Benach J.L., Grunwaldt E. & Davis J.P. 1982. Lyme disease - A tick-borne spirochetosis? *Science (80-.).* 216: 1317–1319.

Caine J.A., Lin Y.P., Kessler J.R., Sato H., Leong J.M. & Coburn J. 2017. Borrelia burgdorferi outer surface protein C (OspC) binds complement component C4b and confers bloodstream survival. *Cell. Microbiol.* 19: e12786.

Canica M.M., Nato F., Merle L. du, Mazie J.C., Baranton G. & Postic D. 1993. Monoclonal antibodies for identification of Borrelia afzelii sp. nov. Associated with late cutaneous manifestations of Lyme borreliosis. *Scand. J. Infect. Dis.* 25: 441–448.

Cardenas-de la Garza J.A., la Cruz-Valadez E. De, Ocampo-Candiani J. & Welsh O. 2019. Clinical spectrum of Lyme disease. *Eur. J. Clin. Microbiol. Infect. Dis.* 38: 201–208.

Carlson D., Hernandez J., Bloom B.J., Coburn J., Aversa J.M. & Steere A.C. 1999. Lack of Borrelia burgdorferi DNA in synovial samples from patients with antibiotic treatment-resistant Lyme arthritis. *Arthritis Rheum.* 42: 2705–2709.

Carrasco S.E., Troxell B., Yang Y., Brandt S.L., Li H., Sandusky G.E., Condon K.W., Serezani C.H. & Yang X.F. 2015. Outer surface protein OspC is an antiphagocytic factor that protects Borrelia burgdorferi from phagocytosis by macrophages. *Infect. Immun.* 83: 4848–4860.

Casjens S., Palmer N., Vugt R. Van, Huang W.M., Stevenson B., Rosa P., Lathigra R., Sutton G., Peterson J., Dodson R.J., Haft D., Hickey E., Gwinn M., White O. & Fraser C.M. 2000. A bacterial genome in flux: The twelve linear and nine circular extrachromosomal DNAs in an infectious isolate of the Lyme disease spirochete Borrelia burgdorferi. *Mol. Microbiol.* 35: 490–516.

Chaconas G., Castellanos M. & Verhey T.B. 2020. Changing of the guard: How

the Lyme disease spirochete subverts the host immune response. *J. Biol. Chem.* 295: 301–313.

Chen L., Li Q., Wang J., Jin S., Zheng H., Lin J., He F., Zhang H., Ma S., Mei J. & Yu J. 2017. MiR-29b-3p promotes chondrocyte apoptosis and facilitates the occurrence and development of osteoarthritis by targeting PGRN. *J. Cell. Mol. Med.* 21: 3347–3359.

Chikezie P.C., Ibegbulem C.O. & Mbagwu F.N. 2015. Bioactive principles from medicinal plants. *Res. J. Phytochem.* 9: 88–115.

Comstock L.E. & Thomas D.D. 1989. Penetration of endothelial cell monolayers by Borrelia burgdorferi. *Infect. Immun.* 57: 1626–1628.

Comstock L.E. & Thomas D.D. 1991. Characterization of Borrelia burgdorferi invasion of cultured endothelial cells. *Microb. Pathog.* 10: 137–148.

Crowley J.T., Toledo A.M., LaRocca T.J., Coleman J.L., London E. & Benach J.L. 2013. Lipid exchange between Borrelia burgdorferi and host cells. *PLoS Pathog.* 9: e1003109.

Cruz A.R., Moore M.W., Vake C.J. La, Eggers C.H., Salazar J.C. & Radolf J.D. 2008. Phagocytosis of Borrelia burgdorferi, the Lyme disease spirochete, potentiates innate immune activation and induces apoptosis in human monocytes. *Infect. Immun.* 76: 56–70.

Dam A.P. Van, Kuiper H., Vos K., Widjojokusumo A., Jongh B.M. De, Spanjaard L., Ramselaar A.C.P., Kramer M.D., Dankert J. & Kuiper H. 1993. Different genospecies of borrelia burgdorferi are associated with distinct clinical manifestations of lyme borreliosis. *Clin. Infect. Dis.* 17: 708–717.

Dever L.L., Jorgensen J.H. & Barbour A.G. 1992. In vitro antimicrobial susceptibility testing of Borrelia burgdorferi: A microdilution MIC method and time-kill studies. *J. Clin. Microbiol.* 30: 2692–2697.

Dhama K., Tiwari R., Chakraborty S., Saminathan M., Kumar A., Karthik K., Wani M.Y., Amarpal, Singh S.V. & Rahal A. 2014. Evidence based antibacterial potentials of medicinal plants and herbs countering bacterial pathogens especially in the era of emerging drug resistance: An integrated update. *Int. J. Pharmacol.* 10: 1–43.

Dorward D.W. & Garon C.F. 1990. DNA is packaged within membrane-derived vesicles of gram-negative but not gram-positive bacteria. *Appl. Environ. Microbiol.* 56: 1960–1962.

Dorward D.W., Garon C.F. & Judd R.C. 1989. Export and intercellular transfer of DNA via membrane blebs of Neisseria gonorrhoeae. *J. Bacteriol.* 171: 2499–2505.

Dorward D.W., Schwan T.G. & Garon C.F. 1991. Immune capture and detection of Borrelia burgdorferi antigens in urine, blood, or tissues from infected ticks, mice, dogs, and humans. *J. Clin. Microbiol.* 29: 1162–1170.

Dulipati V., Meri S. & Panelius J. 2020. Complement evasion strategies of Borrelia burgdorferi sensu lato. *FEBS Lett.* 594: 2645–2656.

Ellis T.N. & Kuehn M.J. 2010. Virulence and immunomodulatory roles of bacterial outer membrane vesicles. *Microbiol. Mol. Biol. Rev.* 74: 81–94.

Embers M.E., Barthold S.W., Borda J.T., Bowers L., Doyle L., Hodzic E., Jacobs M.B., Hasenkampf N.R., Martin D.S., Narasimhan S., Phillippi-Falkenstein

K.M., Purcell J.E., Ratterree M.S. & Philipp M.T. 2012. Persistence of Borrelia burgdorferi in rhesus macaques following antibiotic treatment of disseminated infection. *PLoS One* 7: e29914.

Embers M.E., Ramamoorthy R. & Philipp M.T. 2004. Survival strategies of Borrelia burgdorferi, the etiologic agent of Lyme disease. *Microbes Infect.* 6: 312–318.

Feng J., Shi W., Miklossy J., Tauxe G.M., McMeniman C.J. & Zhang Y. 2018. Identification of essential oils with strong activity against stationary phase Borrelia burgdorferi. *Antibiotics* 7: 89.

Feng J., Zhang S., Shi W. & Zhang Y. 2016. Ceftriaxone pulse dosing fails to eradicate biofilm-like microcolony B. burgdorferi persisters which are sterilized by daptomycin/ doxycycline/cefuroxime without pulse dosing. *Front. Microbiol.* 7: 1744.

Feng J., Zhang S., Shi W., Zubcevik N., Miklossy J. & Zhang Y. 2017. Selective essential oils from spice or culinary herbs have high activity against stationary phase and biofilm Borrelia burgdorferi. *Front. Med.* 4: 169.

Filgueira L., Nestlé F.O., Rittig M., Joller H.I. & Groscurth P. 1996. Human dendritic cells phagocytose and process Borrelia burgdorferi. *J. Immunol.* 157: 2998–3005.

Forsberg C.W., Beveridge T.J. & Hellstrom A. 1981. Cellulase and xylanase release from Bacteroides succinogenes and its importance in the rumen environment. *Appl. Environ. Microbiol.* 42: 886–896.

Fraser C.M., Casjens S., Huang W.M., Sutton G.G., Clayton R., Lathigra R., White O., Ketchum K.A., Dodson R., Hickey E.K., Gwinn M., Dougherty B., Tomb J.F., Fleischmann R.D., Richardson D., Peterson J., Kerlavage A.R., Quackenbush J., Salzberg S., Hanson M., Vugt R. Van, Palmer N., Adams M.D., Gocayne J., Weidman J., Utterback T., Watthey L., McDonald L., Artiach P., Bowman C., Garland S., Fujii C., Cotton M.D., Horst K., Roberts K., Hatch B., Smith H.O. & Venter J.C. 1997. Genomic sequence of a Lyme disease spirochaete, Borrelia burgdorferi. *Nature* 390: 580–586.

Gankema H., Wensink J., Guinee P.A.M., Jansen W.H. & Witholt B. 1980. Some characteristics of the outer membrane material released by growing enterotoxigenic Escherichia coli. *Infect. Immun.* 29: 704–713.

Garon C.F., Dorward D.W. & Corwin M.D. 1989. Structural features of Borrelia burgdorferi - The Lyme disease spirochete: Silver staining for nucleic acids. *Scanning Microsc.* 3: 109–115.

Georgilis K., Peacocke M. & Klempner M.S. 1992. Fibroblasts protect the Lyme disease spirochete, Borrelia burgdorferi, from ceftriaxone in vitro. *J. Infect. Dis.* 166: 440–444.

Girschick H.J., Huppertz H.I., Russman H., Krenn V. & Karch H. 1996. Intracellular persistence of Borrelia burgdorferi in human synovial cells. *Rheumatol. Int.* 16: 125–132.

Goc A., Niedzwiecki A. & Rath M. 2015. In vitro evaluation of antibacterial activity of phytochemicals and micronutrients against Borrelia burgdorferi and Borrelia garinii. *J. Appl. Microbiol.* 119: 1561–1572.

Goc A., Niedzwiecki A. & Rath M. 2016. Cooperation of doxycycline with

phytochemicals and micronutrients against active and persistent forms of Borrelia sp. *Int. J. Biol. Sci.* 12: 1093–1103.

Goc A., Niedzwiecki A. & Rath M. 2017. Reciprocal cooperation of phytochemicals and micronutrients against typical and atypical forms of Borrelia sp. *J. Appl. Microbiol.* 123: 637–650.

Grimm D., Tilly K., Byram R., Stewart P.E., Krum J.G., Bueschel D.M., Schwan T.G., Policastro P.F., Elias A.F. & Rosa P.A. 2004. Outer-surface protein C of the Lyme disease spirochete: A protein induced in ticks for infection of mammals. *Proc. Natl. Acad. Sci. U. S. A.* 101: 3142–3147.

Gruntar I., Malovrh T., Murgia R. & Cinco M. 2001. Conversion of Borrelia garinii cystic forms to motile spirochetes in vivo. *APMIS* 109: 383–388.

Hechemy K.E., Samsonoff W.A., Harris H.L. & McKee M. 1992. Adherence and entry of Borrelia burgdorferi in Vero cells. *J. Med. Microbiol.* 36: 229–238.

Hellman J., Loiselle P.M., Zanzot E.M., Allaire J.E., Tehan M.M., Boyle L.A., Kurnick J.T. & Warren H.S. 2000. Release of gram-negative outer membrane proteins into human serum and septic rat blood and their interactions with immunoglobulin in antiserum to Escherichia coli J5. *J. Infect. Dis.* 181: 1034–1043.

Hodzic E., Imai D., Feng S. & Barthold S.W. 2014. Resurgence of persisting non-cultivable Borrelia burgdorferi following antibiotic treatment in mice. *PLoS One* 9: e86907.

Hoffmann A.K., Naj X. & Linder S. 2014. Daam1 is a regulator of filopodia formation and phagocytic uptake of Borrelia burgdorferi by primary human macrophages. *FASEB J.* 28: 3075–3089.

Hulïnská D., Votýpka J. & Valešová M. 1999. Persistence of Borrelia garinii and Borrelia afzelii in patients with Lyme arthritis. *Zentralblatt fur Bakteriol.* 289: 301–318.

Huttunen M., Waris M., Kajander R., Hyypia T. & Marjomaki V. 2014. Coxsackievirus A9 infects cells via nonacidic multivesicular bodies. *J. Virol.* 88: 5138–5151.

Hynes S.O., Keenan J.I., Ferris J.A., Annuk H. & Moran A.P. 2005. Lewis epitopes on outer membrane vesicles of relevance to Helicobacter pylori pathogenesis. *Helicobacter* 10: 146–156.

Isaacs R.D. 1994. Borrelia burgdorferi bind to epithelial cell proteoglycans. *J. Clin. Invest.* 93: 809–819.

Ismail S., Hampton M.B. & Keenan J.I. 2003. Helicobacter pylori outer membrane vesicles modulate proliferation and interleukin-8 production by gastric epithelial cells. *Infect. Immun.* 71: 5670–5675.

Jungnick S., Margos G., Rieger M., Dzaferovic E., Bent S.J., Overzier E., Silaghi C., Walder G., Wex F., Koloczek J., Sing A. & Fingerle V. 2015. Borrelia burgdorferi sensu stricto and Borrelia afzelii: Population structure and differential pathogenicity. *Int. J. Med. Microbiol.* 305: 673–681.

Jutras B.L., Lochhead R.B., Kloos Z.A., Biboy J., Strle K., Booth C.J., Govers S.K., Gray J., Schumann P., Vollmer W., Bockenstedt L.K., Steere A.C. & Jacobs-Wagner C. 2019. Borrelia burgdorferi peptidoglycan is a persistent antigen in patients with Lyme arthritis. *Proc. Natl. Acad. Sci. U. S. A.* 116: 13498–13507.

Kaparakis-Liaskos M. & Ferrero R.L. 2015. Immune modulation by bacterial outer membrane vesicles. *Nat. Rev. Immunol.* 15: 375–387.

Karvonen K., Nykky J., Marjomäki V. & Gilbert L. 2021. Distinctive evasion mechanisms to allow persistence of Borrelia burgdorferi in different human cell lines. *Front. Microbiol.* 12: 711291.

Kersten A., Poitschek C., Rauch S. & Aberer E. 1995. Effects of penicillin, ceftriaxone, and doxycycline on morphology of Borrelia burgdorferi. *Antimicrob. Agents Chemother.* 39: 1127–1133.

Kesty N.C., Mason K.M., Reedy M., Miller S.E. & Kuehn M.J. 2004. Enterotoxigenic Escherichia coli vesicles target toxin delivery into mammalian cells. *EMBO J.* 23: 4538–4549.

Khan R., Islam B., Akram M., Shakil S., Ahmad A., Ali S.M., Siddiqui M. & Khan A.U. 2009. Antimicrobial activity of five herbal extracts against multi drug resistant (MDR) strains of bacteria and fungus of clinical origin. *Molecules* 14: 586–597.

Kim T.K., Tirloni L., Bencosme-Cuevas E., Kim T.H., Diedrich J.K., Yates J.R. & Mulenga A. 2021. Borrelia burgdorferi infection modifies protein content in saliva of Ixodes scapularis nymphs. *BMC Genomics* 22: 152.

Klempner M.S., Noring R. & Rogers R.A. 1993. Invasion of human skin fibroblasts by the Lyme disease spirochete, Borrelia burgdorferi. *J. Infect. Dis.* 167: 1074–1081.

Klose M., Salloum J.E., Gonschior H. & Linder S. 2019. SNX3 drives maturation of Borrelia phagosomes by forming a hub for PI(3)P, Rab5a, and galectin-9. *J. Cell Biol.* 218: 3039–3059.

Kugeler K.J., Schwartz A.M., Delorey M.J., Mead P.S. & Hinckley A.F. 2021. Estimating the frequency of Lyme disease diagnoses, United States, 2010-2018. *Emerg. Infect. Dis.* 27: 616–619.

Kullberg B.J., Vrijmoeth H.D., Schoor F. Van De & Hovius J.W. 2020. Lyme borreliosis: Diagnosis and management. *BMJ* 369: m1041.

Lantos P.M., Rumbaugh J., Bockenstedt L.K., Falck-Ytter Y.T., Aguero-Rosenfeld M.E., Auwaerter P.G., Baldwin K., Bannuru R.R., Belani K.K., Bowie W.R., Branda J.A., Clifford D.B., Dimario F.J., Halperin J.J., Krause P.J., Lavergne V., Liang M.H., Meissner H.C., Nigrovic L.E., Nocton J.J., Osani M.C., Pruitt A.A., Rips J., Rosenfeld L.E., Savoy M.L., Sood S.K., Steere A.C., Strle F., Sundel R., Tsao J., Vaysbrot E.E., Wormser G.P. & Zemel L.S. 2021. Clinical practice guidelines by the infectious diseases society of America (IDSA), American academy of neurology (AAN), and American college of rheumatology (acr): 2020 guidelines for the prevention, diagnosis and treatment of Lyme disease. *Clin. Infect. Dis.* 72: 1–8.

Lewis K. 2010. Persister cells. *Annu. Rev. Microbiol.* 64: 357–372.

Lin Y.P., Diuk-Wasser M.A., Stevenson B. & Kraiczy P. 2020a. Complement evasion contributes to Lyme Borreliae–host associations. *Trends Parasitol.* 36: 634–645.

Lin Y.P., Tan X., Caine J.A., Castellanos M., Chaconas G., Coburn J. & Leong J.M. 2020b. Strain-specific joint invasion and colonization by Lyme disease spirochetes is promoted by outer surface protein C. *PLoS Pathog.* 16: e1008516.

Liu C.C., Zhang Y., Dai B.L., Ma Y.J., Zhang Q., Wang Y. & Yang H. 2017. Chlorogenic acid prevents inflammatory responses in IL-1β-stimulated human SW-1353 chondrocytes, a model for osteoarthritis. *Mol. Med. Rep.* 16: 1369–1375.

Livengood J.A. & Gilmore R.D. 2006. Invasion of human neuronal and glial cells by an infectious strain of Borrelia burgdorferi. *Microbes Infect.* 8: 2832–2840.

LPSN. 2021. *List of prokaryotic names with standing in nomenclature -web page*. www.bacterio.net (Last visited 20/11/2021).

Ma Y., Sturrock A. & Weis J.J. 1991. Intracellular localization of Borrelia burgdorferi within human endothelial cells. *Infect. Immun.* 59: 671–678.

Malge A., Ghai V., Reddy P.J., Baxter D., Kim T.-K.K., Moritz R.L. & Wang K. 2018. mRNA transcript distribution bias between Borrelia burgdorferi bacteria and their outer membrane vesicles. *FEMS Microbiol. Lett.* 365: 135.

McBroom A.J. & Kuehn M.J. 2005. Outer membrane vesicles. *EcoSal Plus* 1.

Mead P.S. 2015. Epidemiology of Lyme disease. *Infect. Dis. Clin. North Am.* 29: 187–210.

Meriläinen L., Brander H., Herranen A., Schwarzbach A. & Gilbert L. 2016. Pleomorphic forms of Borrelia burgdorferi induce distinct immune responses. *Microbes Infect.* 18: 484–495.

Meriläinen L., Herranen A., Schwarzbach A. & Gilbert L. 2015. Morphological and biochemical features of Borrelia burgdorferi pleomorphic forms. *Microbiology* 161: 516–527.

Miklossy J., Kasas S., Zurn A.D., McCall S., Yu S. & McGeer P.L. 2008. Persisting atypical and cystic forms of Borrelia burgdorferi and local inflammation in Lyme neuroborreliosis. *J. Neuroinflammation* 5: 1–18.

Mirlashari M.R., Høiby E.A., Holst J. & Lyberg T. 2001. Outer membrane vesicles from Neisseria meningitidis: Effects on cytokine production in human whole blood. *Cytokine* 13: 91–97.

Montgomery R.R. & Malawista S.E. 1996. Entry of Borrelia burgdorferi into macrophages is end-on and leads to degradation in lysosomes. *Infect. Immun.* 64: 2867–2872.

Moriarty T.J., Norman M.U., Colarusso P., Bankhead T., Kubes P. & Chaconas G. 2008. Real-time high resolution 3D imaging of the Lyme disease spirochete adhering to and escaping from the vasculature of a living host. *PLoS Pathog.* 4: e1000090.

Murgia R. & Cinco M. 2004. Induction of cystic forms by different stress conditions in Borrelia burgdorferi. *APMIS* 112: 57–62.

Myers T.A., Kaushal D. & Philipp M.T. 2009. Microglia are mediators of Borrelia burgdorferi-induced apoptosis in SH-SY5Y neuronal cells. *PLoS Pathog.* 5: e1000659.

Naj X. & Linder S. 2015. ER-coordinated activities of Rab22a and Rab5a drive phagosomal compaction and intracellular processing of Borrelia burgdorferi by macrophages. *Cell Rep.* 12: 1816–1830.

Nanagara R., Duray P.H. & Schumacher H.R. 1996. Ultrastructural demonstrational of spirochetal antigens in synovial membrane in chronic

Lyme disease: Possible factors contributing to persistence of organisms. *Hum. Pathol.* 27: 1025–1034.

Nascimento G.G.F., Locatelli J., Freitas P.C. & Silva G.L. 2000. Antibacterial activity of plant extracts and phytochemicals on antibiotic-resistant bacteria. *Brazilian J. Microbiol.* 31: 247–256.

Norris S.J. 2014. vls antigenic variation systems of Lyme disease Borrelia: Eluding host immunity through both random, segmental gene conversion and framework heterogeneity. *Microbiol. Spectr.* 2: MDNA3-0038–2014.

Nuttall P.A. 2019. Tick saliva and its role in pathogen transmission. *Wien. Klin. Wochenschr.*

Orench-Rivera N. & Kuehn M.J. 2016. Environmentally controlled bacterial vesicle-mediated export. *Cell. Microbiol.* 18: 1525–1536.

Pal U., Wang P., Bao F., Yang X., Samanta S., Schoen R., Wormser G.P., Schwartz I. & Fikrig E. 2008. Borrelia burgdorferi basic membrane proteins A and B participate in the genesis of Lyme arthritis. *J. Exp. Med.* 205: 133–141.

Perez Vidakovics M.L.A., Jendholm J., Mörgelin M., Månsson A., Larsson C., Cardell L.O. & Riesbeck K. 2010. B cell activation by outer membrane vesicles - A novel virulence mechanism. *PLoS Pathog.* 6: e1000724.

Petricarari S., Presani G., Prodan M., Granzotto M., Murgia R. & Cinco M. 2003. Lymphocyte apoptosis co-cultured with Borrelia burgdorferi. *Microb. Pathog.* 35: 139–145.

Pettit R.K. & Judd R.C. 1992. The interaction of naturally elaborated blebs from serum-susceptible and serum-resistant strains of Neisseria gonorrhoeae with normal human serum. *Mol. Microbiol.* 6: 729–734.

Pícha D., Moravcová L., Vaňousová D., Hercogová J. & Blechová Z. 2014. DNA persistence after treatment of Lyme borreliosis. *Folia Microbiol. (Praha).* 59: 115–125.

Qing G., Gong N., Chen X., Chen J., Zhang H., Wang Y., Wang R., Zhang S., Zhang Z., Zhao X., Luo Y. & Liang X.-J. 2019. Natural and engineered bacterial outer membrane vesicles. *Biophys. Reports* 5: 184–198.

Ramamoorthi N., Narasimhan S., Pal U., Bao F., Yang X.F., Fish D., Anguita J., Norgard M. V., Kantor F.S., Anderson J.F., Koski R.A. & Fikrig E. 2005. The Lyme disease agent exploits a tick protein to infect the mammalian host. *Nature* 436: 573–577.

Ramesh G., Santana-Gould L., Inglis F.M., England J.D. & Philipp M.T. 2013. The Lyme disease spirochete Borrelia burgdorferi induces inflammation and apoptosis in cells from dorsal root ganglia. *J. Neuroinflammation* 10: 88.

Renelli M., Matias V., Lo R.Y. & Beveridge T.J. 2004. DNA-containing membrane vesicles of Pseudomonas aeruginosa PAO1 and their genetic transformation potential. *Microbiology* 150: 2161–2169.

Rittig M.G., Häupl T., Krause A., Kressel M., Groscurth P. & Burmester G.R. 1994. Borrelia burgdorferi-induced ultrastructural alterations in human phacgocytes: A clue to pathogenicity? *J. Pathol.* 173: 269–282.

Rittig M.G., Jagoda J.C., Wilske B., Murgia R., Cinco M., Repp R., Burmester G.R. & Krause A. 1998. Coiling phagocytosis discriminates between different

spirochetes and is enhanced by phorbol myristate acetate and granulocyte-macrophage colony- stimulating factor. *Infect. Immun.* 66: 627–635.

Rittig M.G., Krause A., Haupl T., Schaible U.E., Modolell M., Kramer M.D., Lutjen-Drecoll E., Simon M.M. & Burmester G.R. 1992. Coiling phagocytosis is the preferential phagocytic mechanism for Borrelia burgdorferi. *Infect. Immun.* 60: 4205–4212.

Rittig M.G., Kuhn K.H., Dechant C.A., Gauckler A., Modolell M., Ricciardi-Castagnoli P., Krause A. & Burmester G.R. 1996. Phagocytes from both vertebrate and invertebrate species use 'coiling' phagocytosis. *Dev. Comp. Immunol.* 20: 393–406.

Rozwadowska B., Albertyńska M., Okła H., Jasik K.P., Swinarew A.S., Mazurek U., Dudek S., Urbańska-Jasik D. & Poprawa I. 2017. Induction of apoptosis in normal human dermal fibroblasts infected with Borrelia burgdorferi sensu Lato. *Vector-Borne Zoonotic Dis.* 17: 237–242.

Rudenko N., Golovchenko M., Kybicova K. & Vancova M. 2019. Metamorphoses of Lyme disease spirochetes: Phenomenon of Borrelia persisters. *Parasites and Vectors* 12: 237.

Sapi E., Balasubramanian K., Poruri A., Maghsoudlou J.S., Socarras K.M., Timmaraju A. V., Filush K.R., Gupta K., Shaikh S., Theophilus P.A.S., Luecke D.F., MacDonald A. & Zelger B. 2016. Evidence of in vivo existence of Borrelia biofilm in borrelial lymphocytomas. *Eur. J. Microbiol. Immunol.* 6: 9–24.

Sapi E., Kasliwala R.S., Ismail H., Torres J.P., Oldakowski M., Markland S., Gaur G., Melillo A., Eisendle K., Liegner K.B., Libien J. & Goldman J.E. 2019. The long-term persistence of Borrelia burgdorferi antigens and DNA in the tissues of a patient with lyme disease. *Antibiotics* 8: 183.

Sapi E., Kaur N., Anyanwu S., Luecke D.F., Datar A., Patel S., Rossi M. & Stricker R.B. 2011. Evaluation of in vitro antibiotic susceptibility of different morphological forms of Borrelia burgdorferi. *Infect. Drug Resist.* 4: 97–113.

Schindelin J., Arganda-Carreras I., Frise E., Kaynig V., Longair M., Pietzsch T., Preibisch S., Rueden C., Saalfeld S., Schmid B., Tinevez J.Y., White D.J., Hartenstein V., Eliceiri K., Tomancak P. & Cardona A. 2012. Fiji: An open-source platform for biological-image analysis. *Nat. Methods* 9: 676–682.

Schoen R.T. 2020. Lyme disease: Diagnosis and treatment. *Curr. Opin. Rheumatol.* 32: 247–254.

Schuijt T.J., Hovius J.W.R., Burgel N.D. Van, Ramamoorthi N., Fikrig E. & Dam A.P. Van. 2008. The tick salivary protein Salp15 inhibits the killing of serum-sensitive Borrelia burgdorferi sensu lato isolates. *Infect. Immun.* 76: 2888–2894.

Schwan T.G., Piesman J., Golde W.T., Dolan M.C. & Rosa P.A. 1995. Induction of an outer surface protein on Borrelia burgdorferi during tick feeding. *Proc. Natl. Acad. Sci. U. S. A.* 92: 2909–2913.

Sehgal V.N. & Khurana A. 2015. Lyme disease/borreliosis as a systemic disease. *Clin. Dermatol.* 33: 542–550.

Sharma B., Brown A. V., Matluck N.E., Hu L.T. & Lewis K. 2015. Borrelia burgdorferi, the causative agent of Lyme disease, forms drug-tolerant persister cells. *Antimicrob. Agents Chemother.* 59: 4616–4624.

Shoberg R.J. & Thomas D.D. 1993. Specific adherence of Borrelia burgdorferi extracellular vesicles to human endothelial cells in culture. *Infect. Immun.* 61: 3892–3900.

Shoberg R.J. & Thomas D.D. 1995. Borrelia burgdorferi vesicle production occurs via a mechanism independent of immunoglobulin M involvement. *Infect. Immun.* 63: 4857–4861.

Shor S., Green C., Szantyr B., Phillips S., Liegner K., Burrascano B., Bransfield R. & Maloney E.L. 2019. Chronic Lyme disease: An evidence-based definition by the ILADS working group. *Antibiotics* 8: 269.

Silva A.M. de, Tyson K.R. & Pal U. 2009. Molecular characterization of the tick-Borrelia interface. *Front. Biosci.* Volume: 3051–3063.

Skare J.T., Shang E.S., Foley D.M., Blanco D.R., Champion C.I., Mirzabekov T., Sokolov Y., Kagan B.L., Miller J.N. & Lovett M.A. 1995. Virulent strain associated outer membrane proteins of Borrelia burgdorferi. *J. Clin. Invest.* 96: 2380–2392.

Srivastava S.Y. & Silva A.M. De. 2009. Characterization of Borrelia burgdorferi aggregates. *Vector-Borne Zoonotic Dis.* 9: 323–329.

Stanek G., Wormser G.P., Gray J. & Strle F. 2012. Lyme borreliosis. *Lancet* 379: 461–473.

Strnad M., Elsterová J., Schrenková J., Vancová M., Rego R.O.M., Grubhoffer L. & Nebesářová J. 2015. Correlative cryo-fluorescence and cryo-scanning electron microscopy as a straightforward tool to study host-pathogen interactions. *Sci. Rep.* 5: 18029.

Suhonen J., Komi J., Soukka J., Lassila O. & Viljanen M.K. 2003. Interaction between Borrelia burgdorferi and immature human dendritic cells. *Scand. J. Immunol.* 58: 67–75.

Szczepanski A., Furie M.B., Benach J.L., Lane B.P. & Fleit H.B. 1990. Interaction between Borrelia burgdorferi and endothelium in vitro. *J. Clin. Invest.* 85: 1637–1647.

Tajkarimi M.M., Ibrahim S.A. & Cliver D.O. 2010. Antimicrobial herb and spice compounds in food. *Food Control* 21: 1199–1218.

Theophilus P.A.S., Victoria M.J., Socarras K.M., Filush K.R., Gupta K., Luecke D.F. & Sapi E. 2015. Effectiveness of Stevia rebaudiana whole leaf extract against the various morphological forms of Borrelia burgdorferi in vitro. *Eur. J. Microbiol. Immunol.* 5: 268–280.

Thomas D.D., Cadavid D. & Barbour A.G. 1994. Differential association of borrelia species with cultured neural cells. *J. Infect. Dis.* 169: 445–448.

Thomas D.D. & Comstock L.E. 1989. Interaction of Lyme disease spirochetes with cultured eucaryotic cells. *Infect. Immun.* 57: 1324–1326.

Tilly K., Rosa P.A. & Stewart P.E. 2008. Biology of infection with Borrelia burgdorferi. *Infect. Dis. Clin. North Am.* 22: 217–234.

Toledo A., Coleman L., Kuhlow C.J., Crowley J.T. & Benach J.L. 2012. The enolase of Borrelia burgdorferi is a plasminogen receptor released in outer membrane vesicles. *Infect. Immun.* 80: 359–368.

Toyofuku M., Nomura N. & Eberl L. 2019. Types and origins of bacterial membrane vesicles. *Nat. Rev. Microbiol.* 17: 13–24.

Trevisan G., Cinco M., Trevisini S., Meo N. di, Chersi K., Ruscio M., Forgione P. & Bonin S. 2021. Borreliae part 1: Borrelia Lyme group and Echidna-reptile group. *Biology (Basel).* 10: 1036.

Uddin T.M., Chakraborty A.J., Khusro A., Zidan B.R.M., Mitra S., Emran T. Bin, Dhama K., Ripon M.K.H., Gajdács M., Sahibzada M.U.K., Hossain M.J. & Koirala N. 2021. Antibiotic resistance in microbes: History, mechanisms, therapeutic strategies and future prospects. *J. Infect. Public Health* 14: 1750–1766.

Unal C.M., Schaar V. & Riesbeck K. 2011. Bacterial outer membrane vesicles in disease and preventive medicine. *Semin. Immunopathol.* 33: 395–408.

Vink C., Rudenko G. & Seifert H.S. 2012. Microbial antigenic variation mediated by homologous DNA recombination. *FEMS Microbiol. Rev.* 36: 917–948.

Walport M.J. 2001. Complement. First of two parts. *N. Engl. J. Med.* 344: 1058–1066.

Wawrzeniak K., Gaur G., Sapi E. & Senejani A.G. 2020. Effect of Borrelia burgdorferi outer membrane vesicles on host oxidative stress response. *Antibiotics* 9: 275.

Wen S., Wang F., Ji Z., Pan Y.Y., Jian M., Bi Y.F., Zhou G., Luo L., Chen T., Li L., Ding Z., Abi M.E., Liu A. & Bao F. 2020. Salp15, a multifunctional protein from tick saliva with potential pharmaceutical effects. *Front. Immunol.* 10: 3067.

Whitmire W.M. & Garon C.F. 1993. Specific and nonspecific responses of murine B cells to membrane blebs of Borrelia burgdorferi. *Infect. Immun.* 61: 1460–1467.

Williams S.K., Weiner Z.P. & Gilmore R.D. 2018. Human neuroglial cells internalize Borrelia burgdorferi by coiling phagocytosis mediated by Daam1. *PLoS One* 13: e0197413.

Wolcott K.A., Margos G., Fingerle V. & Becker N.S. 2021. Host association of Borrelia burgdorferi sensu lato: A review. *Ticks Tick. Borne. Dis.* 12: 101766.

Wormser G.P., Dattwyler R.J., Shapiro E.D., Halperin J.J., Steere A.C., Klempner M.S., Krause P.J., Bakken J.S., Strle F., Stanek G., Bockenstedt L., Fish D., Dumler J.S. & Nadelman R.B. 2006. The clinical assessments treatment, and prevention of Lyme disease, human granulocytic anaplasmosis, and babesiosis: Clinical practice guidelines by the Infectious Diseases Society of America. *Clin. Infect. Dis.* 43: 1089–1134.

Wu J., Weening E.H., Faske J.B., Höök M. & Skare J.T. 2011. Invasion of eukaryotic cells by Borrelia burgdorferi requires β1 integrins and Src kinase activity. *Infect. Immun.* 79: 1338–1348.

Yang X., Promnares K., Qin J., He M., Shroder D.Y., Kariu T., Wang Y. & Pal U. 2011. Characterization of multiprotein complexes of the Borrelia burgdorferi outer membrane vesicles. *J. Proteome Res.* 10: 4556–4566.

Yokoyama K., Horii T., Yamashino T., Hashikawa S., Barua S., Hasegawa T., Watanabe H. & Ohta M. 2006. Production of Shiga toxin by Escherichia coli measured with reference to the membrane vesicle-associated toxins. *FEMS Microbiol. Lett.* 192: 139–144.

Yue B. 2014. Biology of the extracellular matrix: An overview. *J. Glaucoma* 23: S20–S23.

Zhang J.R., Hardham J.M., Barbour A.G. & Norris S.J. 1997. Antigenic variation in Lyme disease borreliae by promiscuous recombination of VMP-like sequence cassettes. *Cell* 89: 275–285.

Zipfel P.F. & Skerka C. 2009. Complement regulators and inhibitory proteins. *Nat. Rev. Immunol.* 9: 729–740.

ORIGINAL PAPERS

I

DISTINCTIVE EVASION MECHANISMS TO ALLOW PERSISTENCE OF BORRELIA BURGDORFERI IN DIFFERENT HUMAN CELL LINES

by

Kati Karvonen, Jonna Nykky, Varpu Marjomäki & Leona Gilbert 2021

Frontiers in Microbiology 12: 711291

https://doi.org/10.3389/fmicb.2021.711291

frontiers in Microbiology

ORIGINAL RESEARCH
published: 12 October 2021
doi: 10.3389/fmicb.2021.711291

Distinctive Evasion Mechanisms to Allow Persistence of *Borrelia burgdorferi* in Different Human Cell Lines

Kati Karvonen[1], Jonna Nykky[1], Varpu Marjomäki[1] and Leona Gilbert[2]**

[1] Department of Biological and Environmental Science, Nanoscience Center, University of Jyväskylä, Jyväskylä, Finland,
[2] Te?ted Oy Ltd., Jyväskylä, Finland

Lyme borreliosis is a multisystemic disease caused by the pleomorphic bacteria of the *Borrelia burgdorferi sensu lato* complex. The exact mechanisms for the infection to progress into a prolonged sequelae of the disease are currently unknown, although immune evasion and persistence of the bacteria in the host are thought to be major contributors. The current study investigated *B. burgdorferi* infection processes in two human cell lines, both non-immune and non-phagocytic, to further understand the mechanisms of infection of this bacterium. By utilizing light, confocal, helium ion, and transmission electron microscopy, borrelial infection of chondrosarcoma (SW1353) and dermal fibroblast (BJ) cells were examined from an early 30-min time point to a late 9-days post-infection. Host cell invasion, viability of both the host and *B. burgdorferi*, as well as, co-localization with lysosomes and the presence of different borrelial pleomorphic forms were analyzed. The results demonstrated differences of infection between the cell lines starting from early entry as *B. burgdorferi* invaded BJ cells in coiled forms with less pronounced host cell extensions, whereas in SW1353 cells, micropodial interactions with spirochetes were always seen. Moreover, infection of BJ cells increased in a dose dependent manner throughout the examined 9 days, while the percentage of infection, although dose dependent, decreased in SW1353 cells after reaching a peak at 48 h. Furthermore, blebs, round body and damaged *B. burgdorferi* forms, were mostly observed from the infected SW1353 cells, while spirochetes dominated in BJ cells. Both infected host cell lines grew and remained viable after 9 day post-infection. Although damaged forms were noticed in both cell lines, co-localization with lysosomes was low in both cell lines, especially in BJ cells. The invasion of non-phagocytic cells and the lack of cytopathic effects onto the host cells by *B. burgdorferi* indicated one mechanism of immune evasion for the bacteria. The differences in attachment, pleomorphic form expressions, and the lack of lysosomal involvement between the infected host cells likely explain the ability of a bacterium to adapt to different environments, as well as, a strategy for persistence inside a host.

Keywords: lyme borreliosis, pleomorphic forms, immune evasion, microscopy, persist

OPEN ACCESS

Edited by:
Mattias Collin,
Lund University, Sweden

Reviewed by:
Camilo E. Khatchikian,
Dartmouth College, United States
Eva Sapi,
University of New Haven,
United States

****Correspondence:***
Kati Karvonen
kati.s.karvonen@jyu.fi
Leona Gilbert
leona.gilbert@tezted.com

Specialty section:
This article was submitted to Infectious Agents and Disease, a section of the journal Frontiers in Microbiology

Received: *18 May 2021*
Accepted: *15 September 2021*
Published: *12 October 2021*

Citation:
Karvonen K, Nykky J, Marjomäki V and Gilbert L (2021) Distinctive Evasion Mechanisms to Allow Persistence of Borrelia burgdorferi in Different Human Cell Lines. Front. Microbiol. 12:711291. doi: 10.3389/fmicb.2021.711291

INTRODUCTION

Borrelia burgdorferi, the causative agent of Lyme borreliosis (LB), is a pleomorphic bacterium transmitted *via Ixodes* ticks (Burgdorfer et al., 1982). *Borrelia* bacteria can be found globally and the main species causing LB are *B. burgdorferi sensu stricto*, *Borrelia garinii*, and *Borrelia afzelii*. In normal culture conditions, *Borrelia* is found in the parental spirochete form with a length varying from 10 to 30 μm, as well as, forming vesicles or blebs, as a metabolically inactive round body (RB) and even in biofilms (Meriläinen et al., 2015). Additionally, these pleomorphic forms can be induced by unfavorable culture conditions such as changes in pH, osmotic pressure, temperature, and even with antibiotic treatment (Kersten et al., 1995; Murgia and Cinco, 2004; Srivastava and De Silva, 2009; Meriläinen et al., 2015; Sharma et al., 2015). However, upon return to optimal culture conditions *Borrelia* can revert back to spirochetes (Brorson and Brorson, 1998; Gruntar et al., 2001; Meriläinen et al., 2015; Sharma et al., 2015).

Lyme borreliosis is the most common vector-borne disease in North America and Europe (Mead, 2015). The infection can lead to a multisystemic disorder with signs and symptoms ranging from mild flu-like symptoms and erythema migrans rash, to autoimmune-like disorders such as acrodermatitis chronica atrophicans, Lyme arthritis, and neurological, or cardiac impairments (Wormser et al., 2006; Sehgal and Khurana, 2015). The variety of signs and symptoms are due both to bacterial dissemination into distal tissues, as well as, local inflammatory reactions of the immune system to the bacterial proteins (reviewed in Hyde, 2017; Radolf et al., 2020). Antibiotics usually eradicate *Borrelia* if treatment is given early on in the infection. However, patients who suffer from what is termed post-treatment Lyme disease syndrome (Stanek et al., 2012) or chronic Lyme (Shor et al., 2019) remain. These patients have previously received antibiotic treatment but continue to exhibit different LB related clinical symptoms. *Borrelia* persistence in humans is currently under debate, although the pleomorphic forms of *Borrelia* are thought to play a major role in the persistence of the bacteria (Miklossy et al., 2008; Sharma et al., 2015; Rudenko et al., 2019). However, the exact mechanisms resulting in the long-term sequelae of the disease are currently undetermined.

Pathogens have several mechanisms for entering non-phagocytic cells. Smaller pathogens fit inside, for instance, caveolae or clathrin-coated vesicles, while larger ones internalize *via* more sizeable cellular compartments and progress through such endocytosis pathways as macropinocytosis (Cossart and Helenius, 2014). *Borrelia* have been demonstrated to invade a variety of human cells, for instance, endothelial cells (Comstock and Thomas, 1991; Ma et al., 1991), dermal fibroblasts (Klempner et al., 1993; Rozwadowska et al., 2017), synovial cells (Girschick et al., 1996), and neural cells (Livengood and Gilmore, 2006; Miklossy et al., 2008), among others. Furthermore, it has been demonstrated that *Borrelia* can be internalized by human cells without affecting cell viability, and this has been thought to play a role in host immune evasion (Ma et al., 1991; Girschick et al., 1996; Livengood and Gilmore, 2006). The ability to evade the host immune system is an integral part of *Borrelia* survival and dissemination throughout the body. How exactly *Borrelia* escapes being noticed by the immune system is yet to be resolved. Nevertheless, there are known *Borrelia* immune escape strategies including using tick proteins as a disguise, active suppression of host immune system, antigenic variation of the bacterial membrane proteins and altering its shape into a different pleomorphic form, among others (reviewed in Embers et al., 2004; Berndtson, 2013; Rudenko et al., 2019). Further understanding of the infection mechanisms of these bacteria by investigating the cellular invasion and its outcome in non-phagocytic cells is crucial. In this study, *Borrelia* infection of two non-immune and non-phagocytic human cell lines was examined. The results illustrated that *B. burgdorferi* could maintain a variety of intracellular locations inside non-phagocytic human cells during extended infection periods without instigating cytopathic effects. Moreover, differences in *B. burgdorferi* invasion processes, as well as, in infectivity between the two human cell lines were apparent. Furthermore, different borrelial pleomorphic forms were visualized inside the infected human cells. Consequently, though *B. burgdorferi* infected these human cells in a divergent manner, both the invasion and persistence with pleomorphic forms inside non-phagocytic host cells outlined strategies for *Borrelia* to avoid clearance by the immune system, and thus, initiate a persisting infection.

MATERIALS AND METHODS

Human Cell Cultures

Normal dermal fibroblast cell line (BJ, CRL-2522) and chondrosarcoma cell line (SW1353, HTB-94) were purchased from American Type Culture Collection. Dermal fibroblasts have been previously used in investigations of borrelial infection (Georgilis et al., 1992). Furthermore, the use of chondrosarcoma cells in osteoarthritis research is well documented (Chen et al., 2017; Liu et al., 2017). Therefore, these cell lines, BJ and SW1353, were utilized for their relevance as a disease-related model for skin manifestations and arthritis, respectively. The SW1353 cells were grown at +37°C with 100% air in Leibovitz's L-15 media (Sigma), while the BJ cells were at +37°C, 5% CO_2 in Eagle's minimum essential media (Sigma) as instructed by the manufacturers. Both media were supplemented with 10% fetal bovine serum (Gibco), 2 mM L-glutamine (Gibco), and 100 IU/ml penicillin/0.2 mg/ml streptomycin (Gibco) antibiotic cocktail. Sodium pyruvate (1 mM, Gibco) was also added to the BJ media.

Bacteria Cultures

The infectious *B. burgdorferi* strain GCB726 with green fluorescent protein (GFP) (hereafter referred to as *B. burgdorferi*), a generous gift from George Chakonas, University of Calgary, Canada (Moriarty et al., 2008), was grown, and round bodies (RBs) were induced as previously described (Meriläinen et al., 2015). In all experiments, low-passage number cells (≤p8) in log phase were utilized.

Infection Protocol

In the proceeding experiments ("Helium Ion Microscopy," "*Borrelia burgdorferi* Infection Assay and Wheat Germ Agglutinin Staining," "Human Cell Viability Assays," "*Borrelial* Survival," "Transmission Electron Microscopy," and "Co-localization and Green Fluorescent Protein Signal Analyses With Immunolabeling Procedure" sections) the cell density, multiplicity of infections (MOIs) and time of infection are specific for each experiment. In general, human cells were seeded in antibiotic-free media a day before the infection in order for the cells to fully attach to the culture dishes. *B. burgdorferi* was counted using a C-Chip DHC-N01 Disposable Hemocytometer (System Neubauer Improved; Digital Bio). The specific MOIs (see "Helium Ion Microscopy," "*Borrelia burgdorferi* Infection Assay and Wheat Germ Agglutinin Staining," "Human Cell Viability Assays," "*Borrelial* Survival," "Transmission Electron Microscopy," and "Co-localization and Green Fluorescent Protein Signal Analyses With Immunolabeling Procedure" sections) of *B. burgdorferi* were centrifuged 1,000 × *g* for 15 min and resuspended into the antibiotic-free media of each cell line. Before adding *Borrelia*, the human cells were washed once with +37°C PBS. *B. burgdorferi* entry into the human cells was synchronized with 1-h incubation on ice. After ice incubation, antibiotic-free media was added according to standard culture plates used, and the infection was allowed to proceed according to each respective experiment (sections "Helium Ion Microscopy," "*Borrelia burgdorferi* Infection Assay and Wheat Germ Agglutinin Staining," "Human Cell Viability Assays," "*Borrelial* Survival," "Transmission Electron Microscopy," and "Co-localization and Green Fluorescent Protein Signal Analyses With Immunolabeling Procedure").

Helium Ion Microscopy

Helium ion microscopy (HIM) (Zeiss Orion Nanofab) was utilized to visualize early human cell attachment and invasion by *B. burgdorferi*. The 100,000 cells were seeded onto coverslips with integrated grids in them (High Precision microscope cover glasses, 28 mm, No. 1.5H, Paul Marienfeld GmbH & Co., Germany) in six-well culture plates and incubated overnight accordingly. As controls, samples with only human cells, spirochetes and RBs, individually, were used. The gridded areas of the cover slips used for bacterial controls were coated with 50-μl drop of poly-L-lysine (P8920, Sigma) according to the instructions of the manufacturer (Sigma). Borrelial control samples were allowed to attach onto the coverslips by incubating them in the respective antibiotic-free human cell media for at least 2 h before starting the experiment. Samples were infected as mentioned above at MOI 200 for 30 min. Next, samples were washed twice with PBS, before fixation with 4% paraformaldehyde (PFA) 20 min at room temperature (RT). The PBS was washed away with two dH_2O washes, 3 min each. The samples were stained with 1% osmium tetroxide (O_sO_4, Electron Microscopy Sciences, Hatfield, PA, United States) for 30 min, followed by two dH_2O washes for 3 min, and dehydrated as follows: 50, 70, and 96% ethanol dehydrations, each 3 min, were performed before two 5-min dehydrations in 100% ethanol. Last, the dehydration was finalized with an overnight incubation of samples in ≥99.9% hexamethyldisilazane (Sigma). Coverslips were then plated onto specimen studs with carbon stickers (Ted Pella Inc., United States). Samples were stored in a dehumidifier chamber at RT until imaging with Zeiss Orion Nanofab HIM. Acceleration voltage of approximately 30 kV and an aperture of 10 μm were used at 25° tilt. The spot size varied between 6 and 7, with the ion current in the range of 0.09–0.3 pA. Since the samples were non-conductive, the flood gun charge compensation was utilized. Images were taken using line averaging of 32 with 0.5–2 μm dwell time. In total, 20 infected cells from two separate experiments were imaged and analyzed for *B. burgdorferi* invasion.

Borrelia burgdorferi Infection Assay and Wheat Germ Agglutinin Staining

Analyzing the infectivity of *B. burgdorferi* with the human cells was performed at time points 24, 48, 72, 96 h, 7 and 9 days using MOIs 10, 20, and 40. In each experiment, 30,000 cells/well in a 12-well plate were seeded and incubated overnight before the infection with *B. burgdorferi*.

At each time point, cells were fixed, stained and immunolabeled as previously described (Thammasri et al., 2013). All steps were performed at RT and in the dark after the first staining step. Briefly, the samples were washed twice with PBS after the fixation step mentioned above. Free aldehydes were blocked with 0.15% glycine/PBS solution for 10 min, and unspecific binding was blocked with 2% BSA (Sigma)/PBS solution for 20 min. Cell membranes were stained with wheat germ agglutinin (WGA) with Texas Red-X conjugate (Invitrogen) for 20 min. WGA was used at a concentration of 10 and 5 ng/ml for SW1353 and BJ cells, respectively. After staining, cells were washed twice with PBS for 5 min. Coverslips were mounted onto microscopic slides (Thermo Scientific) with Antifade Prolong Gold with DAPI (Sigma). Leica TCS SP8X Falcon confocal microscope with the 63 × glycerol objective, PMT detector for the 405 nm, and HyD detectors for the 488 and 555 nm excitation wavelengths were used to image the samples. Optimal exposure, gain, and intensity were adjusted with Las X software (Leica) before taking the images. A human cell was considered infected if *B. burgdorferi* was attached to or inside the cell. A total of 300 human cells were counted from three separate experiments.

Human Cell Viability Assays

The viability of *B. burgdorferi* infected human cells at various time points (24, 48, 72, and 96 h) was examined using two separate methods. Uninfected cells were used as a positive control, while 1 μM Staurosporine (S4400 staurosporine from Streptomyces sp., Sigma) was used to stimulate human cell death. MOIs of 20, 40, and 200 were used to infect 30,000 cells in 12-well culture plates (Nunc). After each time point, samples were trypsinized with 0.05% trypsin/EDTA solution (Gibco) and counted with Trypan Blue exclusion method, see below. To further verify the viability of the cells, 100 nM MitoTracker Red CMXRos (MT, Invitrogen) was used to stain viable mitochondria

as instructed by the manufacturer. Samples were prepared for both flow cytometry and confocal microscopy analysis. After the MT staining, the microscopy samples were fixed and mounted onto microscopic slides as mentioned above, while the samples required for flow cytometric analysis were trypsinized and plated onto round bottomed 96-well plate (Corning). Guava® easyCyte 8HT benchtop flow cytometer (Millipore) with blue and red lasers on, 5-decade acquisition, a 3,000 threshold for forward scatter and the 583/26 nm filter, was used to analyze samples. Guava InCyte 3.0 software was used to acquire either 10,000 events or 3 min of event collection, as well as in analyzing the data. Regions for cells and *B. burgdorferi* were drawn in the scatter plots, and the fluorescence gate was adjusted for cells with unstained controls. Each experiment was performed three times with triplicate samples.

Borrelial Survival

To examine the possibility of *B. burgdorferi* to survive and remain viable after being internalized by a human cell, an infection procedure was performed using MOI 200 for 24 and 72 h. After the time points, external bacteria were removed using an acid wash protocol as previously described with modifications (Kameyama et al., 2007). Briefly, the cells were washed three times with cold PBS, before the samples were subjected to a cold acid wash (0.2 M glycine, 0.15 M NaCl, pH 3) for 30 s. Then three 30 s cold PBS washes were performed. The cells were detached from the plates by trypsinization for 5 min at +37°C, and collected into Eppendorf tubes using antibiotic-free media. The viability of the human cells was examined with Trypan Blue. For the Trypan Blue assay, the cells were pelleted (200 g, 5 min, Thermo Scientific MicroCL 17, Germany) and washed twice with RT PBS. After the second wash, the pellet was resuspended into 3 ml of *B. burgdorferi* media (BSK II) and a 10-μl sample containing Trypan Blue was taken into a C-chip hemocytometer for microscopical analysis to ensure that both the human cells were not damaged after the acid wash and that no free *B. burgdorferi* was left in the samples. The pellets were incubated in BSK II containing culture tubes at +37°C for a maximum of 6 weeks. At week 4, the media in the samples was changed by centrifugation (1,000 × *g* for 15 min). Each week, the samples were examined for *B. burgdorferi* growth by taking a 10 μl sample for fluorescence microscopic analysis. *B. burgdorferi* growth was determined if the samples had multiple healthy looking and motile spirochetes. Leica DM5500 fluorescence microscope with ×20 and ×40 objectives and 488 nm filter setup were used in visualizing and imaging the samples. The experiments were carried out in triplicates and repeated three times.

Transmission Electron Microscopy

In order to visualize the intracellular location of *B. burgdorferi*, transmission electron microscopy (TEM) was utilized at 24 h and 9-day time points with MOI 200 (10 cm dish). Samples were prepared for immunolabeling on frozen thin sections as described previously (Huttunen et al., 2014). Samples were washed twice with RT PBS before fixation with 4% PFA, 0.1% glutaraldehyde in 0.1 M phosphate buffer for 10 min. After the fixation, the cells were gently scraped from the culture plates and further fixed for a maximum of 1 h. The cells were pelleted in a swing-out rotor at 2,700 × *g* for 10 min RT (Heraeus Megafuge 1.0 R, Germany). Rabbit anti-GFP primary antibody (Invitrogen) was used in immunolabeling *B. burgdorferi* with 1:100 dilution. Protein A gold (10 nm, 1:200) was used to visualize *B. burgdorferi* as described previously (Huttunen et al., 2014). JEOL JEM1400 transmission electron microscope was utilized in imaging the samples.

Co-localization and Green Fluorescent Protein Signal Analyses With Immunolabeling Procedure

For a co-localization study between *B. burgdorferi* and lysosomes, 30,000 cells on coverslips in 24-well plates were infected with MOI 40 of *B. burgdorferi* for 24 h and 9 days. The cells were fixed, and the membranes were stained with WGA as mentioned above. After the WGA staining, two 5-min PBS washes were performed, and the cell membrane was permeabilized with Triton-X100 solution (0.1% Triton X-100 (Sigma), 0.01% NaN_3 (Sigma), 2% BSA in PBS) for 20 min. The H4B4 mouse anti-human Lamp-2 primary antibody (Developmental Studies Hybridoma Bank, United States) was diluted to 1:50 in the Triton solution, and the samples were incubated for 1 h. Afterward, three PBS washes, 5 min each, was performed. Alexa fluor goat anti-mouse IgG 633 secondary antibody (Invitrogen) was used at 1:200 dilution in the Triton solution and incubated for 30 min. Excess secondary antibody was washed with PBS, three times for 5 min. The samples were mounted with Antifade Prolong Gold with DAPI. Nikon A1R confocal microscope with Galvano scanning, 60× objective and 405 nm (DAPI), 488 nm (GFP), 561 nm (WGA), and 638 nm (Lamp2) lasers were used in the co-localization experiment. Stacks with 0.2 μm steps of 30 cells in total were taken for the co-localization analysis.

For the GFP signal analysis, ×40 objective with the same excitation wavelengths as in the co-localization analysis, except the 638 nm laser, were used. From randomly selected portions of the samples, 30 images of cells were taken from the middle section of stacks (middle of the cell). Both experiments were repeated three times.

Pleomorphic Form Analysis

During the *B. burgdorferi* infection assay, it was noted that there were clear differences in *B. burgdorferi* forms between the infections of the two human cell lines. Therefore, confocal imaging (Nikon A1R microscope with Galvano scanning, ×60 objective with 405, 488, and 561 nm lasers) was utilized to analyze the different pleomorphic forms of *B. burgdorferi* found in the infected samples. In addition, *B. burgdorferi* was subjected to BJ (MEM) and SW1353 (L-15) medias alone for 96 h and analyzed daily with a fluorescence microscope (Leica DM5500). In total, 300 *B. burgdorferi* associated with the human cells were counted from three separate experiments. The included forms (Meriläinen et al., 2015) and their inclusion/exclusion criteria are stated in **Table 1** below.

TABLE 1 | Pleomorphic forms of *Borrelia burgdorferi* and their characteristics.

Form	Description	DNA	GFP	Size
Spirochete	Corkscrew or any other clear spirochete form but in a variety of shapes [e.g., looped, ring (Miklossy et al., 2008), V-shaped etc.]	Yes	Yes	10–30 μm
Bleb	Spirochete with clear blebbing, can have several blebs, OR a detached bleb.	Yes/No	Yes	0.8–1.7 μm
Round body (RB)/coiling RB	Full RB or a forming RB that can include a "tail"	Yes	Yes	Full RB 2.4–3.2 μm Coiling RB >1.7 μm
Aggregate	Cluster of 10 or more bacteria, can include any one or all of the abovementioned pleomorphic forms	Yes	Yes	Varies, must have 10 or more bacterial cells
Damaged	Form/shape difficult to define into any of the abovementioned forms. Must lack either a DNA or GFP signal. Spheres are smaller than 0.8 μm			

GFP, green fluorescent protein.

Image and Statistical Analyses

All confocal images were analyzed using ImageJ software (Schindelin et al., 2012). Brightness and contrast were adjusted, Gaussian blur filter with Sigma radius 0.5–0.7 was added, and stacks were combined with z-projection using max intensity to create a single image.

The co-localization analysis was performed in ImageJ using the JaCoP plugin (Bolte and Cordelières, 2006). Before starting the analysis, Intermodes threshold was used for the stacks with additional manual adjustments. The analysis was executed using Mander's coefficient and Costes' randomization with 100 rounds. Samples with more than 5% co-localization were considered as co-localized if their Costes' *p*-value was $\geq$0.95 (Costes et al., 2004). The representative images were made using the Intermodes threshold.

The HIM images were adjusted for brightness and contrast using ImageJ.

Two-tailed, unequal variance Student's *t*-test was performed in Microsoft Excel. Statistical significance was considered for samples with a *p-value* of $^{*} \leq 0.05$ or $^{**} \leq 0.005$.

RESULTS

Borrelia burgdorferi Formed Coiled Structures During Entry Into Human Cells

With helium ion microscopy the surfaces of biological samples can be examined without any additional metallic coating procedures of samples, which might affect and distort results. Hence, HIM was applied to detect the cell attached *Borrelia* at an early time point (30 min post-infection) onto both human dermal fibroblast and chondrosarcoma cells. To the best of our knowledge, this is the first time HIM has been utilized in analyzing early cellular invasion by *B. burgdorferi*. In the control images, multiple spirochetes, and a cluster of three RBs, respectively, demonstrate the shapes and sizes of *B. burgdorferi* (**Figures 1A,B**). Carcinoma cells have been shown to exhibit lamellipodia and invadopods as adhesion and invasion structures (Lorenz et al., 2004). Here, the uninfected carcinoma cell line SW1353 displayed cell surface extensions in higher amounts than the BJ cell line (**Figures 1C,D**). It was considered that the effect was due to the invasive nature of the cell line, since BJ cells were not a cancer cell line. A total of 20 human cells were counted and analyzed for *B. burgdorferi* entry from the infected samples. Only spirochetes were located on top of the infected SW1353 cell (**Figures 1E,G**), while both spirochetal and coiled forms were observed on the BJ cells (**Figures 1F,G**) 30 min post-infection. The white arrows in **Figure 1** point to *B. burgdorferi* in the infected samples, as well as in the controls. *B. burgdorferi* was found interacting with cell surface constructs of the SW1353 cells as indicated by the black arrow (**Figure 1E**).

Borrelia burgdorferi Infected Human Cells Differently

Two human cell lines, chondrosarcoma (SW1353) and a dermal fibroblast (BJ), were infected with GFP-mutated strain of *B. burgdorferi* in order to investigate the infectivity of the bacterium in these cells. During a 9-day time period, the differences between the infections of the different cell lines was evident. An overall trend in the infected SW1353 cells was that the amount of cell associated bacteria increased until 48 h (**Figure 2A**). Although infectivity increased in a dose-dependent manner inside a time point, the increase was not significant ($p \leq 0.05$) (**Figures 2A,B**). Conversely, the infectivity of *B. burgdorferi* with the BJ cell line increased gradually reaching a peak at day 9 (**Figure 2C**). Similarly to SW1353 cells, infectivity increased in a dose dependent manner with a significant difference between MOIs 10 and 40 ($p \leq 0.05$) at 48 h (**Figures 2C,D**). Furthermore, at 9 days post-infection, there was a significant increase in the infectivity of BJ cells with MOIs 20 and 40 when compared with 24 h. Noticeably, even at 9 days post-infection, *B. burgdorferi* was not cleared from either cell line.

Since the infectivity of *B. burgdorferi* with these two human cell lines demonstrated to be different, an additional experiment measuring the GFP signal from the infected samples at 24 h and 9 days was performed. Using a 40× objective, a total of 30 images of clusters of cells with a confocal microscope were taken, each from the middle of the cells, and analyzed for GFP signal intensities. The mean values for each image were combined and averaged, and a comparison between the time points was carried out (**Supplementary Figure 1**). There was a significant decrease ($p \leq 0.005$) of GFP signal in the later time point in the infected SW1353 cells, while, the GFP signal

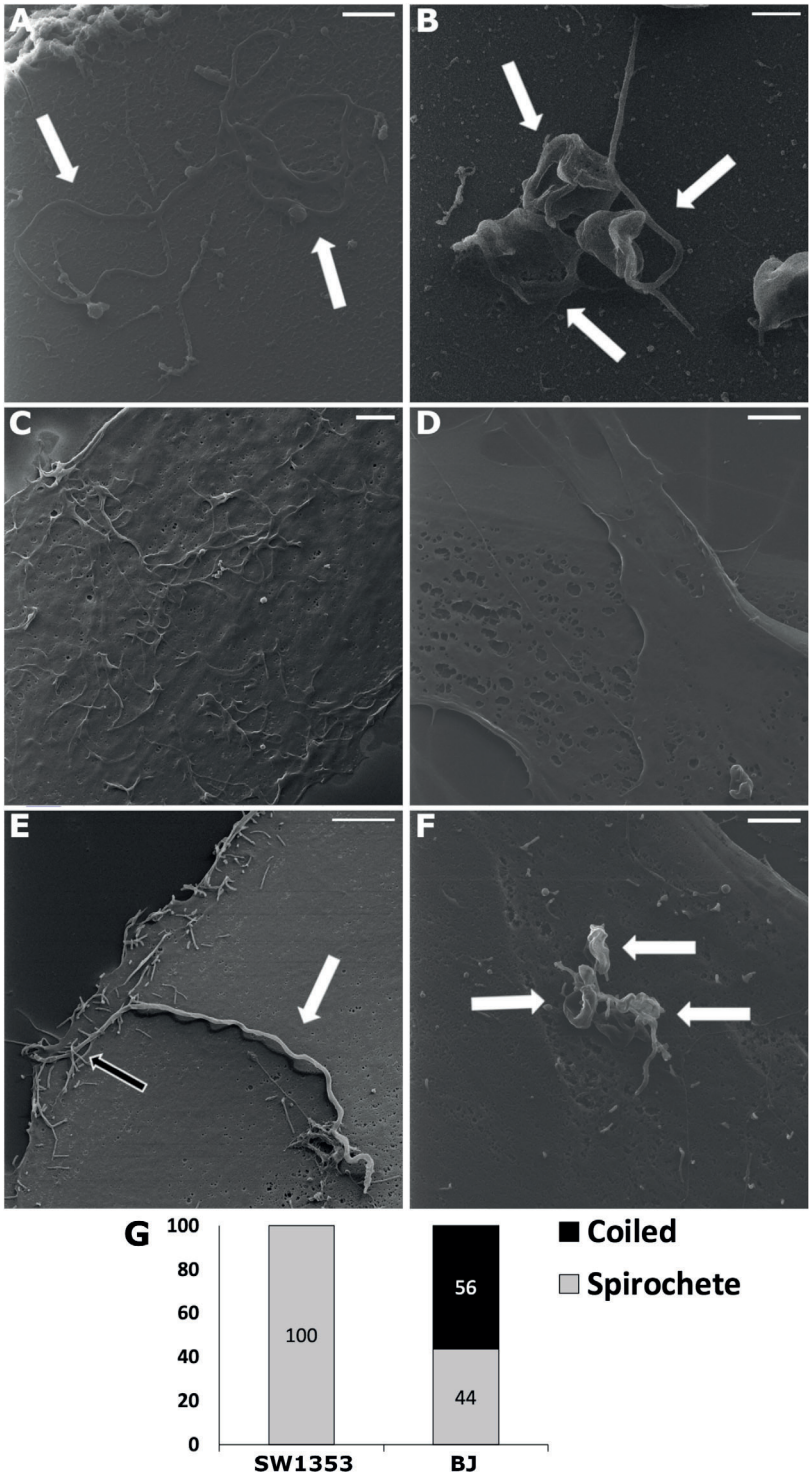

FIGURE 1 | Upon infection, human cell lines demonstrated *Borrelia burgdorferi* forms differently. Helium ion microscopy (Zeiss Orion Nanofab) images of *Borrelia* spirochetes **(A)** and round bodies **(B)**, as well as, uninfected chondrosarcoma (SW1353) **(C)** and dermal fibroblast (BJ) **(D)** cells. **(E,F)** *Borrelia* spirochetes and coiled forms invaded SW1353 and BJ cells, respectively, at 30 min post-infection. **(G)** A total of 20 infected human cells were counted and the different *B. burgdorferi* forms were analyzed. Graph presents spirochete and coiled forms attached to SW1353 and BJ cells in percentages. White arrows indicating *Borrelia*, while the black arrow points to cellular interactions with the bacterium. Scale bars **(A–C)**: 1 μm, **(D–F)**: 2 μm. Representative images from two separate experiments.

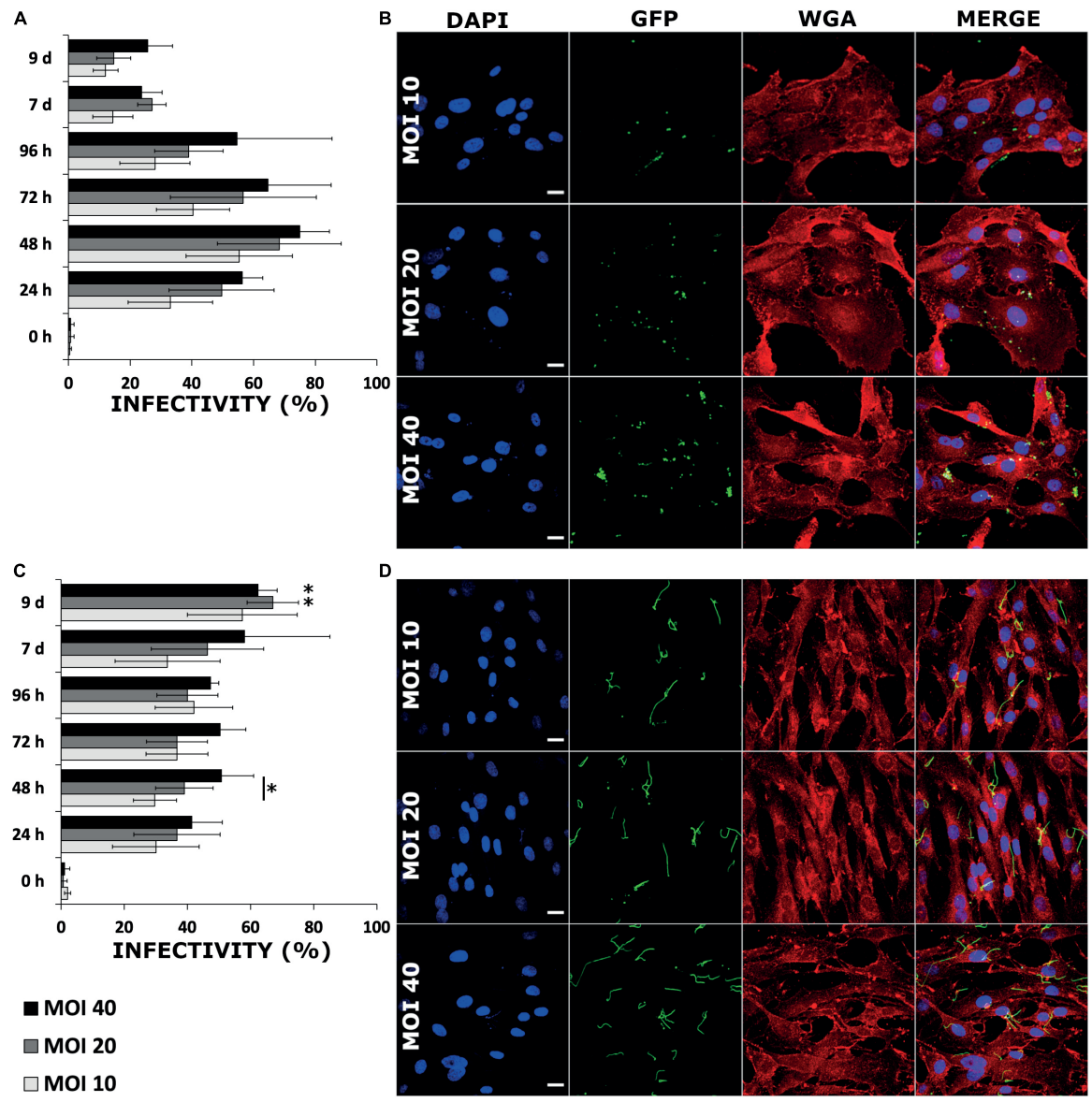

FIGURE 2 | *Borrelia burgdorferi* infected human cells in a dose dependent manner without losing infectivity even after 9 days. SW1353 **(A,B)** and BJ **(C,D)** cells were infected with *B. burgdorferi* strain GCB726 with green fluorescent protein (GFP) (*B. burgdorferi*). A cell was considered infected when *B. burgdorferi* was attached to or inside a cell. Three different multiplicity of infections (MOIs) (10, 20, and 40) were examined over 9 days. In total, 300 cells were counted from three replicate experiments (n = 300). Standard deviation of means from three repeated experiments. Statistical significance with paired independent Student's t-test (*$p \leq 0.05$) was performed for both MOIs in a time point (line with asterisk), as well as, between 24 h and the rest of the time points (asterisk only). Representative confocal micrographs from the 48 h time point for infected SW1353 **(B)**, and BJ **(D)** cells. The nucleus (DAPI) in blue, *B. burgdorferi* (GFP) in green, the cell membrane wheat germ agglutinin (WGA) in red and a merged image of all three channels. Scale bars 20 μm.

intensities did not significantly vary in the BJ cell line between the time points (**Supplementary Figure 1A**). The top two rows in **Supplementary Figure 1B** illustrate the SW1353 cell line for 24 h and 9 days, respectively. The bottom two rows in **Supplementary Figure 1B** represent BJ cell line. As demonstrated in the GFP images, more *B. burgdorferi* were visible in the BJ samples, than in the SW1353 cells.

Human Cells Remained Viable After *Borrelia burgdorferi* Infection

An investigation into cellular viability after *B. burgdorferi* infection was performed. Both human cell lines were infected with three different MOIs (20, 40, and 200) and then counted after four different time points using Trypan Blue. Both infected cell lines grew in a similar manner to the uninfected cells

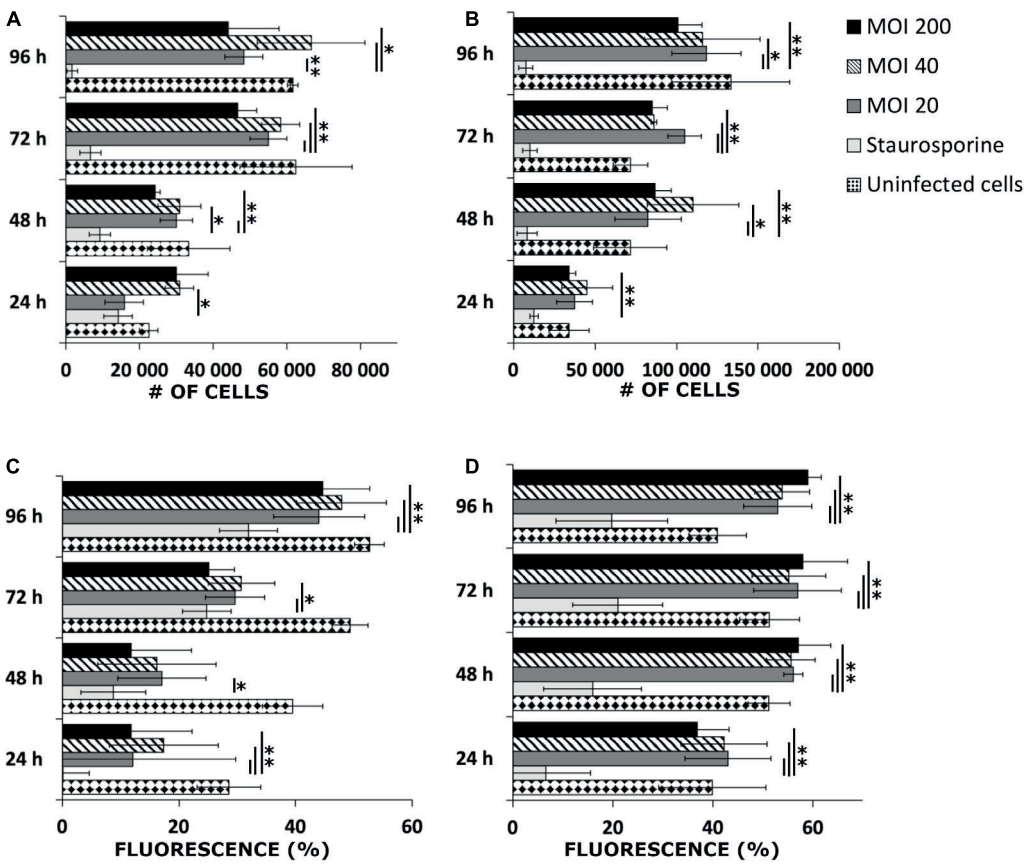

FIGURE 3 | Human cells remained viable after *B. burgdorferi* infection. Representative graphs of viable SW1353 **(A)** and BJ **(B)** cells infected with *B. burgdorferi* at four different time points and cells counted using Trypan Blue stain. Experiments were performed in triplicates and repeated three times. Uninfected cells were negative control, while staurosporine induced apoptotic cells were positive controls for death. MOIs 20, 40, and 200 were used. MitoTracker^{TM} Red CMXRos stain for live mitochondria was used to further verify the viability of the infected cells from three separate experiments. Flow cytometry was used to analyze the samples. A graphical illustration of the fluorescence signal in percentages (%) gathered from SW1353 **(C)** and BJ **(D)** cells, respectively. The same controls and MOIs were used as in the Trypan Blue experiments above. Error bars of standard deviations. Statistical significance was performed with Student's *t*-test ($^{*}p \leq 0.05$; $^{**}p \leq 0.005$).

throughout the 96 h (**Figures 3A,B**). In the infected SW1353 cells, MOI 40 samples had significant replication ($^{*}p \leq 0.05$; $^{**}p \leq 0.005$) in each time point when compared with the staurosporine induced apoptotic cell control (**Figure 3A**). Furthermore, after the first 24 h, each MOI varied significantly from the positive control. Similarly, the infected BJ cells multiplied significantly during the four time points. However, in the BJ cells, MOI 200 samples had significant growth ($p \leq 0.005$) in each time point, with significant growth for MOIs 20 and 40 starting at 48 h (**Figure 3B**). Hence, both cell lines remained viable even with high doses of *B. burgdorferi*.

In addition, viable mitochondria were stained and analyzed with a flow cytometer to further confirm the viability of the human cells. MOI 20 differed significantly in each of the four time points with the infected SW1353 cells when compared with the positive control (**Figure 3C**). Quite markedly, a very strong significance ($p \leq 0.005$) in the SW1353 samples was found at 24 and 96 h timepoints for each MOI. In a similar manner, the infected BJ cells demonstrated significantly strong differences between the positive control and the MOIs at each time point (**Figure 3D**). Both cell lines had viable mitochondria even with high MOIs throughout the experimental time points. Hence, it was deduced that the human cells remained viable 96 h post-infection.

Representative dot plots of the flow cytometry analysis, and confocal microscopy images of mitochondria-stained samples from the 96-h time point can be found in **Supplementary Figure 2**. The unstained controls were used to adjust the fluorescence signal. The cell controls were used to denote the viable cell populations in the middle of the plots (red circles), while *B. burgdorferi* is located in the red squares on the left. The infected samples exhibited similar cell patterns to the negative controls in both cell lines (**Supplementary Figures 2A,B**). The confocal micrographs represent the viability of the infected SW1353 and BJ cells, respectively, as seen by staining of the viable mitochondria (MT) in **Supplementary Figures 2C,D**. Only the highest MOI (200) is presented.

Borrelia burgdorferi Could Be Regrown After Internalization Into Human Cells

During the cell survival experiments, the question of whether *B. burgdorferi* remained viable after internalization into the human cells arose. In order to study borrelial survival, the cell lines were infected with *B. burgdorferi* and, after 24 and 72 h post-infection, the washed cell pellets were placed in BSK II media for 6 weeks. By using a fluorescence microscope, *B. burgdorferi* growth was considered positive once a sample contained multiple motile spirochetes, while samples lacking growth had negligible fluorescence signal. During the 6-week growth period, *B. burgdorferi* was observed to grow in total only in one out of nine samples from the SW1353 cells from triplicate experiments at both time points (**Figure 4**). Also, from the BJ cell samples, *B. burgdorferi* was found growing from one out of nine test samples from the 24-h time point. However, a total of six out of nine from the 72-h time point samples had grown by the end of the 6 weeks (**Figure 4**). The data indicated that *B. burgdorferi* was capable of growth after infection for several days, though growth was not observed in all samples.

Borrelia burgdorferi Was Intracellular Even After 9 Days Post-infection

To investigate the intracellular location of *B. burgdorferi*, cryo-EM was employed. Twenty-four hours and 9 days were considered useful time points for visualizing the expected changes in *B. burgdorferi* infectivity, which were evident in the *B. burgdorferi* infection assay mentioned above. The analysis of the GFP and Protein A-gold immunolabeled samples indicated that *B. burgdorferi* was present in the cells even at 9 days post-infection (**Figures 5C,D**). The immunolabeled *B. burgdorferi* (**Figure 5A**) could be found both inside and outside the human cells at both time points. The intracellular locations varied from close to the nucleus, in the cytosol, attached to the plasma membranes, and inside a cellular vesicle (**Figures 5B–E**).

Borrelia burgdorferi Was Not Targeted to Lysosomes

In an effort to determine a possible processing pathway of *B. burgdorferi* inside the human cells, co-localization analysis of GFP and lysosomes was carried out. The analysis was performed at 24 h and 9 days, with a total of 30 cells from three separate experiments. Only cells with a co-localization value of over 5% were considered as co-localized if the Costes' *p*-value was higher than 0.95 (Costes et al., 2004). In **Figure 6**, the representative images of the co-localization analysis are presented. Lysosomes are represented in magenta, GFP (*Borrelia*) in green, and the co-localized pixels are indicated in white. As displayed in the zoomed images (white boxes) of each figure, very little co-localization occurs with *B. burgdorferi* and the lysosomes (**Figures 6A–D**). This indicated that *B. burgdorferi* was not targeted to lysosomes and could avoid degradation by lysosomal enzymes. However, specifically in the SW1353 cell samples (**Figures 6A,B**), it can be seen that *B. burgdorferi* is not in its spirochetal forms but rather in distinguishable RB or coiled shapes.

Table 2 demonstrates the mean values for both co-localized and non-co-localized pixels for the GFP and Lamp2 signals with the number of cells (n) next to each cell line. **Table 2** indicates that there are only two SW1353 cells with an average of 8.5% co-localization of lysosomes with *B. burgdorferi*, and only four BJ cells with 16.4% co-localization value at 24 h. At day 9, the co-localized SW1353 cell numbers increased to 13 with an average co-localization value of 17.5%. Contrary to SW1353 cells, the number of BJ cells with co-localized lysosomes with *B. burgdorferi* dropped to zero at day 9.

Human Cell Lines Displayed *Borrelia burgdorferi* Pleomorphic Forms Differently

During the *B. burgdorferi* infection analysis, the two human cell lines demonstrated a variety of pleomorphic forms. Therefore, an analysis of 300 *B. burgdorferi* from each cell line and time point was performed from confocal images of GFP-labeled *B. burgdorferi*. The different pleomorphic forms of *B. burgdorferi* were divided into spirochetes, blebs, round bodies, aggregates, and damaged (Meriläinen et al., 2015). The specific requirements for each category can be found in **Table 1** in the "Materials and Methods" section. In **Figures 7A,B**, the division of each category in percentages for infected SW1353 and BJ cells, respectively, are shown. The longer the time point, the more pleomorphic forms were identified from both cell lines. Nonetheless, while both cell lines exhibited each of the pleomorphic form, there was a clear difference between the cell lines. SW1353 cells displayed more blebs and RBs during the first 96 h, with an abundance of damaged forms at 7 and 9 days post-infection (**Figure 7A**). For the SW1353 cell samples, there was a steady increase of RBs and a decrease of blebs during the first 96 h. A sudden drop of RBs and an increase of damaged forms at 7–9 days occurred in the SW1353 cells. Hence, the parental spirochetal form changed to the other pleomorphic forms from the beginning, with less than 40% of the population being spirochetes at 24 h (**Figure 7A**). In the infected BJ cells, on the other hand, the spirochetal forms remained the dominant shape throughout the time points with over 50% still as spirochetes at 9 days post-infection (**Figure 7B**). Although there was a somewhat steady increase of blebs, there were only less than 30% of blebs in the whole population at 96 h (**Figure 7B**). At 7 days post-infection, there were a variety of both pleomorphic and damaged forms visible; however, both blebs and RBs, as well as, the damaged forms, accounted for only less than 20% of the forms observed in the infected BJ cells (**Figure 7B**). Interestingly, the number of both blebs and RBs decreased, while the number of spirochetes increased at 9 days post-infection (**Figure 7B**). Furthermore, aggregates steadily increased in the infected BJ cells throughout the analyzed time points. Therefore, the utilization of pleomorphic forms during infection of different human cell lines was regarded as a mechanism to aid in survival and/or persistence for *Borrelia*.

Previous analysis of *Borrelia* survival in MEM media has indicated the maintenance of spirochetal forms (Murgia and Cinco, 2004), while a separate investigation of RPMI-1640 media indicated the induction of RBs, blebs, and damaged spirochetes

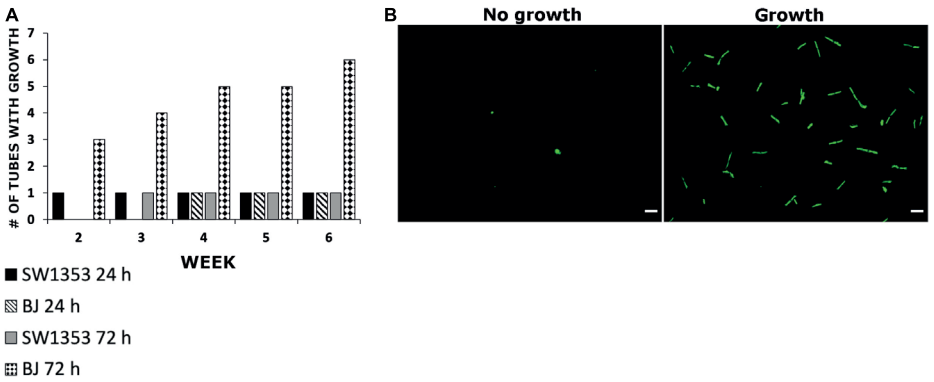

FIGURE 4 | *Borrelia burgdorferi* was able to regrow after being internalized into human cells. **(A)** SW1353 and BJ cells were infected with *B. burgdorferi* for 24 and 72 h, respectively. After each time point, the cells were thoroughly washed with PBS and treated with an acid wash (0.2 M glycine, 0.15 M NaCl, pH 3) for 30 s in order to get rid of any external bacteria. The cells were then placed into BSK II media for 6 weeks and observed weekly for borrelial growth using fluorescence microscopy. Growth was considered when samples contained multiple healthy looking and motile spirochetes **(B)**. The experiments were performed in triplicates and repeated three times, thus, totaling nine tubes for each cell line and time point. Scale bars 30 μm.

(Meriläinen et al., 2016). Therefore, an analysis of *B. burgdorferi* in BJ (MEM) and SW1353 (L-15) media alone for 96 h was performed (data not shown). Mostly spirochetes were seen in MEM, but in L-15, a similar pattern to the formation of especially damaged *Borrelia* as in **Figure 7A** was observed. However, as the included *Borrelia* from the infected cell culture samples had to be either intracellular or attached to the human cells, the formation of different pleomorphic forms could not be solely explained by the unfavorable conditions of the L-15 media even at 9 days. Hence, the results in **Figure 7** are considered valid and due to the differences in the human cells and not in the cell media.

In **Figures 7C–G** representative images of spirochetes, coiling RB, blebs, and RBs, aggregates and damaged forms, respectively, can be observed. As can be seen, the RBs in **Figures 7D,E** have a DNA signal, as well as, a GFP signal, and are wide enough to be categorized as RBs. While the bleb in **Figure 7E** has DNA but lacks the width in the bulge to be considered as an RB. The weak DNA signals in **Figure 7E** have been circled for better visualization. An aggregate with a collection of 10 or more bacterial cells is visualized in **Figure 7F**. A damaged *B. burgdorferi* with a clear lack of DNA signal is exemplified in **Figure 7G**.

DISCUSSION

Borrelia burgdorferi infection can lead to a multisystemic disorder affecting predominantly the skin, joints, and the nervous system. Yet, it remains uncertain how the initial infection can sometimes lead to prolonged distress in patients. *Borrelia* has been shown to infect non-immune cells, such as human foreskin fibroblasts (Georgilis et al., 1992; Klempner et al., 1993), human primary synovial cells (Girschick et al., 1996), human umbilical vein endothelial cells (HUVECs) (Comstock and Thomas, 1989, 1991; Szczepanski et al., 1990; Ma et al., 1991; Livengood and Gilmore, 2006), human neural cells (Strnad et al., 2015), as well as human neuroglial (Rittig et al., 1992; Livengood and Gilmore, 2006; Williams et al., 2018), and neuroblastoma cells (Thomas et al., 1994; Strnad et al., 2015), among others. The bacterium's ability to invade non-phagocytic cells has been suggested as one mechanism for immune evasion (Ma et al., 1991; Klempner et al., 1993; Girschick et al., 1996; Embers et al., 2004; Livengood and Gilmore, 2006; Wu et al., 2011; Naj and Linder, 2015). **Table 3** summarizes studies of different mammalian cell lines infected with *Borrelia* and the adverse outcomes of the infection. In this study, we investigated the infection of two non-phagocytic human cell lines, normal dermal fibroblast (BJ), and chondrosarcoma (SW1353) cells, by *B. burgdorferi*, and the outcome of the infection for both the human, as well as, the bacterial cells.

Differential Borrelial Attachment and Entry Process Exhibited by Different Cell Lines

Pathogens can highjack cellular actin structures and utilize them for invasion purposes (Rottner et al., 2017; Stradal and Schelhaas, 2018). Several bacteria species are known to exploit cellular surface extensions for attachment and invasion into eukaryotic cells. For example, *Salmonella typhimurium*, a flagellated bacterium, stops and scans the surface of the cell, such as membrane ruffles, for the best entry site (Misselwitz et al., 2012). In a study where primary monocytes were infected with a variety of spirochetes, coiling but not conventional phagocytosis of *B. burgdorferi* could be increased with membrane ruffling inducing chemicals (granulocyte-macrophage colony-stimulating factor and phorbol myristate acetate) (Rittig et al., 1998). Studies with the bacterium *Shigella* have demonstrated a capture mechanism by nanometer thin micropodial extensions, which help the bacteria invade the cell by bringing it into close contact with the cell membrane (Romero et al., 2011). Similarly, invasion of a variety of different host cells by *B. burgdorferi* have been exhibited to include protrusions from the host cell. For example, in phagocytic cells such as macrophages

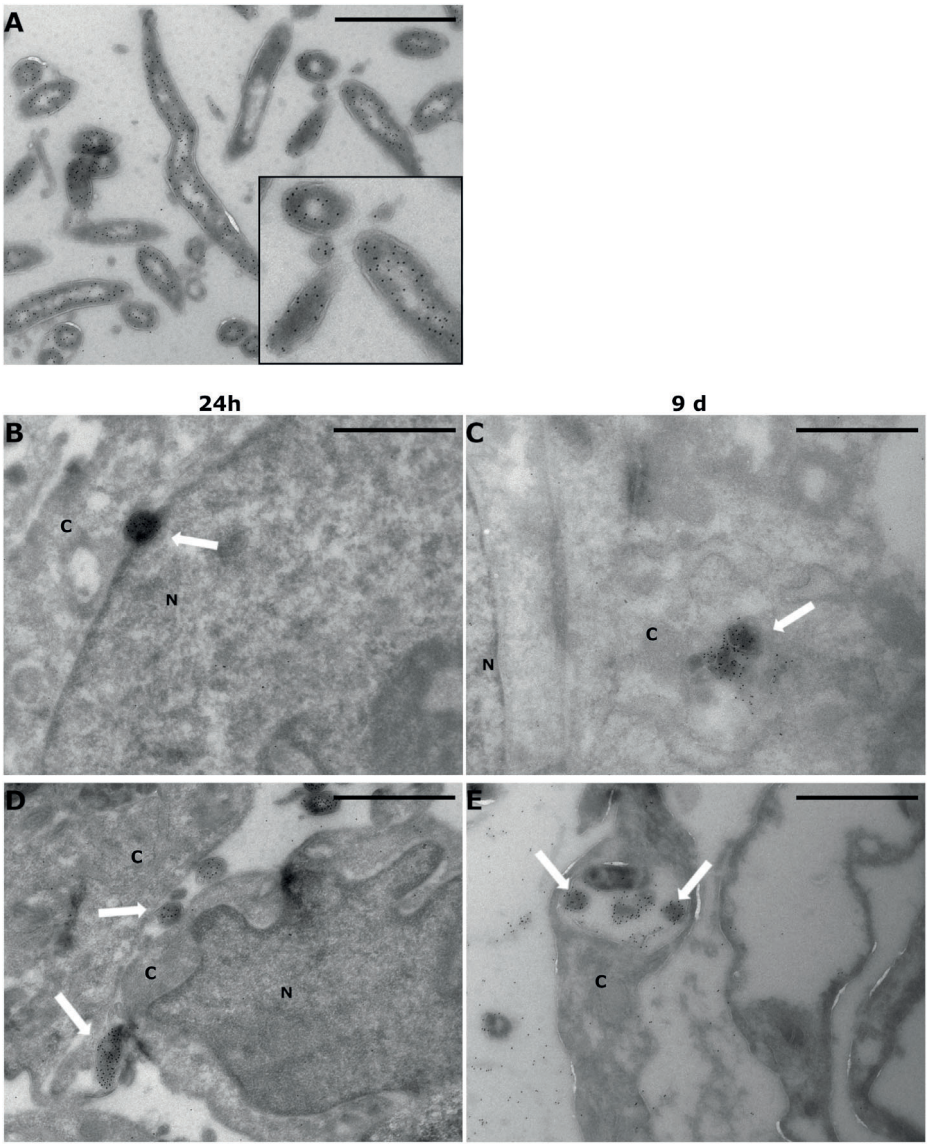

FIGURE 5 | *Borrelia burgdorferi* was found inside human cells even after 9 days post-infection. SW1353 and BJ cells were infected with *Borrelia* GCB726 strain with GFP for 24 h and 9 days. Infected cells were prepared for cryo-electron microscopy with GFP immunolabeling using anti-GFP antibody and Protein A-gold particles (diameter 10 nm). Transmission electron microscopy (JEOL JEM1400) was utilized in visualizing the samples. **(A)** *Borrelia* control with a zoomed image (black box), **(B,C)** SW1353 samples at 24 h and 9 days, respectively, and at the bottom the infected BJ cells **(D,E)**. White arrows indicate *Borrelia* in the infected samples. Cytoplasm (C) and nucleus (N) of the cells are indicated. Scale bars 1 μm.

(Hoffmann et al., 2014; Naj and Linder, 2015; Meriläinen et al., 2016) and dendritic cells (Suhonen et al., 2003), as well as in non-phagocytic neuroglial (Williams et al., 2018) and primary synovial cells (Girschick et al., 1996), *B. burgdorferi* was seen internalized via coiling phagocytosis with pseudopod involvement (**Table 3**). Here *B. burgdorferi* was detected to interact with especially the SW1353 cells, where microscopic, filopodia-like protrusion from the SW1353 cells were observed "grabbing" attached *B. burgdorferi* (**Figure 1E**). In addition, these interactions facilitated a longitudinal but apical tip entry into the SW1353 cells (**Figure 1E**), as outlined in previous studies (Szczepanski et al., 1990; Hechemy et al., 1992; Klempner et al., 1993; Klose et al., 2021). Interaction between BJ cells and *B. burgdorferi* was observed less often (**Figure 1F**) as in other research (Klempner et al., 1993; Rittig et al., 1996), suggesting differences in cellular adhesion by *Borrelia* most likely due to different receptors on the human cells.

Borrelia cell invasion has been investigated in several cell lines, such as macrophages (Rittig et al., 1992, 1994; Montgomery and Malawista, 1996; Naj and Linder, 2015; Meriläinen et al., 2016;

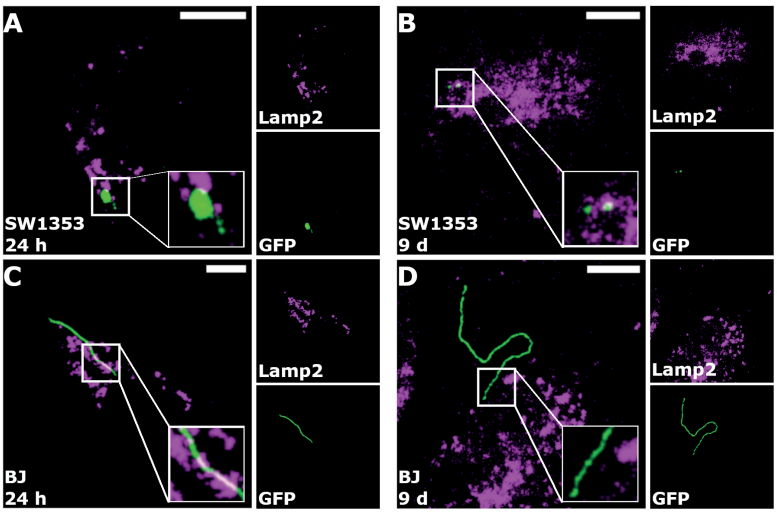

FIGURE 6 | *Borrelia burgdorferi* did not co-localize with lysosomes. Merged representative images of SW1353 **(A,B)** and BJ **(C,D)** cells infected with *B. burgdorferi* at 24 h and 9-day time points, respectively. *Borrelia* fluorescence green, lysosomes in magenta, and co-localized pixels appear white. Zoomed images are shown in the white boxes at the bottom right corners of the merged images. As indicated in the merged images, co-localization of *B. burgdorferi* with lysosomes was not observed. Intermodes threshold was applied to the images before analysis with JaCoP plugin in ImageJ. Scale bars 10 μm.

Klose et al., 2021) and in non-phagocytic cells (Thomas and Comstock, 1989; Georgilis et al., 1992; Klempner et al., 1993; Girschick et al., 1996; Livengood and Gilmore, 2006), as summarized in **Table 3**. *Borrelia* has been described to be internalized by coiling phagocytosis into macrophages (Rittig et al., 1998; Hoffmann et al., 2014; Naj and Linder, 2015; Meriläinen et al., 2016), human dendritic cells (Filgueira et al., 1996; Rittig et al., 1996; Suhonen et al., 2003), as well as, into neuroglial cells (Livengood and Gilmore, 2006; Williams et al., 2018). Specifically, the protein Daam1 (disheveled-associated activator of morphogenesis) has been identified as a regulator for *Borrelia* uptake by filopodia formation and phagocytosis (Hoffmann et al., 2014; Williams et al., 2018). F-actin rich pseudopodia was demonstrated to be used in the pseudopodia engulfment of *Borrelia* in macrophages (Girschick et al., 1996; Meriläinen et al., 2016). We did not observe such coiling by the host in either cell line, which could be due to the early time point (30 min) of the host cell entry experiment (**Figure 1**), or because of a completely different invasion mechanism. However, the interaction between SW1353 cells and *Borrelia* described above, suggest some form of actin filament involvement during host invasion in these cells.

Interestingly, all *B. burgdorferi* attached to SW1353 cells at 30 min were spirochetal formed, while the majority of attached *B. burgdorferi* on infected BJ cells were in coiled forms (**Figure 1G**). *B. burgdorferi* infected murine fibroblast cells exhibited "cyst-like" forms inside these cells (Wu et al., 2011). This suggested alternative entry mechanisms for *Borrelia*, based on the host cell type, as a strategy that may increase immune invasion. Furthermore, Wu et al. (2011) speculated the possibility for the "cyst-like" morphologies to be the result of inactive RB forms, which could revert back to spirochetes after reinstallment into nutritionally replete environment. Moreover, *Borrelia* RBs have been shown to be internalized by coiling phagocytosis less often than spirochetes (Meriläinen et al., 2016), suggesting that the alterations in the membrane receptors affect borrelial invasiveness. Hence, the coiled forms visible in the infected BJ cells observed here (**Figure 1F**) indicate that there could even be different borrelial membrane interactions required for host cell invasion in BJ than in SW1353 cells.

Borrelia infections in HUVEC and HeLa cells have been demonstrated to be time, dose, and temperature dependent (Thomas and Comstock, 1989; Szczepanski et al., 1990; Klempner et al., 1993; Isaacs, 1994). In accordance with previous findings, both infected SW1353 and BJ cells exhibited dose-dependent infectivity by *B. burgdorferi*. However, while the infection increased in a time dependent manner in BJ cells, the amount of infected SW1353 cells peaked at 48 h and decreased subsequently (**Figure 2**). A similar peak at 48 h has been previously shown with HUVE cells (Ma et al., 1991). Curiously, the HUVE cells used in the abovementioned study were normal, non-immortalized cells, similar to our normal dermal fibroblasts, and yet the time dependency results aligned with the immortalized cancerous SW1353 cell line.

Intracellular Persistence

Studies have indicated apoptotic cell death induced by *Borrelia* infection in dermal fibroblasts (Rozwadowska et al., 2017), neural cells (Myers et al., 2009; Ramesh et al., 2013), peripheral T lymphocytes (Sandra et al., 2003), and monocytes (Cruz et al., 2008) among others. Contradictory to previous studies, our dermal fibroblast and chondrosarcoma cells grew similarly to the untreated cells despite being infected with a high MOI (200) (**Figure 3**). However, several other studies have demonstrated corroborating results to ours with viable mammalian cells after

long-term borrelial infection (Thomas et al., 1994; Girschick et al., 1996; Livengood and Gilmore, 2006; Wu et al., 2011).

Furthermore, previous studies have revealed that *B. burgdorferi* can be regrown after being internalized into human cells (Georgilis et al., 1992; Thomas et al., 1994; Livengood and Gilmore, 2006; Wu et al., 2011). Moreover, by analyzing borrelial gene expression with real-time PCR, *Borrelia* have been shown to be metabolically active while internalized inside mouse fibroblast cells (Wu et al., 2011). We also observed *B. burgdorferi* regrowth from washed and pelleted 24 and 72 h infection co-cultures in BSK II supernatant. Although numerous motile spirochetes were observed in only a few samples from both cell lines during the 6-week time period (**Figure 4**), these results supported the previous studies mentioned above, where *B. burgdorferi* regrowth after internalization into human cells was achieved. Hence, similar to previous hypotheses, we propose that both the lack of cytopathic effects and the ability to regrow *Borrelia* from co-cultured samples after removal of external bacteria, suggested that these non-phagocytic cells could serve as a hiding site for *Borrelia* to avoid the host immune system, while simultaneously inducing sustained infection in the host (Ma et al., 1991; Klempner et al., 1993; Girschick et al., 1996; Embers et al., 2004; Livengood and Gilmore, 2006; Wu et al., 2011; Naj and Linder, 2015).

By using cryo-EM, borrelial intracellular location in non-phagocytic human cells could be investigated at an ultrastructural level. Even after 9 days post-infection *B. burgdorferi* was visualized inside the infected human cells at a variety of locations (**Figure 5**). Previous studies have reported *B. burgdorferi* freely in the cytosol, and without signs of degradation, of primary synovial cells after 5 d of co-culture (Girschick et al., 1996). Similarly, in HUVE cells, *B. burgdorferi* was identified moving through the cell monolayer most likely through the tight junctions (Szczepanski et al., 1990), or through the cytoplasm of the host cells (Comstock and Thomas, 1991). Furthermore, in EM visualized infected HUVEC samples, intracellular *B. burgdorferi* was seen surrounded by host membrane (Comstock and Thomas, 1989). Investigation of *B. burgdorferi* infected Vero cells demonstrated the problematic nature of borrelial intracellularity, since the researchers were unable to determine whether *Borrelia* was freely in the cell cytoplasm or enclosed by a membrane (Hechemy et al., 1992). Here, we noticed the bacteria inside these cells both freely in the cytoplasm and enclosed within the host membrane (**Figure 5**). Since the human cells survived, even flourished, during long-term infection with *B. burgdorferi* (**Figure 3**), it was speculated that *B. burgdorferi* utilized the variety of locations inside these cells in order to first escape the possibly hostile external environment, and later being processed by the endosomal processing pathways.

Borrelia have been shown to be processed in the lysosomes of macrophages (Rittig et al., 1994; Montgomery and Malawista, 1996; Naj and Linder, 2015; Meriläinen et al., 2016) and phagolysosomes of dendritic cells (Suhonen et al., 2003). Specifically, we have previously demonstrated that at 24 h, spirochetes co-localized with macrophage lysosome-associated membrane protein 2 (Lamp2) significantly more than RBs (Meriläinen et al., 2016). Here, however, in a co-localization experiment with *Borrelia* and Lamp2, we witnessed a negligible amount of co-localization between *B. burgdorferi* and lysosomes (**Figure 6** and **Table 2**). Similar to previous findings in macrophage (Klose et al., 2019), *B. burgdorferi* was observed in coiled, rounded, and at times damaged-looking forms in SW1353 cells (**Figure 6** and **Table 2**). Additionally, *Borrelia* was more co-localized with lysosomes at day 9 post-infection (**Table 2**), suggesting that *B. burgdorferi* is more actively processed in SW1353 than in BJ cells.

On the other hand, borrelial degradation without lysosomal activity has been demonstrated as well in macrophages and dendritic cells (Rittig et al., 1996). Our previous findings with macrophages have demonstrated that since RBs co-localized with lysosomes less than spirochetes, it would indicate an alternative processing route for RBs in macrophages (Meriläinen et al., 2016). Here, similarly to Meriläinen et al. (2016), since *B. burgdorferi* was observed in other forms than spirochetes in the SW1353 cells (**Figures 6A,B**) it would suggest an alternate processing pathway in these cells.

Furthermore, *Borrelia* has been found as elongated spirochetes in the cytoplasm of macrophages (Naj and Linder, 2015), dendritic cells (Filgueira et al., 1996; Suhonen et al., 2003), fibroblasts (Klempner et al., 1993), HUVECs (Thomas and Comstock, 1989; Szczepanski et al., 1990), and synovial cells (Girschick et al., 1996). Similarly, here *B. burgdorferi* was seen in the cytoplasm of the human cells. Specifically, as exhibited with infected BJ cells (**Figures 2D**, **6C,D**), *Borrelia* did not look damaged and the spirochete appeared free in the cytoplasm, corresponding with the above-mentioned previous results. Again, we demonstrated that *B. burgdorferi* was handled differently between the two human cell lines and indeed can evade the lysosomal pathway aiding in its persistence.

Mechanism of Persistence by Pleomorphic Forms

In order for *Borrelia* to persist in the infected host, it must escape the host immune system. One possible mechanism for borrelial immune evasion currently gaining more support is the persister forms of *Borrelia* (Rudenko et al., 2019). Being a pleomorphic bacterium, *Borrelia* can alter its shape to a metabolically inactive round body, and establish a microcolony or biofilm, especially in unfavorable culture conditions. Specifically, RBs can be induced by osmotic pressure already in 10 min, but also with serum starvation, high temperatures, and changes in pH (Alban et al., 2000; Murgia and Cinco, 2004; Meriläinen et al., 2015; Sharma et al., 2015). Moreover, the formation of biofilms was observed to be temperature, pH, and growth phase dependent (Srivastava and De Silva, 2009). The current investigation demonstrated a

TABLE 2 | *Borrelia burgdorferi* did not co-localize with lysosomes—the number of human cells (n) with average percentages of co-localization between *Borrelia* and lysosomes, and Costes' *p*-value, at 24 h and 9 days post-infection.

	Co-localization (>5%)		*p*-value	No co-localization (<5%)		*p*-value
24 h	SW (*n* = 2)	8.5	100	SW (*n* = 28)	0.32	53.4
	BJ (*n* = 4)	16.4	100	BJ (*n* = 26)	0.55	50.2
9 days	SW (*n* = 13)	17.5	100	SW (*n* = 17)	0.44	43.6
	BJ (*n* = 0)	0	0	BJ (*n* = 30)	0.74	61.2

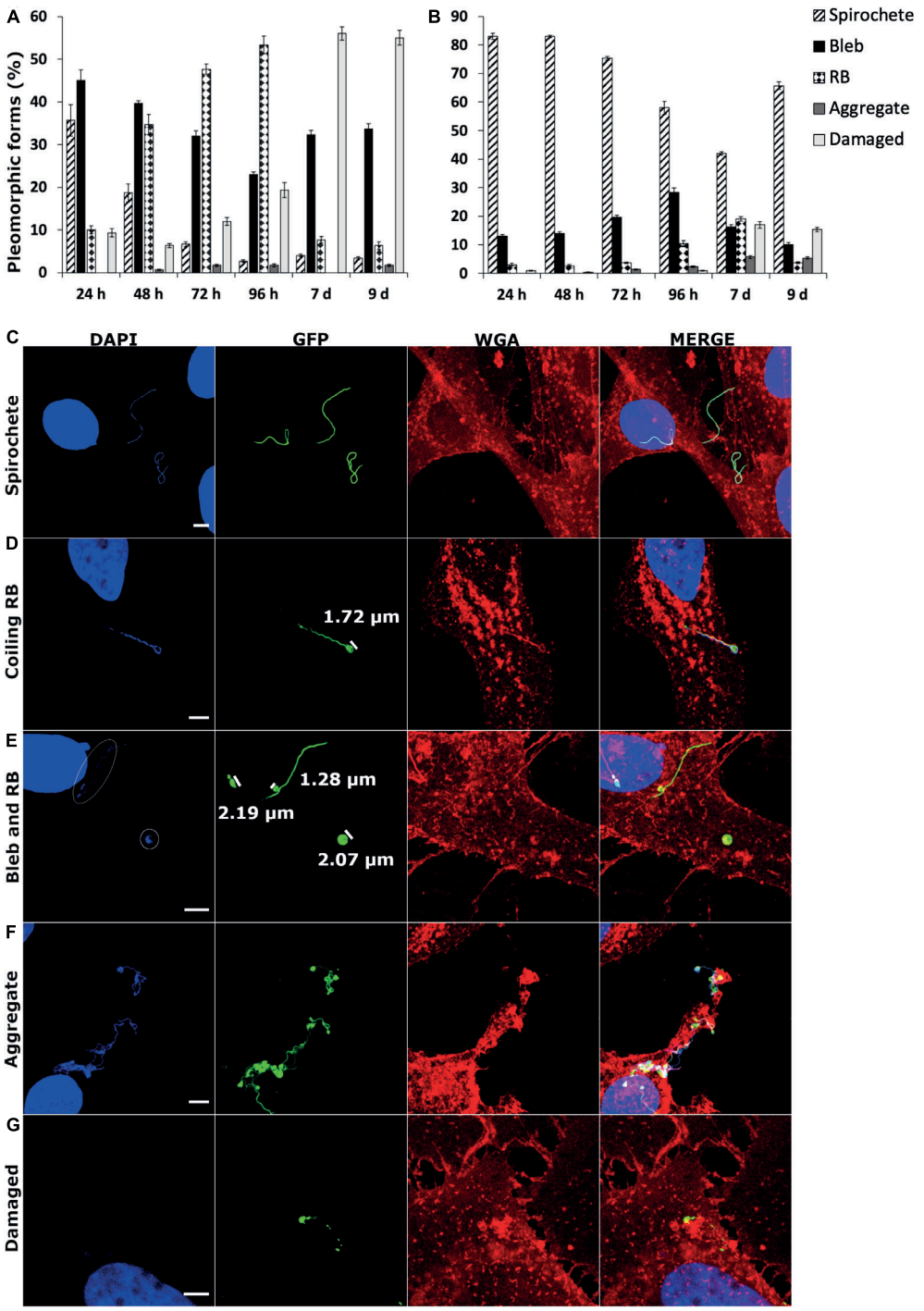

FIGURE 7 | *Borrelia burgdorferi* infection resulted in different formation of pleomorphic forms between the two human cell lines. SW1353 **(A)** and BJ **(B)** cells were infected with *B. burgdorferi* at several time points. A total of 300 *B. burgdorferi* from three experiments were calculated and characterized into spirochete, bleb, round body (RB), aggregate, and damaged categories (the different category definitions can be found in **Table 1** in the "Materials and Methods" section). Different pleomorphic forms in the two human cell lines were observed. **(C)** Three spirochetes are evident, while in panel **(D)**, a coiling RB is visible with the coiling head measuring 1.72 μm. Comparison with a bleb (1.28 μm) to an RB (approximately 2.0 μm) are demonstrated in panel **(E)**. DNA signal from the RB on the right, as well as, from the bleb are indicated in white circles. An aggregate is represented in panel **(F)**, while panel **(G)** indicates a damaged *B. burgdorferi* with a clear lack of bacterial DNA. DNA is visualized in blue (DAPI), *B. burgdorferi* in green (GFP) and the cell membrane in red (WGA). Merged images of the channels are provided. Scale bars 5 μm.

TABLE 3 | Synopsis of previous studies of borrelial infections in a variety of mammalian cell lines.

Host cell (name)	*Borrelia* inoculum	Host cell viability	*Borrelia* viability	Borrelial invasion mechanism	Borrelial location on/inside the cell	Other
HUMAN Endothelial (HUVEC) (Comstock and Thomas, 1989, 1991; Thomas and Comstock, 1989; Szczepanski et al., 1990; Ma et al., 1991; Thomas et al., 1994; Livengood and Gilmore, 2006) Epithelial (HeLa) (Isaacs, 1994)	50×10^6 (Thomas and Comstock, 1989; Comstock and Thomas, 1991; Thomas et al., 1994) MOI 40 (Livengood and Gilmore, 2006) MOI 300 (Isaacs, 1994)	After 4 h (Comstock and Thomas, 1989) and 7 days (Livengood and Gilmore, 2006) of co-culture host cells remained viable (analyzed with trypan blue)		Attachment to the host cell along the length or from the tips of the spirochete (Thomas and Comstock, 1989; Thomas et al., 1994)	Apical surfaces/intercellular spaces/beneath cell monolayer (Szczepanski et al., 1990) and through cytoplasm (Comstock and Thomas, 1991); host membrane bound intracellular bacteria as seen with EM (Comstock and Thomas, 1989)	Attachment was time, dose (Thomas and Comstock, 1989; Szczepanski et al., 1990) and temperature dependent (Isaacs, 1994); internalization peaked at 48 h and was inhibited with 1 μg/ml of cytochalasin D (Ma et al., 1991); attachment could be substantially (60%) inhibited with glycosaminoglycans (Isaacs, 1994)
Primary fibroblast (Georgilis et al., 1992; Klempner et al., 1993; Rittig et al., 1996; Wu et al., 2011)	MOI 10 (Rittig et al., 1996; Wu et al., 2011) $4/40/400 \times 10^6$ (Klempner et al., 1993)	Host remained viable with internalized bacteria (Klempner et al., 1993; Wu et al., 2011)	Internalized *Borrelia* survived 5 days (Klempner et al., 1993) and 14 days (Georgilis et al., 1992) treatment of ceftriaxone, and 5 h treatment with gentamicin (Wu et al., 2011)	Invaginations and extensions into host cytoplasm without any apparent perturbations from the fibroblasts (Klempner et al., 1993; Rittig et al., 1996)	Apical surfaces (Klempner et al., 1993)	Attachment was dose dependent (Klempner et al., 1993); long term internalization and maintenance of viable *Borrelia* by host cells (after 28 days of co-culture) (Wu et al., 2011)
Primary synovial (Girschick et al., 1996)	MOI 100 (Girschick et al., 1996)	Host remained viable in co-culture after 8 weeks (Girschick et al., 1996)	Internalized *Borrelia* survived 9 days treatment of ceftriaxone for 8 weeks (Girschick et al., 1996)	Engulfment without enwrapping of host membrane or phagosome interaction as visualized with EM (Girschick et al., 1996)	After 5 days of co-culture, spirochetes in the host cytoplasm without signs of degradation (Girschick et al., 1996)	Long term internalization and maintenance of viable *Borrelia* by host cells (after over 8 weeks of co-culture) (Girschick et al., 1996)
Neuroglia (H4 and HS-683) (Thomas et al., 1994; Livengood and Gilmore, 2006; Williams et al., 2018) Neuroblastoma (SK-N-MC) (Thomas et al., 1994), (UKF-NB-4) (Strnad et al., 2015)	MOI 10 (Strnad et al., 2015; Williams et al., 2018) MOI 40 (Livengood and Gilmore, 2006) 50×10^6 (Thomas et al., 1994) MOI 100 (Williams et al., 2018)	After 5 h (Strnad et al., 2015) and 7 days (Livengood and Gilmore, 2006) of co-culture host cells remained viable (analyzed with trypan blue)	Viable *Borrelia* after 6 h in DMEM containing 1% antibiotic-antimycotic solution, but motility was lost at 8 h (Strnad et al., 2015); viable internalized *Borrelia* after 4 h incubation with gentamicin (150 g/ml) (Livengood and Gilmore, 2006)	Adherence along the spirochete (Thomas et al., 1994); coiling and conventional phagocytosis as visualized with EM (Livengood and Gilmore, 2006); coiling phagocytosis via Daam1 regulated pseudopods (Williams et al., 2018)		Attachment but no entry in 3 h of co-culture, which might be due to the antibiotics in the culture medium (Strnad et al., 2015)

(Continued)

TABLE 3 | (Continued)

Host cell (name)	*Borrelia* inoculum	Host cell viability	*Borrelia* viability	Borrelial invasion mechanism	Borrelial location on/inside the cell	Other
Primary monocytes and macrophages (Rittig et al., 1992, 1994, 1996, 1998; Girschick et al., 1996; Hoffmann et al., 2014; Naj and Linder, 2015; Klose et al., 2021) Differentiated macrophages (THP-1) (Meriläinen et al., 2016)	MOI 10 (Rittig et al., 1992, 1994, 1996, 1998) MOI 30 (Klose et al., 2021) MOI 40 (Meriläinen et al., 2016) MOI 100 (Hoffmann et al., 2014; Naj and Linder, 2015; Girschick et al., 1996)		Internalized *Borrelia* survived 1 h treatment with 100 mg/ml kanamycin and gentamicin (Naj and Linder, 2015)	Coiled uptake and invagination into the host as visualized with EM (Rittig et al., 1994, 1996); coiling phagocytosis in 40–60% of samples vs. conventional (Rittig et al., 1996, 1998) Daam1 regulated formation of filopodia that capture spirochetes, and formation of coiling pseudopods that enwrap them (Hoffmann et al., 2014; Naj and Linder, 2015); F-actin rich pseudopods in coiling phagocytosis (Girschick et al., 1996; Meriläinen et al., 2016); conventional and coiled phagocytosis (Rittig et al., 1992, 1996; Girschick et al., 1996)	Lysosomal (Rittig et al., 1994; Meriläinen et al., 2016) degradation (Girschick et al., 1996) regulated by Rab5a and Rab22a (Naj and Linder, 2015) with some elongated spirochetes in the cytoplasm (Naj and Linder, 2015); lysosomes localized more with spirochetes than RBs (Meriläinen et al., 2016); *Borrelia* associated membranes contained tunnels, possibly formed when spirochetes had moved, which connected to ER (Klose et al., 2021)	Bacterial degradation lacked lysosomal activity (Rittig et al., 1992, 1996); pseudopods were covered with surplus pseudopods (Rittig et al., 1998); membrane ruffles and coiling but not conventional phagocytosis could be enhanced with specific chemicals (Rittig et al., 1998); cytochalasin D inhibits borrelial entry but not completely (Hoffmann et al., 2014; Meriläinen et al., 2016); *Borrelia* RBs were not internalized using coiling phagocytosis (Meriläinen et al., 2016)
Primary dendritic cell (Filgueira et al., 1996; Rittig et al., 1996; Suhonen et al., 2003)	MOI 10 (Rittig et al., 1996) 100 × 10^6/ml (Klose et al., 2021)			Coiling (Filgueira et al., 1996) and conventional phagocytosis (Rittig et al., 1996); pseudopods coiled along the spirochete or attached to the middle of the bacterium and covered it with a broad pseudopod (Suhonen et al., 2003)	Free in the host cytosol and inside phagolysosomes (Filgueira et al., 1996) or membrane bound but not inside lysosomes (Rittig et al., 1996)	*Borrelia* infection induced IL-8 and DC maturation (Suhonen et al., 2003); bacterial degradation lacked lysosomal activity (Rittig et al., 1996)
PRIMATE Epithelial (Vero) (Georgilis et al., 1992; Hechemy et al., 1992)	200 × 10^6 (Hechemy et al., 1992)		Internalized *Borrelia* survived 14 days treatment with ceftriaxone (Georgilis et al., 1992)	Entry at coated pit associated sites as seen with EM (Hechemy et al., 1992)	Spirochetes were free in the cytoplasm or tightly bound to host membrane (visualized with EM) (Hechemy et al., 1992)	
RODENT Mouse neuroblastoma (N2a) (Strnad et al., 2015) Rat neuroblastoma (B50)* (Rupprecht et al., 2006)	MOI 10 (Strnad et al., 2015) MOI 200 (Rupprecht et al., 2006)	After 5 h (Strnad et al., 2015) of co-culture host cells remained viable (analyzed with trypan blue)	Viable *Borrelia* after 6 h in DMEM containing 1% antibiotic-antimycotic solution, but motility was lost at 8 h (Strnad et al., 2015);	Adherence to host from the tip of the bacterium (Montgomery and Malawista, 1996; Rupprecht et al., 2006)		OspA is necessary for host cell binding; proteoglycans (heparin, heparan sulfate) aid in adherence; formation of blebs was frequent (Rupprecht et al., 2006)
Mouse macrophage (primary) (Rittig et al., 1992, 1996), (J774) (Montgomery and Malawista, 1996)	MOI 10 (Rittig et al., 1992, 1996) 100 × 10^6/ml (Montgomery and Malawista, 1996)			Adherence to host from the tip of the bacterium (Montgomery and Malawista, 1996); conventional and coiling phagocytosis (Rittig et al., 1992), with preference toward coiling phagocytosis (>50%) (Rittig et al., 1996)	Fusion-disintegration of the lamellipodia membranes resulted in the bacteria residing in the cytoplasm (Rittig et al., 1996)	Bacterial degradation lacked lysosomal activity (Rittig et al., 1992, 1996)

(Continued)

TABLE 3 | (Continued)

Host cell (name)	*Borrelia* inoculum	Host cell viability	*Borrelia* viability	Borrelial invasion mechanism	Borrelial location on/inside the cell	Other
Mouse fibroblast (L929) (Wu et al., 2011)	MOI 1/5/10 (Wu et al., 2011)	Host remained viable with internalized bacteria (analyzed with trypan blue) (Wu et al., 2011)	Internalized *Borrelia* survived 5 h treatment with gentamicin for 28 days (Wu et al., 2011)		Extracellular bacteria remained as spirochetes, whilst internalized occasionally were in cyst-like (RB) forms (Wu et al., 2011)	Using RT PCR, *Borrelia* gene transcripts were recovered from lysed co-cultured pellets demonstrating borrelial metabolic activity while internalized; long term internalization and maintenance of viable *Borrelia* by host cells (after 28 days of co-culture); incubation with PP2, a broad-spectrum Src kinase inhibitor, completely inhibited host invasion (Wu et al., 2011)

**Infection with B. garinii.*
MOI = Multiplicity of Infection, RB = round body, RT PCR = Real Time Polymerase Chain Reaction.

marked difference in *B. burgdorferi* pleomorphic forms during a total of 9 days infection period between infected human fibroblast and chondrosarcoma cells. While the majority of *B. burgdorferi* remained as spirochetes during BJ infections, in infected SW1353 cells mostly blebs and RBs, as well as, damaged forms of *B. burgdorferi* were observed (**Figures 7A,B**). "Cyst-like," globular forms of *Borrelia* have been recorded from infected murine fibroblasts (Wu et al., 2011), in HUVE and neuroglial cells (Livengood and Gilmore, 2006), as well as, in macrophages (Naj and Linder, 2015). Naj and Linder (2015) suggested that borrelial compaction into globular forms is in response to the elongated shape of the spirochete, although they also observed a loss of membrane in the phagosomal surface. Since the cell lines used here were non-phagocytic, the observed pleomorphic forms were thought to occur due to the bacterial response to its environment rather than the host cell response to the bacterium.

Studies have noticed that the reversion of long-term H_2O induced RBs took at least 3 months to revert back to spirochetes (Brorson and Brorson, 1998; Gruntar et al., 2001; Murgia and Cinco, 2004). Hence, the attempts to cultivate *Borrelia* from patient samples should take this into account and survey the samples for pleomorphic forms, as well. As can be seen from **Figure 7A**, synovial tissue samples could contain other borrelial pleomorphic forms than spirochetes. Furthermore, the damaged *Borrelia* could cause a prolonged immune reaction, resulting in chronic inflammation of the joints without the existence of live bacteria (Carlson et al., 1999).

CONCLUSION

In this study, we demonstrated how *B. burgdorferi* exploited different mechanisms in two human cell lines, non-immune and non-phagocytic, to aid in its persistence. The utilization of the host cell surface extensions and differences in borrelial shapes while invading the host cells, as well as the differences in intracellular handling of the bacteria, confer *Borrelia* fitness for survival. Intracellular persistence of *Borrelia*, due to avoidance of lysosomal co-localization, lack of cytopathic effects, and the ability to change its shape, all provide strategies *Borrelia* can employ for immune evasion and persistence.

DATA AVAILABILITY STATEMENT

The original contributions presented in the study are included in the article/**Supplementary Material**, further inquiries can be directed to the corresponding author/s.

AUTHOR CONTRIBUTIONS

KK took part in conceptualizing the study, performed all the experiments, analyzed the data, and wrote the original draft. JN provided assistance in the lab, in the data analysis, and reviewed the draft. VM supervised the EM, co-localization, and GFP experiments, and reviewed the draft. LG conceptualized the overall study, participated in data analysis, and reviewed the

draft. All authors contributed to the article and approved the submitted version.

FUNDING

This study was funded by the Schwartz Foundation.

ACKNOWLEDGMENTS

The authors would like to thank lab technician Petri Papponen and Miika Leppänen for their expertise in utilizing the helium ion microscope. Thank you to Visa Ruokolainen for his helpful advice in handling the confocal microscopes and useful tips in processing images with ImageJ. In addition, the authors also thank Biocenter Oulu EM Laboratory for the preparation of the cryo-EM samples.

SUPPLEMENTARY MATERIAL

The Supplementary Material for this article can be found online at: https://www.frontiersin.org/articles/10.3389/fmicb.2021.711291/full#supplementary-material

REFERENCES

Alban, P. S., Johnson, P. W., and Nelson, D. R. (2000). Serum-starvation-induced changes in protein synthesis and morphology of *Borrelia burgdorferi*. *Microbiology* 146, 119–127. doi: 10.1099/00221287-146-1-119

Berndtson, K. (2013). Review of evidence for immune evasion and persistent infection in Lyme disease. *Int. J. Gen. Med.* 6, 291–306. doi: 10.2147/IJGM.S44114

Bolte, S., and Cordelières, F. P. (2006). A guided tour into subcellular colocalization analysis in light microscopy. *J. Microsc.* 224, 213–232. doi: 10.1111/j.1365-2818.2006.01706.x

Brorson, Ø, and Brorson, S. H. (1998). A rapid method for generating cystic forms of *Borrelia burgdorferi*, and their reversal to mobile spirochetes. *APMIS* 106, 1131–1141. doi: 10.1111/j.1699-0463.1998.tb00269.x

Burgdorfer, W., Barbour, A. G., Hayes, S. F., Benach, J. L., Grunwaldt, E., and Davis, J. P. (1982). Lyme disease-a tick-borne spirochetosis? *Science* 216, 1317–1319.

Carlson, D., Hernandez, J., Bloom, B. J., Coburn, J., Aversa, J. M., and Steere, A. C. (1999). Lack of *Borrelia burgdorferi* DNA in synovial samples from patients with antibiotic treatment-resistant Lyme arthritis. *Arthritis Rheum.* 42, 2705–2709. doi: 10.1002/1529-0131(199912)42:12<2705::AID-ANR29<3.0.CO;2-H

Chen, L., Li, Q., Wang, J., Jin, S., Zheng, H., Lin, J., et al. (2017). MiR-29b-3p promotes chondrocyte apoptosis and facilitates the occurrence and development of osteoarthritis by targeting PGRN. *J. Cell. Mol. Med.* 21, 3347–3359. doi: 10.1111/jcmm.13237

Comstock, L. E., and Thomas, D. D. (1989). Penetration of endothelial cell monolayers by *Borrelia burgdorferi*. *Infect. Immun.* 57, 1626–1628. doi: 10.1128/iai.57.5.1626-1628.1989

Comstock, L. E., and Thomas, D. D. (1991). Characterization of *Borrelia burgdorferi* invasion of cultured endothelial cells. *Microb. Pathog.* 10, 137–148. doi: 10.1016/0882-4010(91)90074-K

Cossart, P., and Helenius, A. (2014). Endocytosis of viruses and bacteria. *Cold Spring Harb. Perspect. Biol.* 6:a016972. doi: 10.1101/cshperspect.a016972

Costes, S. V., Daelemans, D., Cho, E. H., Dobbin, Z., Pavlakis, G., and Lockett, S. (2004). Automatic and quantitative measurement of protein-protein colocalization in live cells. *Biophys. J.* 86, 3993–4003.

Cruz, A. R., Moore, M. W., La Vake, C. J., Eggers, C. H., Salazar, J. C., and Radolf, J. D. (2008). Phagocytosis of *Borrelia burgdorferi*, the Lyme disease spirochete, potentiates innate immune activation and induces apoptosis in human monocytes. *Infect. Immun.* 76, 56–70. doi: 10.1128/IAI.01039-07

Embers, M. E., Ramamoorthy, R., and Philipp, M. T. (2004). Survival strategies of *Borrelia burgdorferi*, the etiologic agent of Lyme disease. *Microbes Infect.* 6, 312–318. doi: 10.1016/j.micinf.2003.11.014

Filgueira, L., Nestlé, F. O., Rittig, M., Joller, H. I., and Groscurth, P. (1996). Human dendritic cells phagocytose and process *Borrelia burgdorferi*. *J. Immunol.* 157, 2998–3005.

Georgilis, K., Peacocke, M., and Klempner, M. S. (1992). Fibroblasts protect the lyme disease spirochete, *Borrelia burgdorferi*, from ceftriaxone in vitro. *J. Infect. Dis.* 166, 440–444. doi: 10.1093/infdis/166.2.440

Girschick, H. J., Huppertz, H. I., Russman, H., Krenn, V., and Karch, H. (1996). Intracellular persistence of *Borrelia burgdorferi* in human synovial cells. *Rheumatol. Int.* 16, 125–132. doi: 10.1007/BF01409985

Gruntar, I., Malovrh, T., Murgia, R., and Cinco, M. (2001). Conversion of *Borrelia garinii* cystic forms to motile spirochetes in vivo. *APMIS* 109, 383–388.

Hechemy, K. E., Samsonoff, W. A., Harris, H. L., and McKee, M. (1992). Adherence and entry of *Borrelia burgdorferi* in vero cells. *J. Med. Microbiol.* 36, 229–238. doi: 10.1099/00222615-36-4-229

Hoffmann, A. K., Naj, X., and Linder, S. (2014). Daam1 is a regulator of filopodia formation and phagocytic uptake of *Borrelia burgdorferi* by primary human macrophages. *FASEB J.* 28, 3075–3089. doi: 10.1096/fj.13-247049

Huttunen, M., Waris, M., Kajander, R., Hyypia, T., and Marjomaki, V. (2014). Coxsackievirus A9 infects cells via nonacidic multivesicular bodies. *J. Virol.* 88, 5138–5151. doi: 10.1128/jvi.03275-13

Hyde, J. A. (2017). Borrelia burgdorferi keeps moving and carries on: a review of borrelial dissemination and invasion. *Front. Immunol.* 8:114. doi: 10.3389/fimmu.2017.00114

Isaacs, R. D. (1994). *Borrelia burgdorferi* bind to epithelial cell proteoglycans. *J. Clin. Invest.* 93, 809–819. doi: 10.1172/JCI117035

Kameyama, S., Horie, M., Kikuchi, T., Omura, T., Tadokoro, A., Takeuchi, T., et al. (2007). Acid wash in determining cellular uptake of fab/cell-permeating peptide conjugates. *Biopolymers* 88, 98–107. doi: 10.1002/bip.20689

Kersten, A., Poitschek, C., Rauch, S., and Aberer, E. (1995). Effects of penicillin, ceftriaxone, and doxycycline on morphology of Borrelia burgdorferi. *Antimicrob. Agents Chemother.* 39, 1127–1133. doi: 10.1128/AAC.39.5.1127

Klempner, M. S., Noring, R., and Rogers, R. A. (1993). Invasion of human skin fibroblasts by the lyme disease spirochete, *Borrelia burgdorferi*. *J. Infect. Dis.* 167, 1074–1081. doi: 10.1093/infdis/167.5.1074

Klose, M., Salloum, J. E., Gonschior, H., and Linder, S. (2019). SNX3 drives maturation of *Borrelia* phagosomes by forming a hub for PI(3)P, Rab5a, and galectin-9. *J. Cell Biol.* 218, 3039–3059. doi: 10.1083/JCB.201812106

Klose, M., Scheungrab, M., Luckner, M., Wanner, G., and Linder, S. (2021). FIB-SEM-based analysis of *Borrelia* intracellular processing by human macrophages. *J. Cell Sci.* 134:jcs252320. doi: 10.1242/jcs.252320

Liu, C. C., Zhang, Y., Dai, B. L., Ma, Y. J., Zhang, Q., Wang, Y., et al. (2017). Chlorogenic acid prevents inflammatory responses in IL-1β-stimulated human SW-1353 chondrocytes, a model for osteoarthritis. *Mol. Med. Rep.* 16, 1369–1375. doi: 10.3892/mmr.2017.6698

Livengood, J. A., and Gilmore, R. D. (2006). Invasion of human neuronal and glial cells by an infectious strain of *Borrelia burgdorferi*. *Microbes Infect.* 8, 2832–2840. doi: 10.1016/j.micinf.2006.08.014

Lorenz, M., Yamaguchi, H., Wang, Y., Singer, R. H., and Condeelis, J. (2004). Imaging sites of N-WASP activity in lamellipodia and invadopodia of carcinoma cells. *Curr. Biol.* 14, 697–703. doi: 10.1016/j.cub.2004.04.008

Ma, Y., Sturrock, A., and Weis, J. J. (1991). Intracellular localization of Borrelia burgdorferi within human endothelial cells. *Infect. Immun.* 59, 671–678.

Mead, P. S. (2015). Epidemiology of lyme disease. *Infect. Dis. Clin. North Am.* 29, 187–210. doi: 10.1016/j.idc.2015.02.010

Meriläinen, L., Brander, H., Herranen, A., Schwarzbach, A., and Gilbert, L. (2016). Pleomorphic forms of *Borrelia burgdorferi* induce distinct immune responses. *Microbes Infect.* 18, 484–495. doi: 10.1016/j.micinf.2016.04.002

Meriläinen, L., Herranen, A., Schwarzbach, A., and Gilbert, L. (2015). Morphological and biochemical features of *Borrelia burgdorferi* pleomorphic forms. *Microbiology* 161, 516–527. doi: 10.1099/mic.0.000027

Miklossy, J., Kasas, S., Zurn, A. D., McCall, S., Yu, S., and McGeer, P. L. (2008). Persisting atypical and cystic forms of *Borrelia burgdorferi* and local inflammation in lyme neuroborreliosis. *J. Neuroinflammation* 5, 1–18. doi: 10.1186/1742-2094-5-40

Misselwitz, B., Barrett, N., Kreibich, S., Vonaesch, P., Andritschke, D., Rout, S., et al. (2012). Near surface swimming of *Salmonella* typhimurium explains target-site selection and cooperative invasion. *PLoS Pathog.* 8:9. doi: 10.1371/journal.ppat.1002810

Montgomery, R. R., and Malawista, S. E. (1996). *Entry of Borrelia Burgdorferi into Macrophages Is End-On and Leads to Degradation in Lysosomes Downloaded From*. Available online at: http://iai.asm.org/ (accessed April 15, 2021)

Moriarty, T. J., Norman, M. U., Colarusso, P., Bankhead, T., Kubes, P., and Chaconas, G. (2008). Real-time high resolution 3D imaging of the lyme disease spirochete adhering to and escaping from the vasculature of a living host. *PLoS Pathog.* 4:e1000090. doi: 10.1371/journal.ppat.1000090

Murgia, R., and Cinco, M. (2004). Induction of cystic forms by different stress conditions in *Borrelia burgdorferi*. *APMIS* 112, 57–62.

Myers, T. A., Kaushal, D., and Philipp, M. T. (2009). Microglia are mediators of *Borrelia burgdorferi*-induced apoptosis in SH-SY5Y neuronal cells. *PLoS Pathog.* 5:e1000659. doi: 10.1371/journal.ppat.1000659

Naj, X., and Linder, S. (2015). ER-coordinated activities of Rab22a and Rab5a drive phagosomal compaction and intracellular processing of borrelia burgdorferi by macrophages. *Cell Rep.* 12, 1816–1830. doi: 10.1016/j.celrep.2015.08.027

Radolf, J. D., Strle, K., Lemieux, J. E., and Strle, F. (2020). Lyme disease in humans. *Curr. Issues Mol. Biol.* 42, 333–384. doi: 10.21775/cimb.042.333

Ramesh, G., Santana-Gould, L., Inglis, F. M., England, J. D., and Philipp, M. T. (2013). The lyme disease spirochete *Borrelia burgdorferi* induces inflammation and apoptosis in cells from dorsal root ganglia. *J. Neuroinflammation* 10:865.

Rittig, M. G., Häupl, T., Krause, A., Kressel, M., Groscurth, P., and Burmester, G. R. (1994). Borrelia burgdorferi-induced ultrastructural alterations in human phacgocytes: a clue to pathogenicity? *J. Pathol.* 173, 269–282. doi: 10.1002/path.1711730311

Rittig, M. G., Jagoda, J. C., Wilske, B., Murgia, R., Cinco, M., Repp, R., et al. (1998). Coiling phagocytosis discriminates between different spirochetes and is enhanced by phorbol myristate acetate and granulocyte-macrophage colony-stimulating factor. *Infect. Immun.* 66, 627–635. doi: 10.1128/iai.66.2.627-635.1998

Rittig, M. G., Krause, A., Haupl, T., Schaible, U. E., Modolell, M., Kramer, M. D., et al. (1992). Coiling phagocytosis is the preferential phagocytic mechanism for *Borrelia burgdorferi*. *Infect. Immun.* 60, 4205–4212. doi: 10.1128/iai.60.10.4205-4212.1992

Rittig, M. G., Kuhn, K. H., Dechant, C. A., Gauckler, A., Modolell, M., Ricciardi-Castagnoli, P., et al. (1996). Phagocytes from both vertebrate and invertebrate species use "coiling" phagocytosis. *Dev. Comp. Immunol.* 20, 393–406. doi: 10.1016/S0145-305X(96)00023-7

Romero, S., Grompone, G., Carayol, N., Mounier, J., Guadagnini, S., Prevost, M. C., et al. (2011). ATP-mediated Erk1/2 activation stimulates bacterial capture by filopodia, which precedes *Shigella* invasion of epithelial cells. *Cell Host Microbe* 9, 508–519. doi: 10.1016/j.chom.2011.05.005

Rottner, K., Faix, J., Bogdan, S., Linder, S., and Kerkhoff, E. (2017). Actin assembly mechanisms at a glance. *J. Cell Sci.* 130, 3427–3435. doi: 10.1242/jcs.206433

Rozwadowska, B., Albertyńska, M., Okła, H., Jasik, K. P., Swinarew, A. S., Mazurek, U., et al. (2017). Induction of apoptosis in normal human dermal fibroblasts infected with *Borrelia burgdorferi* Sensu Lato. *Vector Borne Zoonotic Dis.* 17, 237–242.

Rudenko, N., Golovchenko, M., Kybicova, K., and Vancova, M. (2019). Metamorphoses of lyme disease spirochetes: phenomenon of *Borrelia* persisters. *Parasites Vectors* 12:237. doi: 10.1186/s13071-019-3495-7

Rupprecht, T. A., Koedel, U., Heimerl, C., Fingerle, V., Paul, R., Wilske, B., et al. (2006). Adhesion of Borrelia garinii to neuronal cells is mediated by the interaction of OspA with proteoglycans. *J. Neuroimmunol.* 175, 5–11. doi: 10.1016/j.jneuroim.2006.02.007

Sandra, P., Gianni, P., Mario, P., Marilena, G., Rossella, M., and Marina, C. (2003). Lymphocyte apoptosis co-cultured with Borrelia burgdorferi. *Microb. Pathog.* 35, 139–145. doi: 10.1016/S0882-4010(03)00096-2

Schindelin, J., Arganda-Carreras, I., Frise, E., Kaynig, V., Longair, M., Pietzsch, T., et al. (2012). Fiji: an open-source platform for biological-image analysis. *Nat. Methods* 9, 676–682. doi: 10.1038/nmeth.2019

Sehgal, V. N., and Khurana, A. (2015). Lyme disease/borreliosis as a systemic disease. *Clin. Dermatol.* 33, 542–550. doi: 10.1016/j.clindermatol.2015.05.006

Sharma, B., Brown, A. V., Matluck, N. E., Hu, L. T., and Lewis, K. (2015). Borrelia burgdorferi, the causative agent of lyme disease, forms drug-tolerant persister cells. *Antimicrob. Agents Chemother.* 59, 4616–4624. doi: 10.1128/AAC.00864-15

Shor, S., Green, C., Szantyr, B., Phillips, S., Liegner, K., Burrascano, J. J., et al. (2019). Chronic lyme disease: an evidence-based definition by the ILADS working group. *Antibiot. (Basel)* 8:269. doi: 10.3390/antibiotics8040269

Srivastava, S. Y., and De Silva, A. M. (2009). Characterization of borrelia burgdorferi aggregates. *Vector Borne Zoonotic Dis.* 9, 323–329. doi: 10.1089/vbz.2008.0148

Stanek, G., Wormser, G. P., Gray, J., and Strle, F. (2012). Lyme borreliosis. *Lancet* 379, 461–473.

Stradal, T. E. B., and Schelhaas, M. (2018). Actin dynamics in host–pathogen interaction. *FEBS Lett.* 592, 3658–3669. doi: 10.1002/1873-3468.13173

Strnad, M., Elsterová, J., Schrenková, J., Vancová, M., Rego, R. O. M., Grubhoffer, L., et al. (2015). Correlative cryo-fluorescence and cryo-scanning electron microscopy as a straightforward tool to study host-pathogen interactions. *Sci. Rep.* 5:18029. doi: 10.1038/srep18029

Suhonen, J., Komi, J., Soukka, J., Lassila, O., and Viljanen, M. K. (2003). Interaction between *Borrelia burgdorferi* and immature human dendritic cells. *Scand. J. Immunol.* 58, 67–75. doi: 10.1046/j.1365-3083.2003.01284.x

Szczepanski, A., Furie, M. B., Benach, J. L., Lane, B. P., and Fleit, H. B. (1990). Interaction between *Borrelia burgdorferi* and endothelium in vitro. *J. Clin. Invest.* 85, 1637–1647. doi: 10.1172/JCI114615

Thammasri, K., Rauhamäki, S., Wang, L., Filippou, A., Kivovich, V., Marjomäki, V., et al. (2013). Human parvovirus B19 induced apoptotic bodies contain altered self-antigens that are phagocytosed by antigen presenting cells. *PLoS One* 8:e67179. doi: 10.1371/journal.pone.0067179

Thomas, D. D., Cadavid, D., and Barbour, A. G. (1994). Differential association of *Borrelia* species with cultured neural cells. *J. Infect. Dis.* 169, 445–448. doi: 10.1093/infdis/169.2.445

Thomas, D. D., and Comstock, L. E. (1989). Interaction of lyme disease spirochetes with cultured eucaryotic cells. *Infect. Immun.* 57, 1324–1326. doi: 10.1128/iai.57.4.1324-1326.1989

Williams, S. K., Weiner, Z. P., and Gilmore, R. D. (2018). Human neuroglial cells internalize *Borrelia burgdorferi* by coiling phagocytosis mediated by Daam1. *PLoS One* 13:e0197413. doi: 10.1371/journal.pone.0197413

Wormser, G. P., Dattwyler, R. J., Shapiro, E. D., Halperin, J. J., Steere, A. C., Klempner, M. S., et al. (2006). The clinical assessments treatment, and prevention of lyme disease, human granulocytic anaplasmosis, and babesiosis: clinical practice guidelines by the infectious diseases society of America. *Clin. Infect. Dis.* 43, 1089–1134. doi: 10.1086/508667

Wu, J., Weening, E. H., Faske, J. B., Höök, M., and Skare, J. T. (2011). Invasion of eukaryotic cells by *Borrelia burgdorferi* requires β1 integrins and Src kinase activity. *Infect. Immun.* 79, 1338–1348. doi: 10.1128/IAI.01188-10

Conflict of Interest: Author LG is employed by Te?ted Oy, Jyväskylä, Finland.

The remaining authors declare that the research was conducted in the absence of any commercial or financial relationships that could be construed as a potential conflict of interest.

Publisher's Note: All claims expressed in this article are solely those of the authors and do not necessarily represent those of their affiliated organizations, or those of the publisher, the editors and the reviewers. Any product that may be evaluated in this article, or claim that may be made by its manufacturer, is not guaranteed or endorsed by the publisher.

II

BORRELIA BURGDORFERI OUTER MEMBRANE VESICLES CONTAIN ANTIGENIC PROTEINS BUT DO NOT INDUCE CELL DEATH IN HUMAN CELLS

by

Kati Karvonen, Hanna Tammisto, Jonna Nykky & Leona Gilbert 2022

Microorganisms 2022, 10(2), 212

https://doi.org/10.3390/microorganisms10020212

microorganisms

MDPI

Article

Borrelia burgdorferi Outer Membrane Vesicles Contain Antigenic Proteins, but Do Not Induce Cell Death in Human Cells

Kati Karvonen [1,*], Hanna Tammisto [1], Jonna Nykky [1] and Leona Gilbert [2,*]

[1] Department of Biological and Environmental Science and Nanoscience Center, University of Jyvaskyla, P.O. Box 35, FI-40014 Jyvaskyla, Finland; tammisto.hanna@gmail.com (H.T.); jonna.nykky@jyu.fi (J.N.)
[2] Te?ted Oy, Mattilanniemi 6-8, FI-40100 Jyvaskyla, Finland
* Correspondence: kati.s.karvonen@jyu.fi (K.K.); leona.gilbert@tezted.com (L.G.)

Abstract: Like many bacterial species, *Borrelia burgdorferi*, the pleomorphic bacterium that causes Lyme borreliosis, produces outer membrane vesicles (OMVs). Borrelial OMVs (BbOMVs) have been identified as containing virulence factors, such as outer surface proteins (Osps) A, B, and C, as well as DNA. However, the pathogenicity of BbOMVs in disease development is still unclear. In this study, we characterized purified BbOMVs by analyzing their size and immunolabeling for known antigenic markers: OspA, OspC, p39, and peptidoglycan. In addition, BbOMVs were cocultured with human non-immune cells for cytotoxicity analysis. The results demonstrated that, on average, the vesicles were small, ranging between 11 and 108 nm in diameter. In addition, both OspA and OspC, as well as Lyme arthritis markers p39 and peptidoglycan, were detected from BbOMVs. Furthermore, BbOMVs were cocultured with non-immune cells, which did not result in cell death. Combined, these results suggested that BbOMVs could participate in the induction of infection by functioning as a decoy for the host immune system. Furthermore, BbOMVs might serve as a means for persistent antigens to remain in the host for prolonged periods of time.

Keywords: Lyme borreliosis; bleb; extracellular vesicle; persistent antigen

Citation: Karvonen, K.; Tammisto, H.; Nykky, J.; Gilbert, L. *Borrelia burgdorferi* Outer Membrane Vesicles Contain Antigenic Proteins, but Do Not Induce Cell Death in Human Cells. *Microorganisms* **2022**, *10*, 212. https://doi.org/10.3390/microorganisms10020212

Academic Editors: Natália Cruz-Martins and Célia F. Rodrigues

Received: 14 December 2021
Accepted: 17 January 2022
Published: 19 January 2022

1. Introduction

Lyme borreliosis (LB), the most common vector-borne disease in North America and Europe [1], is caused by the pleomorphic spirochete bacteria *Borrelia burgdorferi* (*B. burgdorferi*) [2]. LB can present with mild flu-like symptoms with or without a red rash called erythema migrans; however, especially if not treated early, the infection can develop into a more severe multisystemic disorder with manifestations in the skin, joints, central nervous system, and/or heart [3,4]. Currently, the exact mechanisms resulting in prolonged sequelae of the disease are still unknown. However, persistence of the bacterium or bacterial antigens in the host tissue are considered as one possible explanation for continued disease manifestations [5–10].

Bacterial outer membrane vesicles (OMVs) are produced in normal growth cultures by Gram-negative bacteria [11]. Currently, it is believed that OMVs are produced either by blebbing of the bacterial outer membrane or explosive cell lysis [12]. OMVs are spherical, 10–300 nm in size, and contain a single membrane bilayer [11,13]. Furthermore, OMVs consist of similar outer membrane proteins, polysaccharides, and lipids as the membranes of the originating bacterium, and can carry a variety of cargo, including genetic information [11,12,14]. Moreover, OMVs have been identified from in vitro growth cultures, as well as in vivo animal and human fluid and tissue samples [15–20]. Hence, it has been suggested that OMVs function, for example, as a means for the bacterium to react to the surrounding environment, or in inter- and intracellular communication, the transport of biological signals far away from the originating bacterium, the removal of harmful factors

from the surface of the bacterial cell, or as decoy targets for host immune response and transforming agents, among other things [11,12,14,21,22].

B. burgdorferi OMVs (BbOMVs), or blebs, have been purified from naturally producing in vitro cell cultures [23,24] and by chemically inducing the formation of blebs in *Borrelia* cultures [25]. Furthermore, BbOMVs have been visualized from in vivo samples [16]. BbOMVs have been revealed to contain outer surface proteins (Osps) A, B, C, and D, as well as several unidentified proteins with sizes of 14–110 kDa [16,24,26–28], but lack flagellar proteins [16,24,26]. Both linear and circular DNA, from mostly plasmid origin [23,29], as well as plasmid-encoded RNA transcripts, are contained in BbOMVs [30]. In Table 1 below, some of the known characteristics of BbOMVs are listed. Furthermore, BbOMVs have been demonstrated to attach to human umbilical vein endothelial cells [24], as well as bind and enter human fibroblast, dendritic, T, and B cells [31], thus proving the ability of these vesicles to interact with host cells.

Table 1. Known characteristics of *B. burgdorferi* outer membrane vesicles.

Marker	Molecular Mass (kDa)	Reference
OspA	29/31	[16,24–26,28]
OspB	32/34	[16,24–26,28]
OspC	18	[28]
OspD	28/29	[24,25,28]
Lp6.6/La7/p66	8/22/68	[28]
p13	19	[28,32]
p39 (BmpA)	37	[28,32]
Lack of flagella	37.5/41	[16,24,26]
Other unidentified proteins	110/50	[27]
	64/30/28/21/19/15/14	[16]
	23	[26]
	19.5	[25]
Enolase	47	[32]
BSA	66	[27]
Nucleotide form and Origin		
DNA	Linear/circular	[23]
	Linear/circular plasmids	[29]
	Linear chromosomal	[29]
RNA transcripts	Mostly from plasmids	[30]
Other Markers		
Porins	0.6/12–13 nS	[25]
Diameter (chemically produced)	300–1000 nm	[25]

Borrelial whole-cell antigens, as well as peptidoglycan, RNA, and DNA have been detected from tissue samples of both animal and human patients after receiving antibiotic treatment [7–10]. BbOMVs could provide a locus for these antigens, thus affording an explanation for antigenic persistence without the discovery of viable spirochetes from antibiotic treated samples. In this study, the diameter of naturally formed BbOMVs was measured for the first time. Further characterization of BbOMVs by electron microscopic analysis and immunostaining methods was performed. Furthermore, the purified vesicles were cocultured with human non-immune cells for cytotoxicity analysis. The results indicated that BbOMVs were, on average, 33 nm in diameter, and that they contained known antigenic markers OspA, OspC, p39, and peptidoglycan. However, the vesicles did not induce cell death in chondrosarcoma or dermal fibroblast cells after 72 h of coculture.

2. Materials and Methods

2.1. Bacteria Cultures

Infectious *B. burgdorferi* strains B31 (ATCC, 35210) and GCB726 with fluorescent green protein (GCBC), kindly provided by Georges Chaconas [33], were utilized in the experiments. Barbour–Stoenner–Kelly (BSK II) medium [34], without gelatin and supplemented with 6% heat inactivated rabbit serum (Sigma, St. Louis, MO, USA), was used to grow both bacteria at immunologically relevant +37 °C. Low passage number (p8 or less) bacterial cells were used in all experiments. In caspase activation analysis (Section 2.6), round body forms (RBs), used as a control, were induced as previously described [35]. Before each experiment, *B. burgdorferi* cells were counted with a C-Chip DHC-N01 Disposable Haemocytometer (System Neubauer Improved; Digital Bio, Washington, DC, USA).

2.2. Human Cell Cultures

Chondrosarcoma (SW1353, HTB-94) and normal dermal fibroblast (BJ, CRL-2522) cell lines were acquired from American Type Culture Collection. SW1353 and BJ cell lines were utilized for their relevance as a disease-related model for arthritis and skin manifestations, respectively [36,37]. SW1353 cells were grown in Leibovitz's L-15 media (Sigma), supplemented with 10% fetal bovine serum (Gibco, Paisley, UK), 2 mM L-glutamine (Gibco), and 100 IU/mL Penicillin/0.2 mg/mL streptomycin (Gibco) antibiotic cocktail, and incubated at +37 °C with 100% air. BJ cells were grown in Eagle's minimum essential media (Sigma), with the above-mentioned supplements and an additional 1 mM sodium pyruvate (Gibco), and incubated at +37 °C, 5% CO_2.

2.3. BbOMV Purification

BbOMVs were purified as previously described with modifications [24,38]. First, BbOMVs were produced by culturing 100 million *B. burgdorferi* cells in 25 mL of BSK II media to log phased (four days) growth. The bacterial cells were removed by centrifugation at 1000× *g* for 30 min (Thermo Scientific SL 16R Centrifuge, Waltham, MA, USA). By using 0.2 µm filters (Filtropur S plus 0.2, Sarstedt, Numbrecht, Germany) and syringe gravity filtering, the supernatant was further cleared from any bacterial remains. A Leica DM5500 fluorescence microscope with 20× objective, was utilized to confirm the lack of bacteria in the supernatants. Next, the samples were concentrated with 100 kDa Amicon Ultra-15 centrifugal filter unit (Merck, Kenilworth, NJ, USA) spinning at 3000× *g* for 15 min at RT, before ultracentrifugation at 100,000× *g* for 120 min at +4 °C (Beckman Coulter Optima L90-K Ultracentrifuge, 70 Ti-rotor, Brea, CA, USA). The formed BbOMV pellets were resuspended into 50–100 µL of cold 5 mM $MgCl_2$ in PBS, and the protein concentrations were measured using NanoDrop. BbOMVs were stored at +4 °C before being cocultured with human cells within 7 days, and, for SDS-PAGE, stored at −20 °C. Negative stained transmission electron microscopy (TEM) samples were prepared immediately after purification.

2.4. Transmission Electron Microscopy

TEM was utilized in visualizing negatively stained freshly purified and epon embedded BbOMVs. A 10 µL drop of freshly purified BbOMVs, with a protein concentration of 20 mg/mL, was placed on glow discharged (EMS/SC7620 Mini Sputter Coater, Hatfield, PA, USA) grid for 20 s before negative staining with 1% phosphotungstic acid for 30 s. For better visualization of the double membrane of BbOMVs both BbOMV and control sample of *B. burgdorferi* spirochetes were prepared for epon embedded thin sections as previously described [39]. In brief, after BbOMV purification several pellets were combined by centrifugation with Airfuge centrifuge (Beckman Coulter, Brea, CA, USA, A-95 rotor, 22 psi, 30 min) and fixed with 2% glutaraldehyde in 0.1 M phosphate buffer for 10 min. For the control sample, the bacterial cell pellet from the vesicle purification was washed twice with PBS and fixed as above. Both samples were pelleted in a swing-out rotor at 2700× *g* for 10 min RT (Heraus Megafuge 1.0 R, Hanau, Germany). 1% uranyl acetate was

used to stain epon embedded thin sections as previously described [39]. JEOL JEM1400 transmission electron microscope was utilized in imaging all the samples.

During imaging, residual *Borrelia* structures from the purified BbOMV samples was detected. Hence, the ratio of the residual *Borrelia* and BbOMVs was analyzed by counting BbOMVs and *B. burgdorferi* cells from 30 randomly selected images with 20,000× magnification and an area of 5.04 mm^2. Particles with a heterogeneous but rounded shape, sized < 200 nm, with a visible membrane, even if partial, and light or dense inside, were considered as BbOMVs. On the other hand, particles with round or spherical shapes, sized > 200 nm, and visible membrane layer enclosing a dense structure were determined as borrelial residues.

2.5. Characterization of BbOMVs

2.5.1. BbOMV Size Analysis

The size of purified BbOMVs was determined from TEM images of freshly-purified, negatively-stained, and epon-embedded BbOMV samples using ImageJ [40]. After brightness and contrast adjustments, a binary image was formed, from which the number of particles and their surface areas were automatically calculated, and the diameter of each vesicle was determined. The sizes were calculated from three separate BbOMV purifications, with a total of 600 BbOMVs analyzed.

2.5.2. Qubit Analysis

The presence of DNA in the purified BbOMVs was quantified with a Qubit 2.0 fluorometer (Life Technologies, Carlsbad, CA, USA). *B. burgdorferi* cell lysates, from both GCBC and B31 strains, were utilized as positive controls, while albumin was a negative control, and BbOMVs from both borrelial strains were analyzed. A 1 mg/mL protein concentration stock solution from each sample was prepared. Using the broad range assay kit (Qubit dsDNA BR assay kit, 2–1000 ng range, Invitrogen, Eugene, OR, USA) and a sample volume of 5 µL, in 195 µL of Qubit working solution, the samples were analyzed as instructed by the manufacturer. Standard deviations from three replications are presented.

2.5.3. SDS-PAGE

To resolve proteins in BbOMV samples, 12% SDS-PAGE gels were used. The protein concentrations were determined with a NanoDrop One spectrophotometer (Thermo Scientific, Madison, WI, USA) and 20 µg per sample were analyzed. A pre-stained ladder (precision plus protein kaleidoscope pre-stained protein standards, 10–250 kDa, BioRad, Hercules, CA, USA) was used. Albumin (Sigma) was utilized as a positive control for Coomassie staining. Borrelial cell lysates from GCBC and B31 strains, positive controls for borrelial proteins, were lysed by boiling and sonicating *Borrelia* cell pellets at +95 °C for 15 min each. Water was used as a negative control for staining. Both GCBC and B31 *B. burgdorferi* purified BbOMVs were examined. All samples were prepared in Laemmli buffer and boiled twice, for 5 min at +95 °C, before running the gels in 200 V for 30–45 min. Coomassie Brilliant Blue (10–15 min, shaking) and a de-staining solution (10% acetic acid, 20% MeOH) were utilized in visualizing protein bands.

For glycoprotein detection, a Pierce Glycoprotein staining kit (Thermo Fisher Scientific, Rockford, IL, USA) was used, according to manufacturer's instructions. A total of 60 µg of protein for each sample, except for positive and negative controls (provided by the kit), which had 20 µg of protein each, as instructed by the manufacturer, was utilized. Horseradish peroxidase and soybean trypsin inhibitor were the positive and negative controls, respectively, provided by the kit.

Both Coomassie- and glycoprotein-stained gels were imaged with ChemiDoc MP (Bio-Rad, Hercules, CA, USA), and the images further quantified by each lane with the ImageJ gel analyzer tool. The experiments were performed three times.

2.5.4. Western Blot

Western blotting and immunolabeling were utilized in further characterizing the BbOMVs. Proteins were separated by SDS-PAGE, similar to the protocol mentioned above in Section 2.5.3. *B. burgdorferi* cell lysates, from both GCBC and B31 strains, were utilized as positive controls, while albumin was a negative control, for the labels. A total of 100 µg of protein for the BbOMV samples was used. Similarly, for OspC, p39, and peptidoglycan labels, the amount of *B. burgdorferi* cell lysates was 100 µg, while 5 µg was utilized for OspA and *B. burgdorferi* labels. A total of 50 µg of albumin was used in each blot. The proteins were transferred onto nitrocellulose membranes (Protran BA 83, GE Healthcare, Chalfont Saint Giles, UK) by blotting at 100 V for 60 min. The membranes were blocked for unspecific binding with 3% bovine serum albumin (BSA) in TBS, for at least 30 min at RT, or overnight at +4 °C. Immunostaining was performed with the following five primary antibodies: mouse anti-*Borrelia burgdorferi* OspA (Santa Cruz Biotechnology, Dallas, TX, USA, sc-58093), mouse anti-peptidoglycan clone 3F6B3 (Bio Rad, 7263-1006), rabbit anti-p39 (Rockland Antibodies and Assays, 200-401-C17S), rabbit anti-OspC (antibodies-online.com, ABIN964717), and rabbit anti-*Borrelia burgdorferi* (Bio Rad, 1439-9406). The primary antibodies were diluted into 3% BSA, 0.2% Tween20-TBS at a 1:1000 dilution, except for the anti-peptidoglycan, which was used at a 1:200 dilution. The blots were incubated with the primary antibodies for 1 h at RT, while shaken. Four washes followed, 5 min each with washing buffer (0.2% Tween20-TBS), after which the secondary antibodies were incubated for 30 min at RT, while shaken. The secondary antibodies were rabbit anti-mouse (D0306) and swine anti-rabbit (D0314) AP-conjugated antibodies (Agilent Dako, Glostrup, Denmark), and both were used at a 1:500 dilution in 3% BSA, 0.2% Tween20-TBS. Another five washes with washing buffer preceded the equilibration of the membranes in APA buffer (0.1 M tris/HCl, 0.1 M NaCl, 5 mM $MgCl_2$) for 5–10 min, followed by the colorimetric solution (APA buffer, Nitro Blue Tetrazolium (330 µg/mL), 5-bromo-4-chloro-3-indolyl phosphate (165 µg/mL)), which was stopped using dH_2O.

The membranes were imaged with ChemiDoc MP. The specific bands for OspA, OspC, and p39, and the whole lanes for peptidoglycan and *B. burgdorferi* labeled blots were further quantified with the gel analyzer tool in ImageJ. The densitometry values were normalized to the GCBC lysate, except the B31 BbOMV, which was normalized to the B31 lysate. The amount of residual *Borrelia* was taken into consideration by subtracting the percentage value from the analyzed signal intensities of BbOMVs. The experiments were repeated three times.

2.6. Caspase Activation Analysis

In order to investigate the cytotoxic effect of BbOMVs on human cells, flow cytometry analysis of cell viability was performed. The cells were infected as previously described [41]. Briefly, 30,000 SW1353 and BJ cells were seeded onto 24-well plates and allowed to attach overnight. The plates were washed with +37 °C PBS before the addition of *B. burgdorferi* spirochetes and RBs (MOIs 40), as well as 50 µg/mL of BbOMVs. The plates were incubated on ice for 1 h in order to synchronize cell entry, after which each cell line's antibiotic-free media was added to the wells, and the plates were incubated for 72 h at +37 °C. Untreated cells were used as negative control, while 2 h incubation with 1 µM staurosporine (S4400 staurosporine from *Streptomyces* sp., Sigma) was a positive control for apoptosis. After 72 h, the samples were washed twice with +37 °C PBS and trypsinized by placing 150 µL of 0.05% trypsin/EDTA (Sigma) into each well and incubating the plates at +37 °C for 5 min. Once the cells detached from the wells, the activity of trypsin was stopped by the addition of each cell line's media. Guava MultiCaspase FAM kit (4500-0530, Merck, Darmstadt, Germany) utilizes a pan-caspase inhibitor (VAD), which is conjugated to carboxyfluorescein (FAM) fluorochrome and a fluoromethyl ketone group (FMK), which covalently binds the inhibitor to an activated caspase. Furthermore, the kit includes a DNA dye (7-AAD) as an indicator of membrane integrity. Hence, the FAM-VAD-FMK pan-caspase inhibitor, together with the 7-AAD DNA dye, was used to analyze the stage of apoptosis initiated

by caspases in the human cells, according to the manufacturer's instructions. The samples were analyzed in round-bottomed 96-well plates (Corning, Corning, NY, USA) with a Guava® easyCyte 8HT benchtop flow cytometer (Millipore, Burlington, MA, USA), using the following settings: blue and red lasers on, 5-decade acquisition, threshold for forward scatter at 3000, 525/30, and 695/50 nm filters, with 10.6% compensation in the red channel for green signal. The appropriate settings were adjusted using unstained, as well as separately stained, negative and positive control samples. Either 10,000 events or 3 min acquisition time was utilized in acquiring the data in the Guava InCyte 3.0 software, which was also used for data analysis. The viable, early apoptotic, late apoptotic/necrotic, and dead cell populations were distinguished using quadrant regions in the dot plots. Each experiment was performed three times with triplicate samples.

2.7. Statistical Analysis

Statistical analysis was performed for the Caspase activation analysis samples (Section 2.6). A two-tailed, unequal variance student's *t*-test was utilized to compare both the untreated and staurosporine treated controls to the *B. burgdorferi* samples. Significance was assumed for samples with the following levels: * $p \leq 0.05$; ** $p \leq 0.01$; *** $p \leq 0.001$. Microsoft excel was employed in the analysis.

3. Results

3.1. BbOMVs Were on Average 33 nm in Diameter

Ultracentrifugation with filtering and concentration steps was utilized in purifying BbOMVs from log phased *B. burgdorferi* cultures. The purified vesicles were measured from negatively stained TEM micrographs, and their diameters calculated from the widest section of the vesicles (Figure 1). In total, 600 BbOMVs were analyzed with ImageJ, and, based on the diameters, four size categories were established: 0–20 nm, 20.1–60 nm, 60.1–100 nm, and 100.1–140 nm (Figure 1). Most of the analyzed BbOMVs belonged to the 20.1–60 nm category, which contained over 418 vesicles. Only three analyzed vesicles were over 100 nm in diameter (Figure 1). The smallest diameter was 11.41 nm and the largest 107.70 nm, while the average was 33.00 nm. Often, the smaller (<60 nm) vesicles were in clusters while larger ones were found separately.

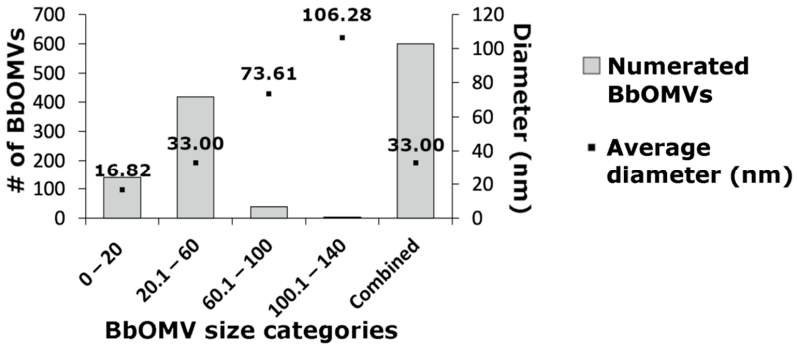

Figure 1. *B. burgdorferi* outer membrane vesicles (BbOMVs) were, on average, 33 nm in diameter. Purified BbOMVs were numerated (n = 600) and their diameters measured from negatively stained transmission electron micrographs, and were then divided into four size categories: 0–20, 20.1–60, 60.1–100, and 100.1–140 nm. The average diameters in each category are presented. The combined average diameter of a BbOMV was 33 nm.

In Figure 2A, BbOMVs of heterogenic, but mostly rounded, shapes with a single membrane bilayer can be observed. Both light and dense BbOMVs were detected. The difference in opacity of the vesicles was most likely due to ruptured membranes, which allowed the stain to leak inside the vesicles (Figure 2A). A control image of *B. burgdorferi* spirochetes with vesicles blebbing off can be distinguished in Figure 2B (white arrows and zoomed image).

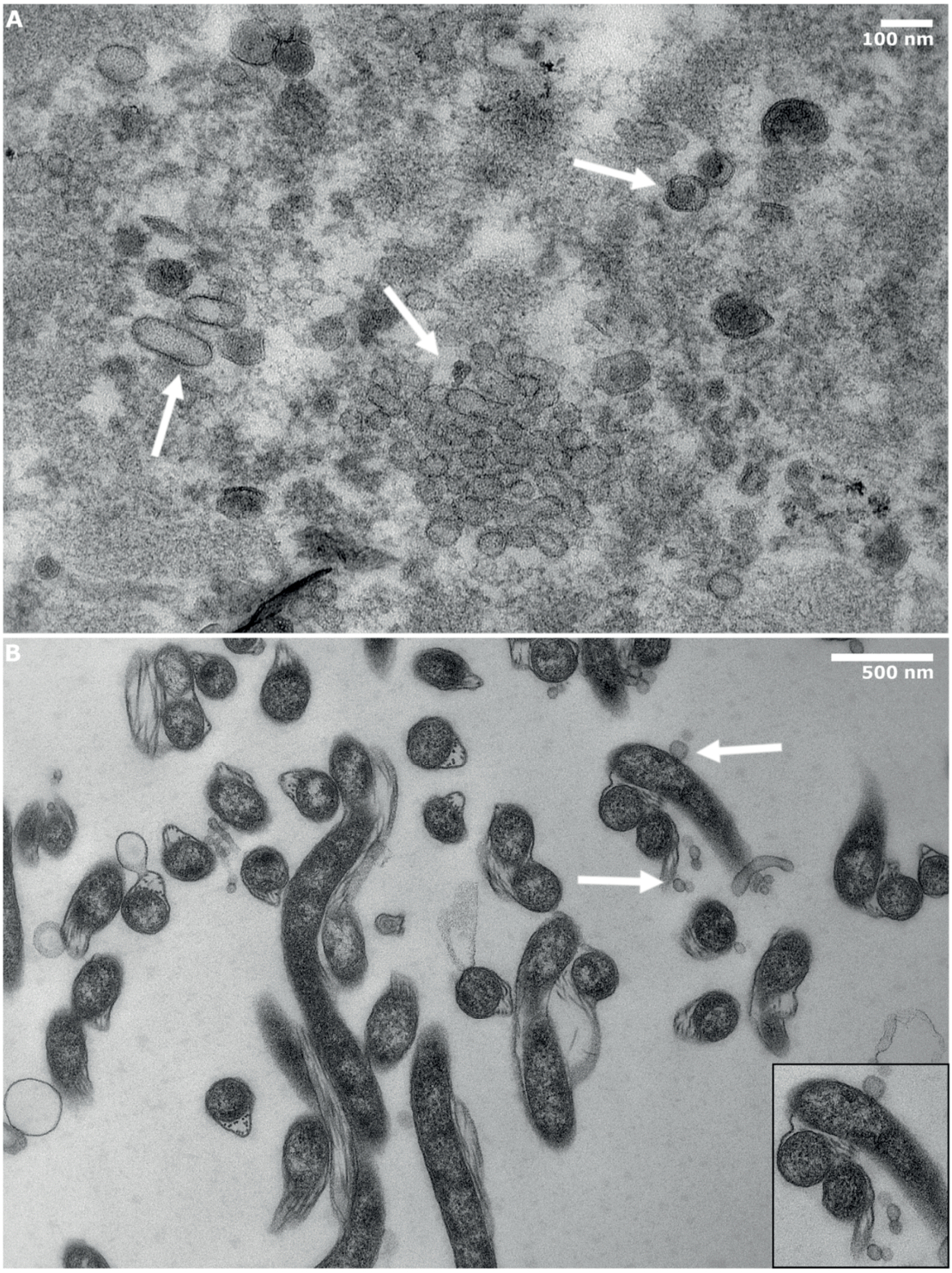

Figure 2. BbOMVs could be successfully and reproducibly purified from *Borrelia* cultures. (**A**) Transmission electron micrographs of epon embedded samples of purified BbOMVs demonstrating spherical shapes with single bilayer membranes. (**B**) As a control for purification, epon embedded *B. burgdorferi* spirochetes with a zoomed image (black box) of blebbing and BbOMVs directly originating from the bacterial cells are presented. White arrows indicate both clusters and separate BbOMVs in the purified vesicle and spirochete samples. Scale bars: A: 100 nm, B: 500 nm.

From epon-embedded BbOMV micrographs, residual *B. burgdorferi* were located (Figure S1). Therefore, the ratio between BbOMVs and residual *Borrelia* was calculated from 30 randomly selected images, where only 1.8% of borrelial spirochetes were detected. Hence, the purification protocol was still considered successful, and the characterization and further utilization of purified BbOMVs was valid.

3.2. Known Antigenic Markers Were Located in BbOMVs

Purified BbOMVs were further characterized for the presence of double-stranded DNA, as well as a variety of proteins and glycoproteins (Figure 3A–C). By utilizing a Qubit assay kit and fluorometer, dsDNA could be easily detected from the purified BbOMVs (Figure 3A, lanes 3–5). Although some background was evident as demonstrated by the signal in the negative control (albumin, lane 2), there was still more signal in the BbOMV samples, suggesting the presence of dsDNA inside the vesicles (Figure 3A, lanes 3–5).

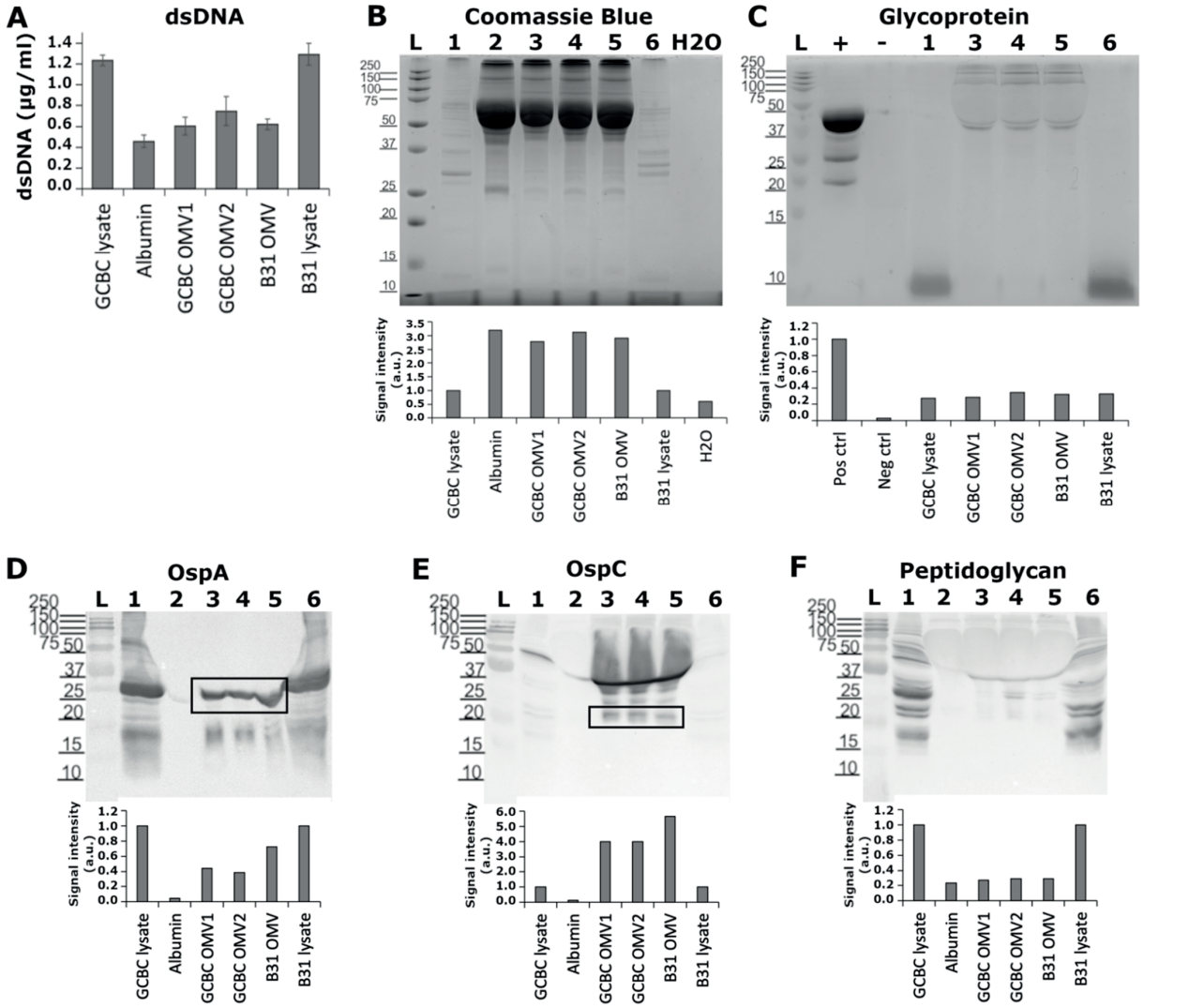

Figure 3. *Cont.*

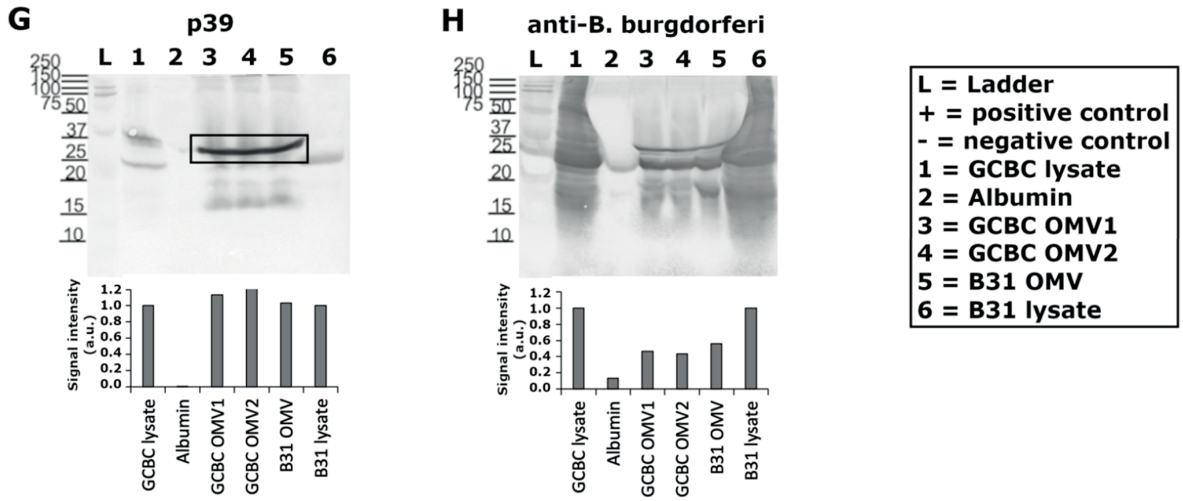

Figure 3. *B. burgdorferi* outer membrane vesicles contained several antigenic markers. (**A**) BbOMVs contained double stranded DNA, which was measured using a Qubit 2.0 fluorometer with a broad-range stain. Standard deviations from triplicate experiments. (**B**) Proteins were resolved with SDS-PAGE and stained with Coomassie Blue, while a Pierce Glycoprotein staining kit (Thermo scientific) was used for visualizing glycoproteins (**C**). Western blot analysis demonstrated known borrelial antigens OspA (**D**), OspC (**E**), peptidoglycan (**F**), and p39 (**G**). Anti-*B. burgdorferi* whole cell antibody was examined as a control (**H**). For the protein analysis, H_2O was used as a negative control, and albumin (lane 2) as a positive control, for the staining. The negative (−, soybean trypsin inhibitor) and positive (+, horseradish peroxidase) controls provided by the glycoprotein staining kit were employed in the analysis. In the Western blots, albumin was utilized as a negative control for the immunolabel. *B. burgdorferi* strains GCBC (lane 1) and B31 (lane 6) bacterial cell lysates were used as positive controls for the labels in each experiment. Lanes 3 and 4 demonstrate BbOMVs purified from CGBC culture, while lane 5 has B31 purified BbOMVs. In order to obtain the full range of signals, the intensity values were analyzed from each lane in the Coomassie Blue and glycoprotein gels, as well as in the peptidoglycan and anti-*B. burgdorferi* labeled blots. Whereas the signals from specific bands representing each expected protein (black box) in OspA, OspC, and p39 blots were examined. Values were normalized to the positive controls: borrelial cell lysates in Coomassie Blue stained gel and western blots, and the kit provided positive control (horseradish peroxidase) in the glycoprotein gel. GCBC BbOMVs and albumin were normalized to GCBC lysates, and the B31 BbOMVs to the B31 lysate. Representative images from three separate experiments.

In Figure 3B–H, the respective images of gels and blots of BbOMVs analyzed for proteins, glycoproteins, and specific protein immunolabels, respectively, are shown. Below each image, the respective densitometry analyses of the labels are reported. Firstly, proteins were visualized with Coomassie Blue stain, which demonstrated visible bands in each lane except the negative control (H_2O) (Figure 3B). Both GCBC and B31 bacterial cell lysates (lanes 1 and 6) demonstrated visible protein bands ranging from 10–250 kDa in size (Figure 3B). The positive control for proteins, albumin (lane 2), exhibited several bands, although the most visible band was ~66 kDa in size, as expected (Figure 3B). However, BbOMVs (lanes 3–5) presented comparable bands, suggesting traces of albumin from the media in the purified vesicle samples. From the densitometry analysis below the gel, this trend can be observed, since albumin (lane 2) had the highest value, closely followed by the BbOMV samples (Figure 3B, lanes 3–5).

Secondly, glycoprotein bands in the BbOMV samples (lanes 3–5) were visible in the range of ~40–250 kDa, while in the lysate controls (lanes 1 and 6) only very small (below 10 kDa) bands were detected (Figure 3C). Moreover, the signal intensity analysis clearly demonstrated the existence of glycoproteins in each sample, as the lysates and BbOMVs had similar intensity values (Figure 3C).

Lastly, the western blot analysis of OspA, OspC, and p39 illustrated visible bands in BbOMV lanes at the expected sizes for each protein: 28, 20.7, and 39 kDa, respectively, as demonstrated by both the representative images and the densitometry analysis for each protein (Figure 3D,E,G, respectively). Curiously, OspC bands were almost undetectable in both bacterial cell lysate lanes, as visualized by the blot and the low signal intensity values in Figure 3E (lanes 1 and 6). Additionally, the lysate bands in the peptidoglycan blot demonstrated a variety of sizes, while BbOMVs illustrated a 37 kDa protein in each lane, and two smaller bands with sizes of 25 and ~26 kDa in one of the BbOMVs (lane 4) (Figure 3F). The signal intensities for BbOMVs (lanes 3–5) in the glycoprotein blot mirrored the blot image, as the signals were not as strong as in the lysate lanes (1 and 6). The final antibody, anti-*B. burgdorferi,* raised against borrelial whole cell lysate, was hence utilized here as a control for the experiment, since it should detect undetermined proteins from BbOMVs. As expected, the lysate bands exhibited strong signals throughout the lanes (Figure 3H, lanes 1 and 6). BbOMV lanes, on the other hand, illustrated smaller proteins, with bands at approximately the same locations as OspA, OspC, and p39, mentioned above (Figure 3H, lanes 3–5), suggesting the validity of the previous labels. Two additional bands were located from the BbOMV lanes (3–5), indicating either labelling of fragmented proteins or further proteins unspecified here (Figure 3H).

3.3. BbOMVs Did Not Induce Cell Death in Human Cells

Flow cytometry was utilized in analyzing the cytotoxic effect of BbOMVs in chondrosarcoma (SW1353) and skin fibroblast (BJ) cells. The cells were treated with *B. burgdorferi* spirochetes, RBs, and BbOMVs for 72 h, and double stained with pan-caspase inhibitor peptide conjugated to a fluorochrome and a ketone group (FAM-VAD-FMK) and a DNA label (7-AAD). Untreated and staurosporine (1 μM) treated cells were controls for viability and death, respectively. The double staining produced quadrant sections by which four different cell populations could be located: viable, early apoptotic, late apoptotic/necrotic and dead cells.

The results demonstrated that neither *B. burgdorferi* spirochetes, nor RBs, nor BbOMVs induced apoptosis in the human cells, since both cell lines, SW1353 and BJ, had over 80% viability after 72 h (Figure 4A,B, respectively). Specifically, in the viable cell population of the SW1353 cells a significant difference ($p \leq 0.05$) was observed between the staurosporine treated cells and the untreated and BbOMV coculture samples (Figure 4A). Moreover, a higher significant difference was detected between staurosporine and *B. burgdorferi* spirochete and RB samples ($p \leq 0.01$) (Figure 4A). In the SW1353 cells, less than 10% of both the untreated and *Borrelia* cocultured samples had early apoptotic or late apoptotic/necrotic cells, respectively, after 72 h (Figure 4A). Furthermore, there were very few dead cells in each sample of SW1353 cells, thus further exhibiting the viability of SW1353 cells even after 72 h co-incubation with *B. burgdorferi* spirochetes, RBs, or BbOMVs.

Similarly, in BJ cells there was minimal amount of early apoptotic (<2%) or dead (<1%) cells in both the untreated and each *Borrelia* cocultured samples (Figure 4B). However, significant differences were observed in both the viable and necrotic cell population of BJ cells. Specifically in the viable BJ cell population a significant difference between the staurosporine treated and untreated ($p \leq 0.01$), and each *Borrelia* cocultured and staurosporine treated sample ($p \leq 0.001$) were observed (Figure 4B). In the necrotic cell population significant differences were analyzed between the staurosporine and the untreated and BbOMV samples ($p \leq 0.01$), as well as, between the staurosporine and *B. burgdorferi* spirochete and RB samples ($p \leq 0.001$) (Figure 4B). Nevertheless, the untreated control exemplified more necrotic cells than *B. burgdorferi* spirochete, RB, or BbOMV cocultured samples, thus, further demonstrating the non-lethal effect of *B. burgdorferi* on BJ cells.

In Figure 4C, a representative dot plot of flow cytometry analysis of SW1353 (top) and BJ (bottom) staurosporine treated, untreated and *B. burgdorferi* BbOMVs, spirochete and RB cocultured samples can be located. In the quadrant plots the viable cell population is in the bottom left corner; the early apoptotic in the bottom right corner; the late apoptotic/

necrotic in the top right corner, and the dead cells in the top left corner. As can be seen from the plots of each sample, the majority of the cell populations are in the viable, bottom left corner, in both human cell lines (Figure 4C).

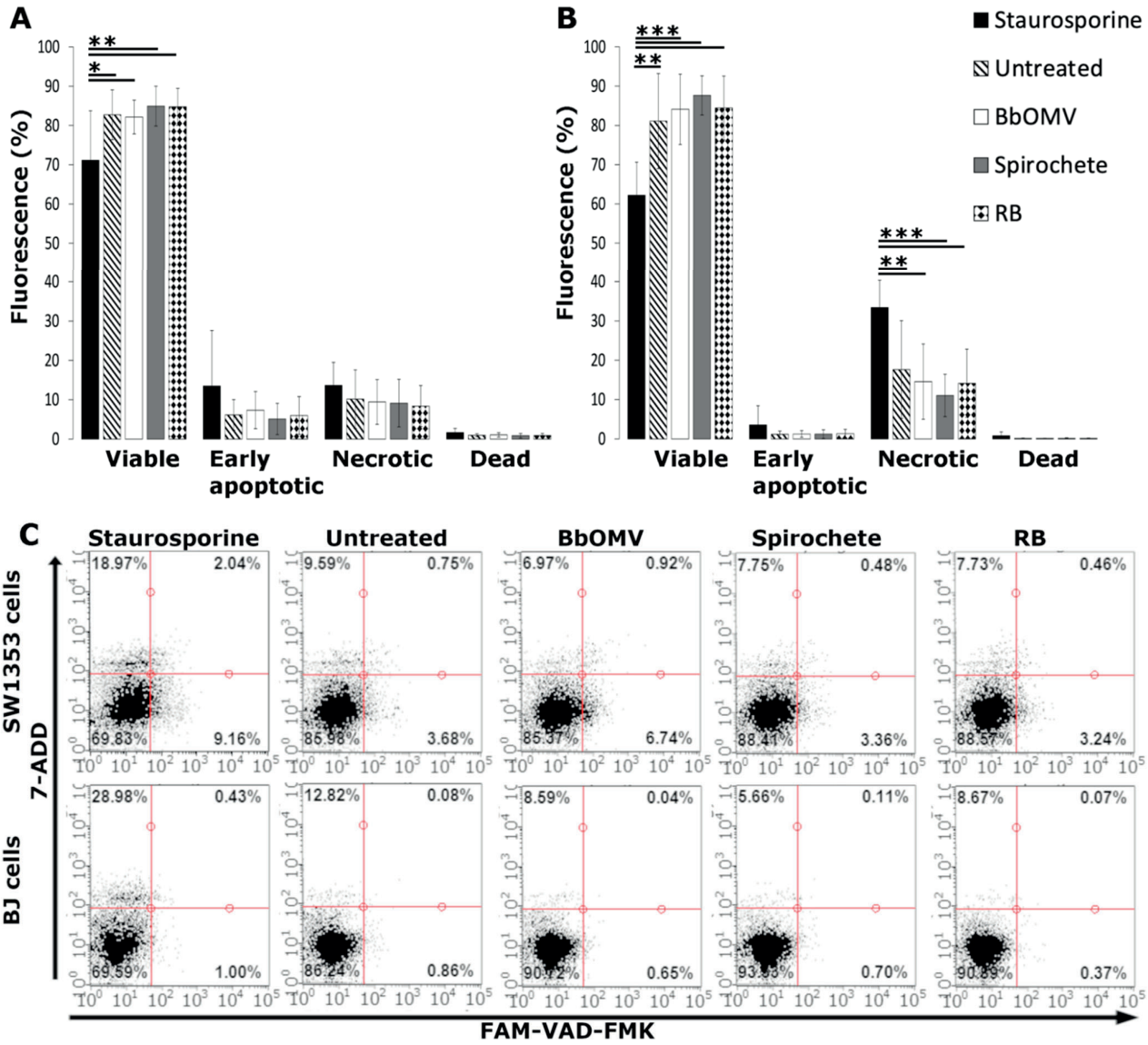

Figure 4. BbOMVs did not induce cell death in human cells. In order to detect different stages of cellular viability after infection, SW1353 (**A**) and BJ (**B**) cells were infected with *B. burgdorferi* spirochetes (MOI 40), RBs (MOI 40) and BbOMVs (50 μg/mL), respectively, for 72 h and double labelled with DNA (7-AAD) and pan-caspase inhibitor-fluorochrome complex (FAM-VAD-FMK) markers. Untreated cells were used as negative control and 1 μM staurosporine treated (2 h) cells were a positive control for apoptosis (cell death). The samples were analyzed with Guava easyCyte 8HT flow cytometer. Standard deviations from triplicate experiments. Statistical significance was compared to both negative and positive controls. * $p \leq 0.05$; ** $p \leq 0.01$; *** $p \leq 0.001$. (**C**) Representative dot plots of SW1353 (top row) and BJ (bottom row) cells from the abovementioned experiment. In the graphs, viable cells are located at the bottom left corner, early apoptotic at the bottom right corner, late apoptotic/ necrotic cells at the top right corner, and dead cells at the top left corner.

4. Discussion

LB can progress into a debilitating and prolonged multisystemic disorder. Currently, it remains unclear how a *B. burgdorferi* infection can, at times, lead to such a sustained state of distress in patients. *Borrelia* is a pleomorphic bacterium with known persister morphologies such as round bodies and biofilms, which might contribute to the persistence of the disease [42–44]. However, the role of borrelial membrane vesicles in the pathogenicity of the disease has not been fully considered. After all, both whole bacterial cells, as well as borrelial antigens, have been detected in human and animal samples after antibiotic treatment [7–10]. The mechanism by which these antigens remain in tissues is not clear, but OMVs could potentially provide both a convenient hiding place and transport system for such persistent antigens. This study examined BbOMVs, first by characterizing them, and later by analyzing the cytotoxic consequences of these vesicles on human cells.

Bacterial OMVs vary in sizes. For instance, enterotoxigenic *Escherichia coli* has been shown to produce extracellular vesicles as large as 300 nm in diameter [45], while *Neisseria gonorrhoeae* produced membrane vesicles as tiny as 6 nm in diameter [23]. In a previous study, the researchers chemically induced borrelial membrane blebbing with citrate buffer and reported the formed BbOMVs to be 300–1000 nm in diameter [25]. Contrarily, we analyzed a total of 600 naturally formed BbOMVs from negatively stained EM micrographs and measured the diameters to range from 11 nm to ~108 nm, with an average of 33 nm (Figure 1). To the best of our knowledge, this is the first time the size of naturally occurring BbOMVs has been reported. Hence, naturally blebbed BbOMVs were 10–30 times smaller on average, than the chemically produced vesicles [25].

Analysis of TEM images demonstrated heterogeneously spherical vesicles with single bilayer membranes with both light and dense contents, thus confirming the purified material as BbOMVs (Figure 2A). Previous work on *Pseudomonas aeruginosa* demonstrated that empty membrane vesicles can take up extracellular DNA [46], further validating the role of extracellular vesicles as an instrument of communication for both the "sender" and the "receiver" of the vesicle. Hence, it was considered that some of the lighter BbOMVs seen here (Figure 2A) might be empty inside, and that *Borrelia* might utilize its vesicles in a similar manner as *Pseudomonas aeruginosa*. Therefore, BbOMVs might participate in LB-related autoimmune disorders by intaking host extracellular DNA and fooling the host immune system into perceiving it as foreign, thus instigating the host to attack itself. However, further validation for this hypothesis is required.

Bacterial membrane vesicles have been identified to carry different types of cargoes [11,12,47]. In Table 1, some of the characteristics of BbOMVs identified thus far can be located. Here, further characterization of BbOMVs confirmed the presence of nucleotides in the form of double stranded DNA (Figure 3A), as has been previously described [29,38]. Furthermore, Malge and colleagues have identified plasmid-encoded RNA transcripts to be enriched in BbOMVs [30]. The containment of genetic information inside BbOMVs would suggest the transfer of information between bacterial cells, if not also, between the bacterium and the host.

Previous analyses have identified several known antigenic lipoproteins, such as OspA, OspB, OspC, and OspD, contained in BbOMVs [16,24,26,28]. Similar to previous findings [16,24,26,28], we confirmed the expression of OspA and OspC in BbOMVs (Figure 3D,E). OspA is expressed while the spirochete is in the tick gut, but both temperature and tick feeding trigger a change to OspC expression [48]. Hence, *Borrelia* utilizes OspC during transmission from the tick vector to the mammalian host, and the lipoprotein is required for establishing an infection [49]. Furthermore, a recent study established that OspC has antiphagocytic properties, thus promoting borrelial immune evasion during early dissemination [50]. Both OspA and OspC have been demonstrated to be immunogenic in patients with arthritic symptoms, with increased IgG response to OspA during later stages (months to years) of Lyme arthritis [51]. Therefore, the presence of both OspA and OspC in BbOMVs could affect the pathology of LB by inducing an inflammatory response in the host.

Curiously, OspC bands were barely visible in the bacterial whole cell lysate controls (lanes 1 and 6 in Figure 3E). Enterotoxin, from enterotoxigenic *Escherichia coli,* and aminopeptidase, from *Pseudomonas aeruginosa,* have been demonstrated to be enriched in the OMVs of these bacteria [52,53]. Both proteins, enterotoxin and aminopeptidase, were shown to increase vesicle association with endothelial cells [52,53]. Thus, the immunoblot results examined here might suggest a similar occurrence for OspC in *B. burgdorferi*, since OspC is necessary for borrelial infectivity [49]. Moreover, as OspC can protect the bacterial cell from phagocytosis [50], it could be possible for the bacterium to disseminate OspC in advance to establish a suitable environment for the bacterium to initiate infection and survive the host immune response.

We further analyzed, and detected, immunogenic proteins peptidoglycan and p39 (basic membrane protein A) in the vesicles (Figure 3F,G, respectively). Both p39 and borrelial peptidoglycan have been identified as markers for Lyme arthritis [7,54]. Since Lyme arthritis is a late manifestation of *B. burgdorferi* infection [55], both peptidoglycan and p39 would have to remain long-term in the host. BbOMVs would provide a convenient mechanism for these antigenic markers to persist in the host during the course of LB, and to survive antibiotic treatment.

Bacterial OMVs can induce immunological consequences in the host. *Helicobacter pylori*, for instance, has been observed to induce growth arrest, increased cytotoxicity, and IL-8 production in gastric epithelial cells through OMV production [56]. *E. coli*, on the other hand, has been shown to secrete Shiga toxins via its OMVs [57]. In one study, bacterial lipopeptides were found to induce neuronal dysfunction both in mice and cultured neurons, suggesting a pathogenic role for lipoproteins without the presence of live bacteria [58]. As the investigated BbOMVs contained lipoproteins OspA, OspC, and p39 (Figure 3D,E,G), some of the neurological symptoms in patients seen post-treatment could be the result of BbOMV-induced pathology.

BbOMVs contain immunogenic antigens and can adhere to endothelial cells; however, the vesicles do not induce cell death in these cells [24]. Similarly, in our study, BbOMVs cocultured with human chondrosarcoma (SW1353) and skin fibroblast (BJ) cells did not increase cell death as compared to the staurosporine treated controls (Figure 4). Furthermore, corresponding to our previous findings [41], neither spirochetes nor RBs induced cell death in these two human cell lines. Hence, as none of the *B. burgdorferi* samples, spirochetes, RBs, or BbOMVs induced death in these two human cell lines, it would seem that *Borrelia* is not cytotoxic to chondrosarcoma or dermal fibroblast cells.

Currently, the persistence of *Borrelia* or borrelial antigens in LB patients requires further examination and validation. Moreover, the role of BbOMVs in the pathology of LB should be investigated to a greater extent. However, due to the presence of known immunogenic markers OspA, OspC, peptidoglycan, and p39, examined here, it could be suggested that BbOMVs hold the potential for inducing an immune response in the host. Furthermore, it has been suggested that BbOMVs could participate in the induction of autoimmune-related consequences in patients via membrane lipid exchange with host cells [59]. Moreover, as bacterial OMVs have been demonstrated to be capable of intaking extracellular DNA [46], BbOMVs could function in a similar manner. Therefore, BbOMVs possess several mechanisms for aiding *Borrelia* in both initiating an infection, as well as sustaining a prolonged immune response, and possibly even initiating an autoimmune response via self-antigens in the form of host lipids and/or DNA.

5. Conclusions

We examined the characteristics of borrelial outer membrane vesicles, and the possible cytotoxic consequences induced by these vesicles in human cells. For the first time, the size of naturally formed BbOMVs was reported, as well as the lack of cell death in chondrosarcoma and dermal fibroblast cells. We demonstrated that BbOMVs contained known antigenic markers OspA, OspC, peptidoglycan, and p39. We propose that *Borrelia* could utilize BbOMVs as a decoy for the host immune system by disseminating immunogenic

proteins such as OspA, OspC, peptidoglycan, and p39, thus avoiding detection and elimination itself. Moreover, BbOMVs could be utilized by the bacterium as persistent antigens, consequently sustaining a prolonged immune response by the host. Hence, the pathogenic role of BbOMVs should be recognized and further examined.

Supplementary Materials: The following supporting information can be downloaded at: https://www.mdpi.com/article/10.3390/microorganisms10020212/s1, Figure S1: Only 1.8% of residual borrelial particles were located from BbOMV purification.

Author Contributions: Conceptualization, K.K. and L.G.; methodology, K.K., H.T., and L.G.; formal analysis, K.K.; investigation, K.K., H.T., and J.N.; resources, K.K. and L.G.; writing—original draft preparation, K.K.; writing—review and editing, K.K., H.T., J.N., and L.G.; visualization, K.K.; supervision, L.G.; project administration, K.K. and L.G.; funding acquisition, L.G. All authors have read and agreed to the published version of the manuscript.

Funding: This research was funded by the Schwartz foundation.

Institutional Review Board Statement: Not applicable.

Informed Consent Statement: Not applicable.

Data Availability Statement: Data is contained within the article or Supplementary Material.

Acknowledgments: The authors would like to thank Visa Ruokolainen for his assistance with ImageJ. In addition, the authors thank Biocenter Oulu EM laboratory for the preparation of epon-embedded TEM samples.

Conflicts of Interest: L.G. is chief executive officer and shareholder of Te?ted Oy, Jyvaskyla, Finland. This work is unrelated to the author's commercial activities. There is no conflict of interest. K.K., H.T., and J.N. declare no conflict of interest.

References

1. Mead, P.S. Epidemiology of Lyme Disease. *Infect. Dis. Clin. N. Am.* **2015**, *29*, 187–210. [CrossRef]
2. Burgdorfer, W.; Barbour, A.G.; Hayes, S.F.; Benach, J.L.; Grunwaldt, E.; Davis, J.P. Lyme disease—A tick-borne spirochetosis? *Science* **1982**, *216*, 1317–1319. [CrossRef]
3. Wormser, G.P.; Dattwyler, R.J.; Shapiro, E.D.; Halperin, J.J.; Steere, A.C.; Klempner, M.S.; Krause, P.J.; Bakken, J.S.; Strle, F.; Stanek, G.; et al. The clinical assessments treatment, and prevention of lyme disease, human granulocytic anaplasmosis, and babesiosis: Clinical practice guidelines by the Infectious Diseases Society of America. *Clin. Infect. Dis.* **2006**, *43*, 1089–1134. [CrossRef]
4. Sehgal, V.N.; Khurana, A. Lyme disease/borreliosis as a systemic disease. *Clin. Dermatol.* **2015**, *33*, 542–550. [CrossRef]
5. Nanagara, R.; Duray, P.H.; Schumacher, H.R. Ultrastructural demonstrational of spirochetal antigens in synovial membrane in chronic lyme disease: Possible factors contributing to persistence of organisms. *Hum. Pathol.* **1996**, *27*, 1025–1034. [CrossRef]
6. Hulïnská, D.; Votýpka, J.; Valešová, M. Persistence of Borrelia garinii and Borrelia afzelii in patients with Lyme arthritis. *Zent. Bakteriol.* **1999**, *289*, 301–318. [CrossRef]
7. Jutras, B.L.; Lochhead, R.B.; Kloos, Z.A.; Biboy, J.; Strle, K.; Booth, C.J.; Govers, S.K.; Gray, J.; Schumann, P.; Vollmer, W.; et al. *Borrelia burgdorferi* peptidoglycan is a persistent antigen in patients with Lyme arthritis. *Proc. Natl. Acad. Sci. USA* **2019**, *116*, 13498–13507. [CrossRef] [PubMed]
8. Embers, M.E.; Barthold, S.W.; Borda, J.T.; Bowers, L.; Doyle, L.; Hodzic, E.; Jacobs, M.B.; Hasenkampf, N.R.; Martin, D.S.; Narasimhan, S.; et al. Persistence of *Borrelia burgdorferi* in rhesus macaques following antibiotic treatment of disseminated infection. *PLoS ONE* **2012**, *7*, e29914. [CrossRef]
9. Hodzic, E.; Imai, D.; Feng, S.; Barthold, S.W. Resurgence of persisting non-cultivable *Borrelia burgdorferi* following antibiotic treatment in mice. *PLoS ONE* **2014**, *9*, e86907. [CrossRef] [PubMed]
10. Bockenstedt, L.K.; Gonzalez, D.G.; Haberman, A.M.; Belperron, A.A. Spirochete antigens persist near cartilage after murine Lyme borreliosis therapy. *J. Clin. Invest.* **2012**, *122*, 2652–2660. [CrossRef]
11. McBroom, A.J.; Kuehn, M.J. Outer Membrane Vesicles. *EcoSal Plus* **2005**, *1*. [CrossRef]
12. Toyofuku, M.; Nomura, N.; Eberl, L. Types and origins of bacterial membrane vesicles. *Nat. Rev. Microbiol.* **2019**, *17*, 13–24. [CrossRef]
13. Orench-Rivera, N.; Kuehn, M.J. Environmentally controlled bacterial vesicle-mediated export. *Cell. Microbiol.* **2016**, *18*, 1525–1536. [CrossRef] [PubMed]
14. Unal, C.M.; Schaar, V.; Riesbeck, K. Bacterial outer membrane vesicles in disease and preventive medicine. *Semin. Immunopathol.* **2011**, *33*, 395–408. [CrossRef] [PubMed]

15. Forsberg, C.W.; Beveridge, T.J.; Hellstrom, A. Cellulase and xylanase release from Bacteroides succinogenes and its importance in the rumen environment. *Appl. Environ. Microbiol.* **1981**, *42*, 886–896. [CrossRef] [PubMed]
16. Dorward, D.W.; Schwan, T.G.; Garon, C.F. Immune capture and detection of *Borrelia burgdorferi* antigens in urine, blood, or tissues from infected ticks, mice, dogs, and humans. *J. Clin. Microbiol.* **1991**, *29*, 1162–1170. [CrossRef] [PubMed]
17. Brandtzaeg, P.; Bryn, K.; Kierulf, P.; Øvstebø, R.; Namork, E.; Aase, B.; Jantzen, E. Meningococcal endotoxin in lethal septic shock plasma studied by gas chromatography, mass-spectrometry, ultracentrifugation, and electron microscopy. *J. Clin. Investig.* **1992**, *89*, 816–823. [CrossRef]
18. Hellman, J.; Loiselle, P.M.; Zanzot, E.M.; Allaire, J.E.; Tehan, M.M.; Boyle, L.A.; Kurnick, J.T.; Warren, H.S. Release of gram-negative outer-membrane proteins into human serum and septic rat blood and their interactions with immunoglobulin in antiserum to Escherichia coli J5. *J. Infect. Dis.* **2000**, *181*, 1034–1043. [CrossRef]
19. Hynes, S.O.; Keenan, J.I.; Ferris, J.A.; Annuk, H.; Moran, A.P. Lewis epitopes on outer membrane vesicles of relevance to Helicobacter pylori pathogenesis. *Helicobacter* **2005**, *10*, 146–156. [CrossRef]
20. Perez Vidakovics, M.L.A.; Jendholm, J.; Mörgelin, M.; Månsson, A.; Larsson, C.; Cardell, L.O.; Riesbeck, K. B cell activation by outer membrane vesicles—A novel virulence mechanism. *PLoS Pathog.* **2010**, *6*, e1000724. [CrossRef]
21. Avila-Calderón, E.D.; Araiza-Villanueva, M.G.; Cancino-Diaz, J.C.; López-Villegas, E.O.; Sriranganathan, N.; Boyle, S.M.; Contreras-Rodríguez, A. Roles of bacterial membrane vesicles. *Arch. Microbiol.* **2015**, *197*, 1–10. [CrossRef]
22. Ellis, T.N.; Kuehn, M.J. Virulence and Immunomodulatory Roles of Bacterial Outer Membrane Vesicles. *Microbiol. Mol. Biol. Rev.* **2010**, *74*, 81–94. [CrossRef]
23. Dorward, D.W.; Garon, C.F.; Judd, R.C. Export and intercellular transfer of DNA via membrane blebs of Neisseria gonorrhoeae. *J. Bacteriol.* **1989**, *171*, 2499–2505. [CrossRef]
24. Shoberg, R.J.; Thomas, D.D. Specific adherence of *Borrelia burgdorferi* extracellular vesicles to human endothelial cells in culture. *Infect. Immun.* **1993**, *61*, 3892–3900. [CrossRef]
25. Skare, J.T.; Shang, E.S.; Foley, D.M.; Blanco, D.R.; Champion, C.I.; Mirzabekov, T.; Sokolov, Y.; Kagan, B.L.; Miller, J.N.; Lovett, M.A. Virulent strain associated outer membrane proteins of *Borrelia burgdorferi*. *J. Clin. Investig.* **1995**, *96*, 2380–2392. [CrossRef]
26. Whitmire, W.M.; Garon, C.F. Specific and nonspecific responses of murine B cells to membrane blebs of *Borrelia burgdorferi*. *Infect. Immun.* **1993**, *61*, 1460–1467. [CrossRef]
27. Shoberg, R.J.; Thomas, D.D. *Borrelia burgdorferi* vesicle production occurs via a mechanism independent of immunoglobulin M involvement. *Infect. Immun.* **1995**, *63*, 4857–4861. [CrossRef] [PubMed]
28. Yang, X.; Promnares, K.; Qin, J.; He, M.; Shroder, D.Y.; Kariu, T.; Wang, Y.; Pal, U. Characterization of multiprotein complexes of the *Borrelia burgdorferi* outer membrane vesicles. *J. Proteome Res.* **2011**, *10*, 4556–4566. [CrossRef]
29. Dorward, D.W.; Garon, C.F. DNA is packaged within membrane-derived vesicles of gram-negative but not gram-positive bacteria. *Appl. Environ. Microbiol.* **1990**, *56*, 1960–1962. [CrossRef] [PubMed]
30. Malge, A.; Ghai, V.; Reddy, P.J.; Baxter, D.; Kim, T.-K.K.; Moritz, R.L.; Wang, K. mRNA transcript distribution bias between *Borrelia burgdorferi* bacteria and their outer membrane vesicles. *FEMS Microbiol. Lett.* **2018**, *365*, 135. [CrossRef] [PubMed]
31. Beermann, C.; Groscurth, P.; Filgueira, L.; Wunderli-Allenspach, H. Lipoproteins from *Borrelia burgdorferi* applied in liposomes and presented by dendritic cells induce CD8+ T-lymphocytes in vitro. *Cell. Immunol.* **2000**, *201*, 124–131. [CrossRef] [PubMed]
32. Toledo, A.; Coleman, L.; Kuhlow, C.J.; Crowley, J.T.; Benach, J.L. The enolase of *Borrelia burgdorferi* is a plasminogen receptor released in outer membrane vesicles. *Infect. Immun.* **2012**, *80*, 359–368. [CrossRef]
33. Moriarty, T.J.; Norman, M.U.; Colarusso, P.; Bankhead, T.; Kubes, P.; Chaconas, G. Real-time high resolution 3D imaging of the lyme disease spirochete adhering to and escaping from the vasculature of a living host. *PLoS Pathog.* **2008**, *4*, e1000090. [CrossRef] [PubMed]
34. Barbour, A.G. Isolation and cultivation of Lyme disease spirochetes. *Yale J. Biol. Med.* **1984**, *57*, 521–525. [PubMed]
35. Meriläinen, L.; Herranen, A.; Schwarzbach, A.; Gilbert, L. Morphological and biochemical features of *Borrelia burgdorferi* pleomorphic forms. *Microbiology* **2015**, *161*, 516–527. [CrossRef]
36. Georgilis, K.; Peacocke, M.; Klempner, M.S. Fibroblasts Protect the Lyme Disease Spirochete, *Borrelia burgdorferi*, from Ceftriaxone In Vitro. *J. Infect. Dis.* **1992**, *166*, 440–444. [CrossRef]
37. Chen, L.; Li, Q.; Wang, J.; Jin, S.; Zheng, H.; Lin, J.; He, F.; Zhang, H.; Ma, S.; Mei, J.; et al. MiR-29b-3p promotes chondrocyte apoptosis and facilitates the occurrence and development of osteoarthritis by targeting PGRN. *J. Cell. Mol. Med.* **2017**, *21*, 3347–3359. [CrossRef]
38. Garon, C.F.; Dorward, D.W.; Corwin, M.D. Structural features of *Borrelia burgdorferi*—The lyme disease spirochete: Silver staining for nucleic acids. *Scanning Microsc.* **1989**, *3*, 109–115.
39. Huttunen, M.; Waris, M.; Kajander, R.; Hyypia, T.; Marjomaki, V. Coxsackievirus A9 Infects Cells via Nonacidic Multivesicular Bodies. *J. Virol.* **2014**, *88*, 5138–5151. [CrossRef]
40. Schindelin, J.; Arganda-Carreras, I.; Frise, E.; Kaynig, V.; Longair, M.; Pietzsch, T.; Preibisch, S.; Rueden, C.; Saalfeld, S.; Schmid, B.; et al. Fiji: An open-source platform for biological-image analysis. *Nat. Methods* **2012**, *9*, 676–682. [CrossRef] [PubMed]
41. Karvonen, K.; Nykky, J.; Marjomäki, V.; Gilbert, L. Distinctive Evasion Mechanisms to Allow Persistence of *Borrelia burgdorferi* in Different Human Cell Lines. *Front. Microbiol.* **2021**, *12*, 3004. [CrossRef] [PubMed]
42. Sapi, E.; Kaur, N.; Anyanwu, S.; Luecke, D.F.; Datar, A.; Patel, S.; Rossi, M.; Stricker, R.B. Evaluation of in-vitro antibiotic susceptibility of different morphological forms of *Borrelia burgdorferi*. *Infect. Drug Resist.* **2011**, *4*, 97–113. [CrossRef]

43. Sharma, B.; Brown, A.V.; Matluck, N.E.; Hu, L.T.; Lewis, K. *Borrelia burgdorferi*, the causative agent of Lyme disease, forms drug-tolerant persister cells. *Antimicrob. Agents Chemother.* **2015**, *59*, 4616–4624. [CrossRef]
44. Rudenko, N.; Golovchenko, M.; Kybicova, K.; Vancova, M. Metamorphoses of Lyme disease spirochetes: Phenomenon of Borrelia persisters. *Parasites Vectors* **2019**, *12*, 237. [CrossRef]
45. Gankema, H.; Wensink, J.; Guinee, P.A.M.; Jansen, W.H.; Witholt, B. Some characteristics of the outer membrane material released by growing enterotoxigenic Escherichia coli. *Infect. Immun.* **1980**, *29*, 704–713. [CrossRef] [PubMed]
46. Renelli, M.; Matias, V.; Lo, R.Y.; Beveridge, T.J. DNA-containing membrane vesicles of Pseudomonas aeruginosa PAO1 and their genetic transformation potential. *Microbiology* **2004**, *150*, 2161–2169. [CrossRef]
47. Kaparakis-Liaskos, M.; Ferrero, R.L. Immune modulation by bacterial outer membrane vesicles. *Nat. Rev. Immunol.* **2015**, *15*, 375–387. [CrossRef] [PubMed]
48. Schwan, T.G.; Piesman, J.; Golde, W.T.; Dolan, M.C.; Rosa, P.A. Induction of an outer surface protein on *Borrelia burgdorferi* during tick feeding. *Proc. Natl. Acad. Sci. USA* **1995**, *92*, 2909–2913. [CrossRef]
49. Grimm, D.; Tilly, K.; Byram, R.; Stewart, P.E.; Krum, J.G.; Bueschel, D.M.; Schwan, T.G.; Policastro, P.F.; Elias, A.F.; Rosa, P.A. Outer-surface protein C of the Lyme disease spirochete: A protein induced in ticks for infection of mammals. *Proc. Natl. Acad. Sci. USA* **2004**, *101*, 3142–3147. [CrossRef]
50. Carrasco, S.E.; Troxell, B.; Yang, Y.; Brandt, S.L.; Li, H.; Sandusky, G.E.; Condon, K.W.; Serezani, C.H.; Yang, X.F. Outer surface protein OspC is an antiphagocytic factor that protects *Borrelia burgdorferi* from phagocytosis by macrophages. *Infect. Immun.* **2015**, *83*, 4848–4860. [CrossRef] [PubMed]
51. Akin, E.; McHugh, G.L.; Flavell, R.A.; Fikrig, E.; Steere, A.C. The immunoglobulin (IgG) antibody response to OspA and OspB correlates with severe and prolonged lyme arthritis and the IgG response to P35 correlates with mild and brief arthritis. *Infect. Immun.* **1999**, *67*, 173–181. [CrossRef]
52. Kesty, N.C.; Mason, K.M.; Reedy, M.; Miller, S.E.; Kuehn, M.J. Enterotoxigenic Escherichia coli vesicles target toxin delivery into mammalian cells. *EMBO J.* **2004**, *23*, 4538–4549. [CrossRef]
53. Bauman, S.J.; Kuehn, M.J. Pseudomonas aeruginosa vesicles associate with and are internalized by human lung epithelial cells. *BMC Microbiol.* **2009**, *9*, 26. [CrossRef]
54. Pal, U.; Wang, P.; Bao, F.; Yang, X.; Samanta, S.; Schoen, R.; Wormser, G.P.; Schwartz, I.; Fikrig, E. *Borrelia burgdorferi* basic membrane proteins A and B participate in the genesis of Lyme arthritis. *J. Exp. Med.* **2008**, *205*, 133–141. [CrossRef] [PubMed]
55. Cardenas-de la Garza, J.A.; De la Cruz-Valadez, E.; Ocampo-Candiani, J.; Welsh, O. Clinical spectrum of Lyme disease. *Eur. J. Clin. Microbiol. Infect. Dis.* **2019**, *38*, 201–208. [CrossRef]
56. Ismail, S.; Hampton, M.B.; Keenan, J.I. Helicobacter pylori outer membrane vesicles modulate proliferation and interleukin-8 production by gastric epithelial cells. *Infect. Immun.* **2003**, *71*, 5670–5675. [CrossRef] [PubMed]
57. Yokoyama, K.; Horii, T.; Yamashino, T.; Hashikawa, S.; Barua, S.; Hasegawa, T.; Watanabe, H.; Ohta, M. Production of Shiga toxin by Escherichia coli measured with reference to the membrane vesicle-associated toxins. *FEMS Microbiol. Lett.* **2006**, *192*, 139–144. [CrossRef]
58. Kim, K.M.; Zamaleeva, A.I.; Lee, Y.W.; Ahmed, M.R.; Kim, E.; Lee, H.R.; Pothineni, V.R.; Tao, J.; Rhee, S.; Jayakumar, M.; et al. Characterization of brain dysfunction induced by bacterial lipopeptides that alter neuronal activity and network in rodent brains. *J. Neurosci.* **2018**, *38*, 10672–10691. [CrossRef] [PubMed]
59. Crowley, J.T.; Toledo, A.M.; LaRocca, T.J.; Coleman, J.L.; London, E.; Benach, J.L. Lipid Exchange between *Borrelia burgdorferi* and Host Cells. *PLoS Pathog.* **2013**, *9*, e1003109. [CrossRef]

III

EFFECTIVE KILLING OF BORRELIA BURGDORFERI IN VITRO WITH NOVEL HERBAL COMPOUNDS

by

Kati Karvonen & Leona Gilbert 2018

General Medicine Open 2 (6): 1–4

https://doi.org/10.15761/GMO.1000153

General Medicine Open

Research Article

ISSN: 2515-4737

Effective killing of *Borrelia burgdorferi in vitro* with novel herbal compounds

Kati Karvonen* and Leona Gilbert

Department of Biological and Environmental Science and Nanoscience Center, PO Box 35, FI-40014, University of Jyvaskyla, Finland

Abstract

Introduction: The tick-borne disease Lyme Borreliosis is caused by *Borrelia* bacteria. The disease can persist even after treatment with antibiotics, which is why other methods of treatment are needed. Herbal compounds and phytochemicals have been recently examined in relation to eradicating *Borrelia* bacteria *in vitro*.

Objective: The possible antimicrobial effect of two novel compounds, Biocidin® Liquid and LSF Broad-Spectrum Liposomal formulas, was examined in the hopes of discovering an alternative method for eradication of *Borrelia* bacteria.

Methods: The minimum inhibitory concentrations (MICs) and minimum bacterial deaths (MBDs), as well as, time-kill effect of each compound were utilized in the study.

Results: The Liquid formula effectively killed the spirochetes with 1:10 dilution, while the MIC for the Liposomal formula was 1:25. Moreover, the MIC for both compounds with Round Bodies was 1:50 and for biofilms 1:10. Though long-term effect (MBD) was seen only with 1:5 dilutions for both formulas. Additionally, the killing effect of each compound was observed already at 10 min post-treatment.

Conclusion: The study conducted here provides new insight into the antimicrobial effect of herbal compounds. Furthermore, studies such as these are required in order to discover possible alternatives to antibiotics in the battle against *Borrelia* infections.

Abbreviations: B. burgdorferi: Borrelia burgdorferi; MIC: minimum inhibitory concentration; MBD: minimum bacterial death; RB: Round Body.

Introduction

The spirochete bacteria *Borrelia burgdorferi,* found in *Ixodes* ticks, is the causative agent for Lyme Borreliosis [1]. Unfavorable conditions, such as changes in pH, nutritional depletion, even antibiotics can lead the pleomorphic bacteria to reversibly alter their form into Round Bodies (RBs) or biofilms [2,3]. Furthermore, the immune system reacts differently to the pleomorphic forms with macrophages digesting and processing RBs differently than spirochetes [4]. Hence, examinations of *B. burgdorferi* need to include these various forms.

Borrelia infected patients report signs and symptoms ranging from skin inflammation, arthritis and neurological or cardiac impairments [5]. Treatment with antibiotics early on the infection can clear the pathogen from the body, however, post-treatment persistence by the bacteria as asymptomatic or with a multiplicity of symptoms can occur [5]. It has been suggested that the different pleomorphic forms of *Borrelia* are involved in the avoidance of the immune system, and thus, in the persistence of the disease [6].

Current treatment for Lyme borreliosis relies solely on antibiotics [5]. However, studies on antibiotic efficiency with different pleomorphic forms of *Borrelia* have shown to demonstrate varying effectiveness of antibiotics in killing the bacteria [6,7]. Therefore, new approaches for better treatment are required.

For centuries herbal compounds have been used as remedies for various ailments. Recently, the antimicrobial possibilities of a variety of phytochemicals and herbal extracts against *Borrelia* have been studied [8-10]. Hence, studies on natural composites might offer new possibilities for remedies to Lyme Borreliosis. Here, two commercially available herbal compounds, Biocidin® Liquid and LSF Broad-Spectrum Liposomal formulas, were tested for their efficiency in eliminating different pleomorphic forms of *B. burgdorferi in vitro*.

Materials and methods

Bacterial strain, culturing conditions and test compounds

All experiments were conducted with infectious, fluorescent *B. burgdorferi* strain GCB726 with GFP, which was graciously provided by Georges Chaconas, University of Calgary, Canada [11]. Barbour-Stoenner-Kelly medium (BSK II) [12], without gelatin and supplemented with 6% heat inactivated rabbit serum (Sigma-Aldrich, St. Louis, USA) was used in the culturing of cells at +37 ºC. Low-passage number cells (≤ passage 8) were used in all of the experiments.

The tested compounds, Biocidin® Liquid formula and Biocidin® LSF Broad-Spectrum Liposomal formula, were acquired from Bio-Botanical Research Inc. (CA, USA). As negative controls for growth 100 µg/ml of doxycycline (Hexal®, Germany) and 0.02 % H_2O_2 (Sigma-Aldrich) were used. Untreated cells were a positive control for growth.

Correspondence to: Kati Karvonen, M.Sc, Department of Biological and Environmental Science and Nanoscience Center, PO Box 35, FI-40014, University of Jyvaskyla, Finland, E-mail: kati.s.karvonen@jyu.fi

Key words: *Borrelia burgdorferi, pleomorphic form, antimicrobial, persister*

Received: December 18, 2018; **Accepted:** December 28, 2018; **Published:** December 31, 2018

Minimum inhibitory concentration and minimum bacterial death experiments

The minimum inhibitory concentrations (MICs) of Biocidin® Liquid and Liposomal formulas were determined by incubating 15 x 10^6 *B. burgdorferi* spirochetes in 3 ml of culture media with different dilutions (1:5, 1:10, 1:25 and 1:50) of the compounds for 96 h [13]. The samples were measured for fluorescence with a spectrophotometer (Perkin Elmer, 2030 Multilabel reader Victor™ x4) every 24 h.

RBs were induced as previously described [13]. Briefly, 15 x 10^6 *B. burgdorferi* spirochetes were incubated in sterile distilled H_2O at +37 °C for 2 h before placing the cells into 3 ml of fresh media and adding the same dilutions of each Biocidin® compound as with the spirochete samples. Fluorescence measurements were done in the above-mentioned manner.

The MICs for both compounds with biofilms were determined by counting a 10 µl area in a C-Chip DHC-N01 Disposable Haemocytometer (System Neubauer Improved, Digital Bio) at 0 h and 72 h post-treatment. Approximately 9000 biofilms in 3 ml of fresh media were treated the previously mentioned dilutions of Biocidin® compounds and incubated at +37 °C for 72 h after which the samples were counted. Cell clusters of over 10 cells were regarded as biofilms.

The minimum bacterial death (MBD) were determined as has been done previously with alterations [13]. Samples of 300 µl from the MIC experiments from each pleomorphic form from the 72-h time point, respectively, were reseeded into 3 ml of fresh media and incubated for 3 weeks at +37 °C. At weeks 1 and 3 the change in pH (color change) of the media was used to indicate growth (yes/no) and microscopy (Leica CTR5500, Germany) was utilized at week 3 to confirm the observations.

Time-kill experiments

The rate of cell death of *B. burgdorferi* was analyzed by adding the MIC dilutions of the compounds (Liquid formula = 1:10; Liposomal formula = 1:25) to 6 x 10^6 spirochetes in 3 ml of culture media and counting the cells using a C-Chip haemocytometer at 10, 20, 30, 60- and 120-min post-treatment. The means of three separate experiments were counted and Excel was used in producing the graph.

Results

MIC and MBD experiments

The MICs for Biocidin® Liquid and Liposomal formulas with spirochetes, RBs and biofilms of *B. burgdorferi* were determined (Figure 1). The MICs for both compounds with each *B. burgdorferi* form in Figure 1 are highlighted with a black star. First, the MIC for the Liquid formula with spirochetes demonstrated 1:10 dilution (Figure 1A), while 1:25 dilution was enough with the Liposomal formula (Figure 1B), as these were the lowest dilutions at which no growth was observed. Second, the MICs for both formulas with RBs was determined to be the 1:50 dilution (Figure 1C and 1D), as the relative fluorescence values followed those of the negative controls. Last, the MICs of both formulas with biofilms were deduced by counting the biofilms in 10 µl of each sample. Both compounds demonstrated an MIC of 1:10 dilution when cultured with biofilms (Figure 1E).

At 72 h time point of the MIC experiments, samples were put to fresh media and incubated for three weeks with the purpose of determining the MBDs for both compound with each *B. burgdorferi* pleomorphic form. Below table exemplifies the results from two separate experiments for each *B. burgdorferi* form (Table 1). Firstly, the Liquid formula demonstrated no growth with the 1:5 dilution during the whole three-week time period in all of the bacterial forms. On the third week growth was observed in each pleomorphic form with the 1:10, 1:25 and 1:50 dilutions except the 1:10 dilution in RBs. Moreover, both spirochete and biofilm samples had growth with the 1:25 and 1:50 dilutions already at week one, while the RB samples showed none. Hence, the short-term dilutions of the Liquid formula for each pleomorphic form correlated those of the MIC results. However, only the 1:5 dilution resulted in no growth long-term with all pleomorphic forms.

Secondly, the results for the Liposomal formula followed those of the Liquid formula, although most of the spirochete samples have been examined only once and the third week of 1:10 dilution with RBs is completely missing because of inapplicable data. However, similarly to the Liquid formula, the Liposomal formula demonstrated no growth in the 1:5 dilution with each of the pleomorphic form. Furthermore, both spirochetes and biofilms indicated growth at week one already in the 1:25 and 1:50 dilutions, while RBs expressed no growth at week one in any of the dilutions. The first week MBD results for the Liposomal formula with RBs and biofilms corresponded to the MIC results. However, when cultured with spirochetes the 1:25 dilution already indicated growth at week one. Thus, contradicting the MIC for the Liposomal formula determined earlier.

Time-kill experiments

The effectiveness of the Biocidin® compounds on *B. burgdorferi* spirochetes was determined in time-kill experiments (Figure 2). *B. burgdorferi* spirochetes were treated with the MICs of the compounds: 1:10 dilution for the Liquid formula; 1:25 for the Liposomal formula, and the cells were counted at 10, 20, 30, 60- and 120-min post-treatment. Both compounds induced cell death of *B. burgdorferi*, with the Liquid formula being slightly more effective.

Discussion

Lyme borreliosis is currently the most common tick-borne disease in the Northern hemisphere (Stanek *et al*. 2012) [14]. Antibiotics are usually effective against *Borrelia* sp., however, persisting forms have been uncovered capable of resisting certain antibiotics [6,15]. Therefore, investigating novel possibilities for eliminating the persisting bacteria from the body is crucial. Here two dietary supplement compounds from Bio-Botanical Research Inc. were examined for their ability to eradicate the different pleomorphic forms of *B. burgdorferi in vitro*.

In recent years, the effects of several phytochemicals on *Borrelia* have been studied and found to be effective against the different pleomorphic forms of the bacteria [8-10,16-18]. For instance, Stevia whole leaf extract has been found to reduce the size and number of *Borrelia* biofilms [10]. Additionally, grapefruit seed extract has been demonstrated to work against *Borrelia* spirochetes and RBs [16]. Recently though, oregano oil was found to be highly active against persistent (7day growth) forms of Borrelia even at low concentrations [17]. Similarly, to previous studies, both of the compounds used here diminished the growth of all *B. burgdorferi* forms as was demonstrated by the MIC and MBD experiments. The active ingredients in both compounds vary from berry extracts to essential oils from plants. Interestingly, both of the compounds used here also have oregano oil, as well as, grapefruit seed extract as active agents in them.

Additionally, the number of spirochetes were drastically reduced after only 2 h post-treatment with the Biocidin® compounds. This suggests that these compounds could offer a possible treatment for Lyme borreliosis, if not solely on their own but possibly when used

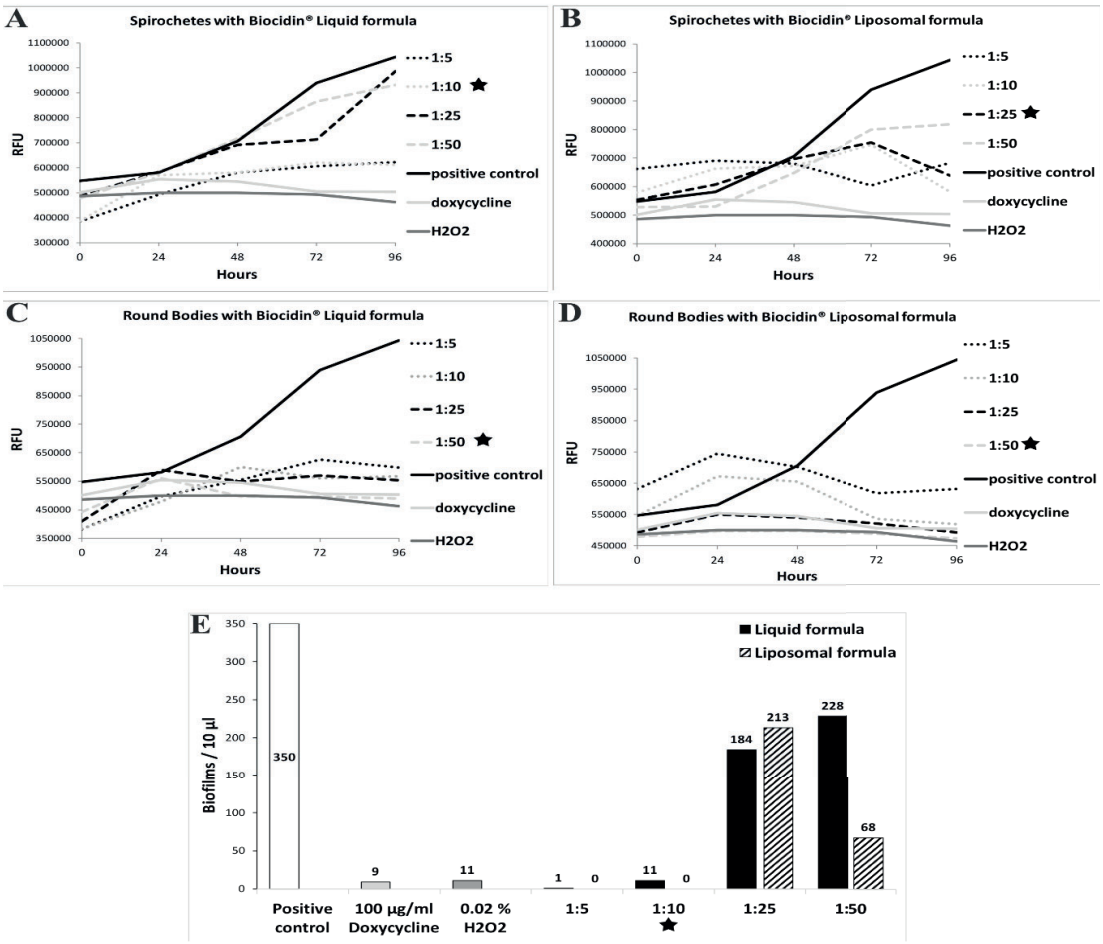

Figure 1. Minimum inhibitory concentrations of Biocidin® compounds with *B. burgdorferi* at various time points

15 x 10^6 spirochetes (A and B) or Round Bodies (C and D) in 3 ml of culture media were mixed with either Biocidin® Liquid (A and C) or Liposomal formula (B and D) in various dilutions (1:5, 1:10, 1:25 and 1:50) for 96 h. Panel E illustrates 9000 *B. burgdorferi* biofilms in 3 ml of culture media with the same dilutions as above of Liquid or Liposomal formula for 72 h. Cells without a treatment were a positive control for growth, while 100 µg/ml of doxycycline and 0.02 % H_2O_2 were used as negative control for growth. Values for spirochetes and Round Bodies are means from two separate experiments. The values for biofilms with Liquid formula are from just one experiment, while those for the Liposomal formula are the means of three experiments. The black stars indicate the minimum inhibitory concentrations (MICs) for each compound for the different pleomorphic forms.

Table 1. Minimum bacterial death of *B. burgdorferi* spirochetes, Round Bodies and biofilms treated with Biocidin® compounds

Dilutions of 1:5, 1:10, 1:25 and 1:50 were used and growth was observed (yes/no) for three weeks. Cells without a treatment were a positive control for growth, while 100 µg/ml of doxycycline and 0.02% H_2O_2 were used as negative control for growth. Results are mainly from two separate assays. Dashed lines indicate incomplete data, while the asterisk indicates only 1 repeat

	Spirochetes		Round Bodies		Biofilms	
	Week 1	**Week 3**	**Week 1**	**Week 3**	**Week 1**	**Week 3**
Positive control	Yes	Yes	Yes	Yes	Yes	Yes
Doxycycline	No	No	No	No	No	No
H_2O_2	No	No	No	No	No	No
Liquid formula						
1:5	No	No	No	No	No	No
1:10	No	Yes	No	No	No	Yes
1:25	Yes	Yes	No	Yes	Yes	Yes
1:50	Yes	Yes	No	Yes	Yes	Yes
Liposomal formula						
1:5	No*	No*	No	No	No	No
1:10	No	Yes*	No	---	No	Yes
1:25	Yes*	Yes*	No	Yes	Yes	Yes
1:50	Yes*	Yes*	No	Yes	Yes	Yes

*only 1 repeat
--- data incomplete

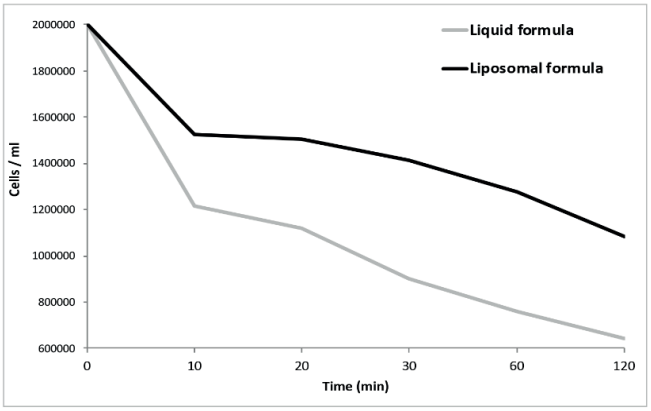

Figure 2. Rate of cell death after Biocidin® treatments

6 x 10^6 *Borrelia burgdorferi* spirochetes in 3 ml of media were treated with 1:10 Biocidin® Liquid formula or 1:25 Biocidin® Liposomal formula to check the rate of cell death. Cells were counted at 10, 20, 30, 60 and 120 min post-treatment. Represented are the mean values of three separate experiments. Both compounds drastically reduced *B. burgdorferi* spirochete count after 2 h post-treatment

synergistically with antibiotics as has been done before with other phytochemicals [19]. Naturally, studies involving antibiotics, as well as, RBs and biofilms should be conducted in order to realize the full potential of these compounds. Still, the promising results gained here for these two compounds indicate new possibilities to combat *B. burgdorferi* infections.

Authorship and Contributorship

All authors meet the criteria for authorship.

Acknowledgements

We'd like to acknowledge the Schwartz foundation for their continuous support of our research endeavors.

Funding

This work was supported by Bio-Botanical research Inc. However, the authors devised the study design, collected and analyzed the data, and prepared the manuscript without input from the company. The decision to publish was the authors.

Conflicts of interest

The authors have no conflicts of interest.

References

1. Burgdorfer W, Barbour AG, Hayes SF, Benach JL, Grunwaldt E (1982) Lyme disease-a tick-borne spirochetosis? *Science* 216: 1317-1319. [Crossref]

2. Meriläinen L, Herranen A, Schwarzbach A, Gilbert L (2015) Morphological and biochemical features of Borrelia burgdorferi pleomorphic forms. *Microbiology* 161: 516-527. [Crossref]

3. Murgia R, Cinco M (2004) Induction of cystic forms by different stress conditions in Borrelia burgdorferi. *APMIS* 112: 57-62. [Crossref]

4. Meriläinen L, Brander H, Herranen A, Schwarzbach A, Gilbert L (2016) Pleomorphic forms of Borrelia burgdorferi induce distinct immune responses. *Microb.Infect* [Crossref]

5. Stanek G, Wormser GP, Gray J, Strle F (2012) Lyme borreliosis. *The Lancet* 379: 461-473.

6. Sharma B, Brown AV, Matluck NE, Hu LT, Lewis K (2015) Borrelia burgdorferi, the Causative Agent of Lyme Disease, Forms Drug-Tolerant Persister Cells. *Antimicrob. Agents Chemother* 59: 4616-4624.

7. Sapi E, Kaur N, Anyanwu S, Luecke D, Datar A et al. (2011) Evaluation of in-vitro antibiotic susceptibility of different morphological forms of Borrelia burgdorferi. *Infect Drug Resist* 4: 97-113 [Crossref]

8. Feng J, Weitner M, Shi W, Zhang S, Sullivan D, et al. (2015) Identification of additional anti-persister activity against Borrelia burgdorferi from an FDA drug library. *Antibiotics* 4: 397-410. [Crossref]

9. Goc A, Niedzwiecki A, Rath M (2015) In vitro evaluation of antibacterial activity of phytochemicals and micronutrients against Borrelia burgdorferi and Borrelia garinii. *J.Appl.Microbiol* 119: 1561-1572. [Crossref]

10. Theophilus PAS, Victoria MJ, Socarras K, Filush KR, Gupta K, et al. (2015) Effectiveness of Stevia rebaudiana whole leaf extract against the various morphological forms of Borrelia burgdorferi in vitro. *European Journal of Microbiology and Immunology* 5: 268-280. [Crossref]

11. Moriarty TJ, Norman MU, Colarusso P, Bankhead T, Kubes P, et al. (2008) Real-time high resolution 3D imaging of the lyme disease spirochete adhering to and escaping from the vasculature of a living host. *PLoS Pathog* 4: e1000090. [Crossref]

12. Barbour AG (1984) Isolation and cultivation of Lyme disease spirochetes. *Yale J.Biol. Med* 57: 521-525. [Crossref]

13. Dever LL, Jorgensen JH, Barbour AG (1992) In vitro antimicrobial susceptibility testing of Borrelia burgdorferi: a microdilution MIC method and time-kill studies. *J Clin Microbiol* 30: 2692-2697.

14. Hubalek Z (2009) Epidemiology of lyme borreliosis. *Curr Probl Dermatol* 37: 31-50. [Crossref]

15. Sapi E, Bastian SL, Mpoy CM, Scott S, Rattelle A, et al. (2012) Characterization of biofilm formation by Borrelia burgdorferi in vitro. *PloS one* 7: e48277. [Crossref]

16. Brorson Ø, Brorson S (2007) Grapefruit seed extract is a powerful in vitro agent against motile and cystic forms of Borrelia burgdorferi sensu lato. *Infection* 35: 206-208. [Crossref]

17. Feng J, Zhang S, Shi W, Zubcevik N, Miklossy J, et al. (2017) Selective essential Oils from spice or culinary herbs have high activity against stationary Phase and Biofilm Borrelia burgdorferi. *Frontiers in medicine* 4: 169. [Crossref]

18. Goc A, Niedzwiecki A, Rath M (2017) Reciprocal cooperation of phytochemicals and micronutrients against typical and atypical forms of Borrelia spp. *J.Appl.Microbiol.* [Crossref]

19. Goc A, Niedzwiecki A, Rath M (2016) Cooperation of Doxycycline with Phytochemicals and Micronutrients Against Active and Persistent Forms of Borrelia sp. *International Journal of Biological Sciences* 12: 1093. [Crossref]